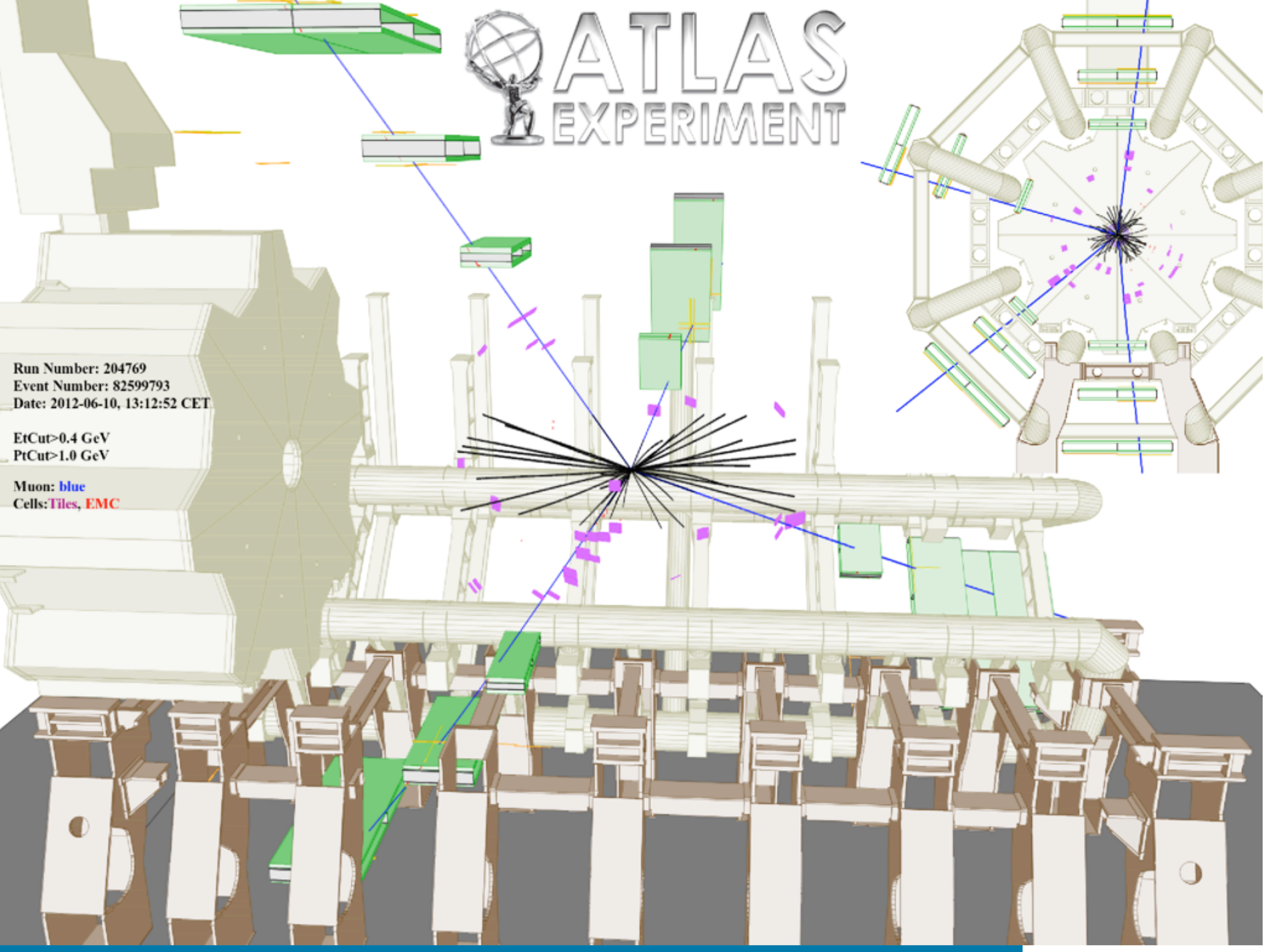

ATLAS measurements of Higgs boson properties in bosonic decay channels

K. Nikolopoulos
University of Birmingham
On behalf of the ATLAS Collaboration

1st August 2014
3rd International Conference in Frontiers in Physics
Kolymvari, Chania, Greece

UNIVERSITY OF BIRMINGHAM

LHC and ATLAS

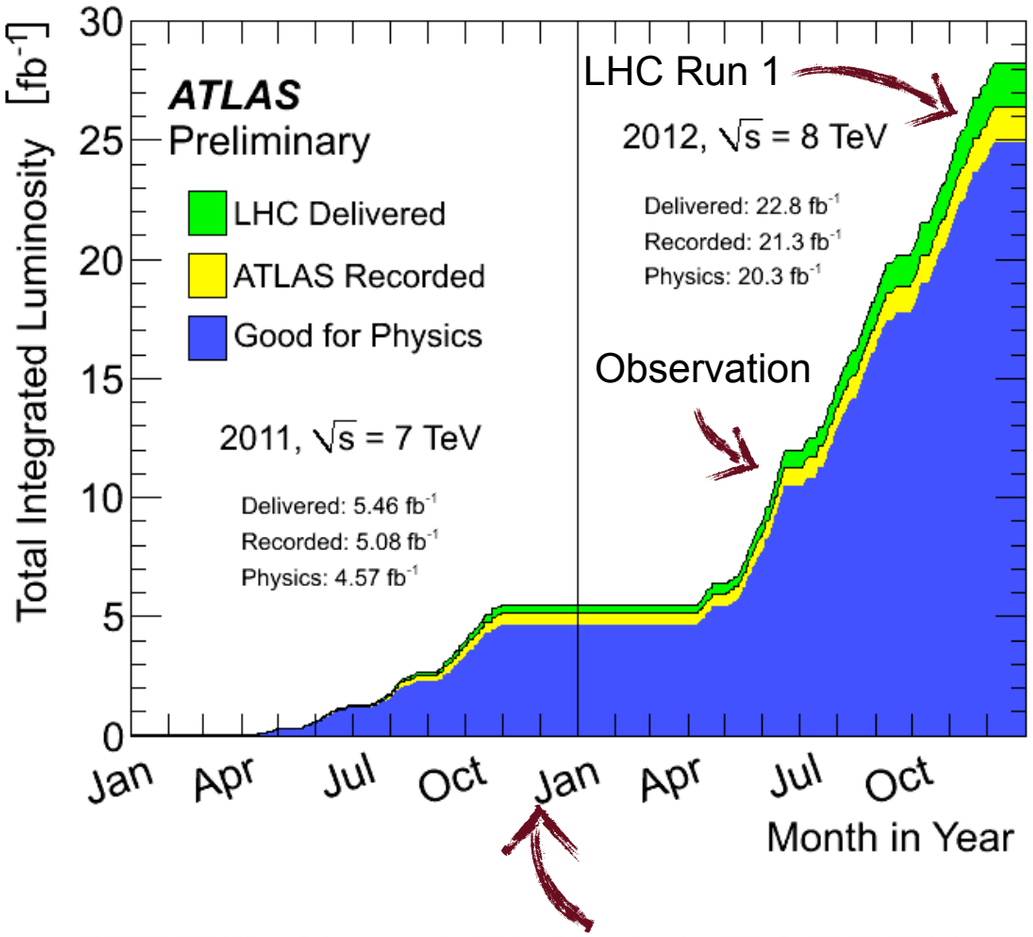

Excellent LHC/ATLAS operations
Overall efficiency 90%

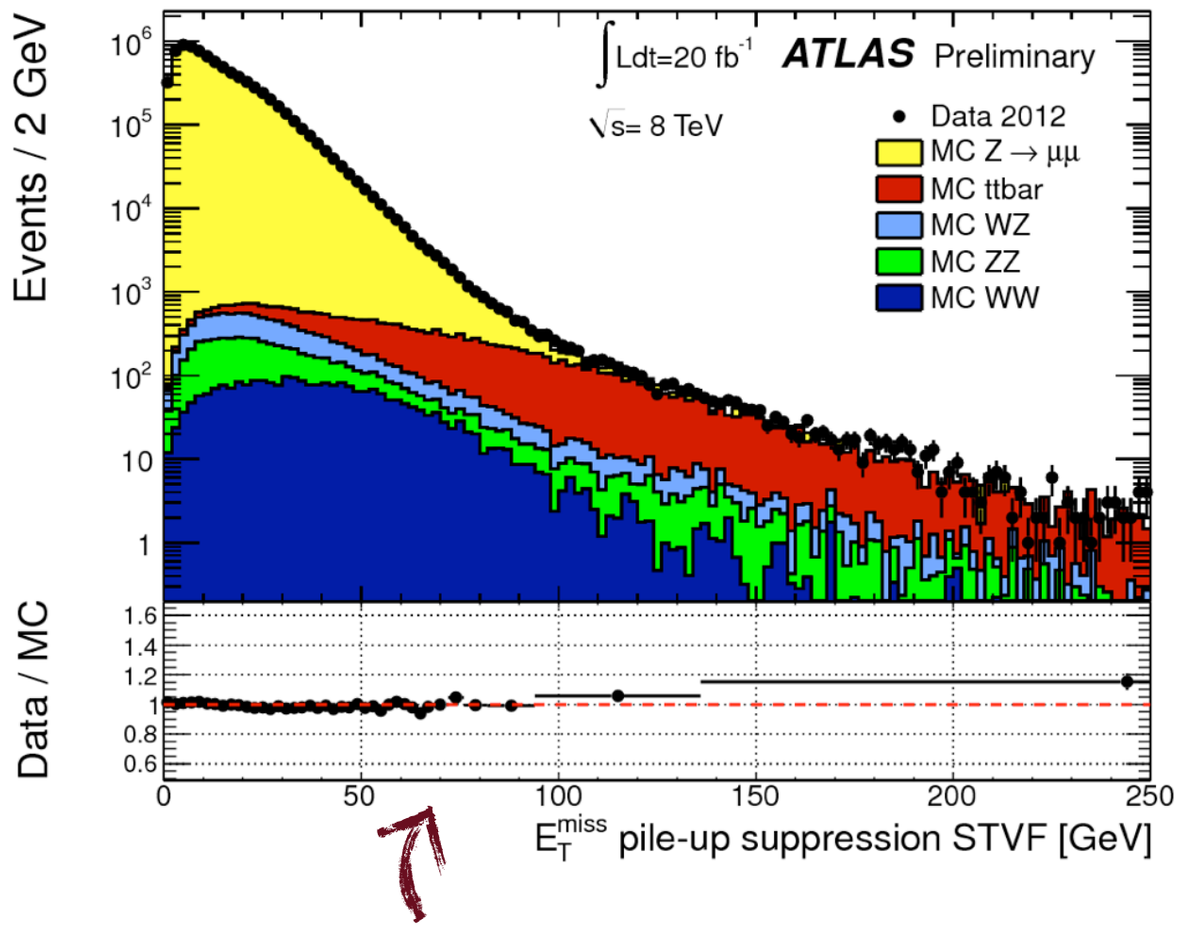

Excellent understanding of the detector performance!

The wealth of high quality data allows detailed studies of the properties of the Higgs boson!

SM Higgs boson production at the LHC

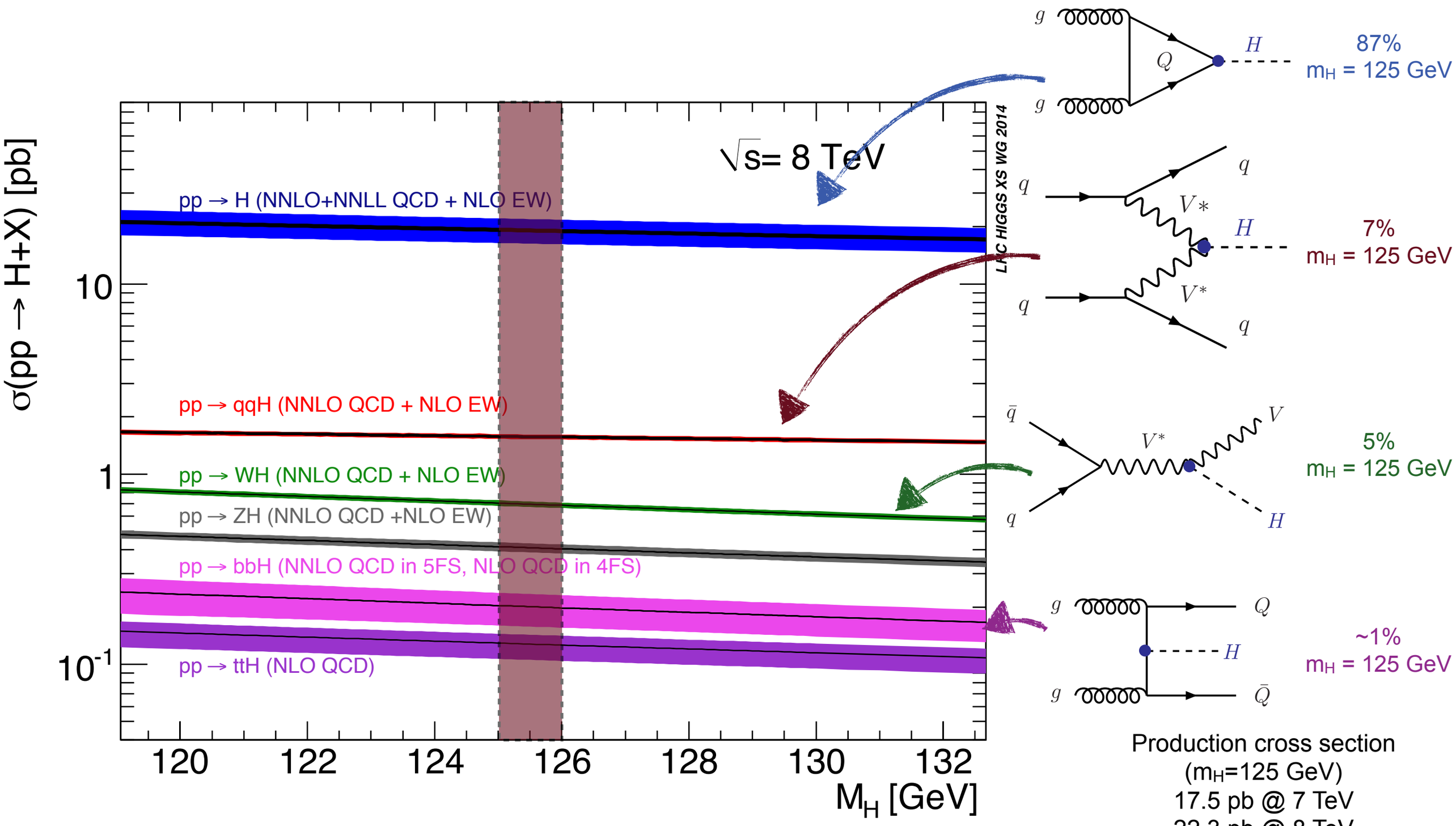

Production cross section
(m_H=125 GeV)
17.5 pb @ 7 TeV
22.3 pb @ 8 TeV
50.9 pb @ 13 TeV
57.4 pb @ 14 TeV

SM Higgs boson decays

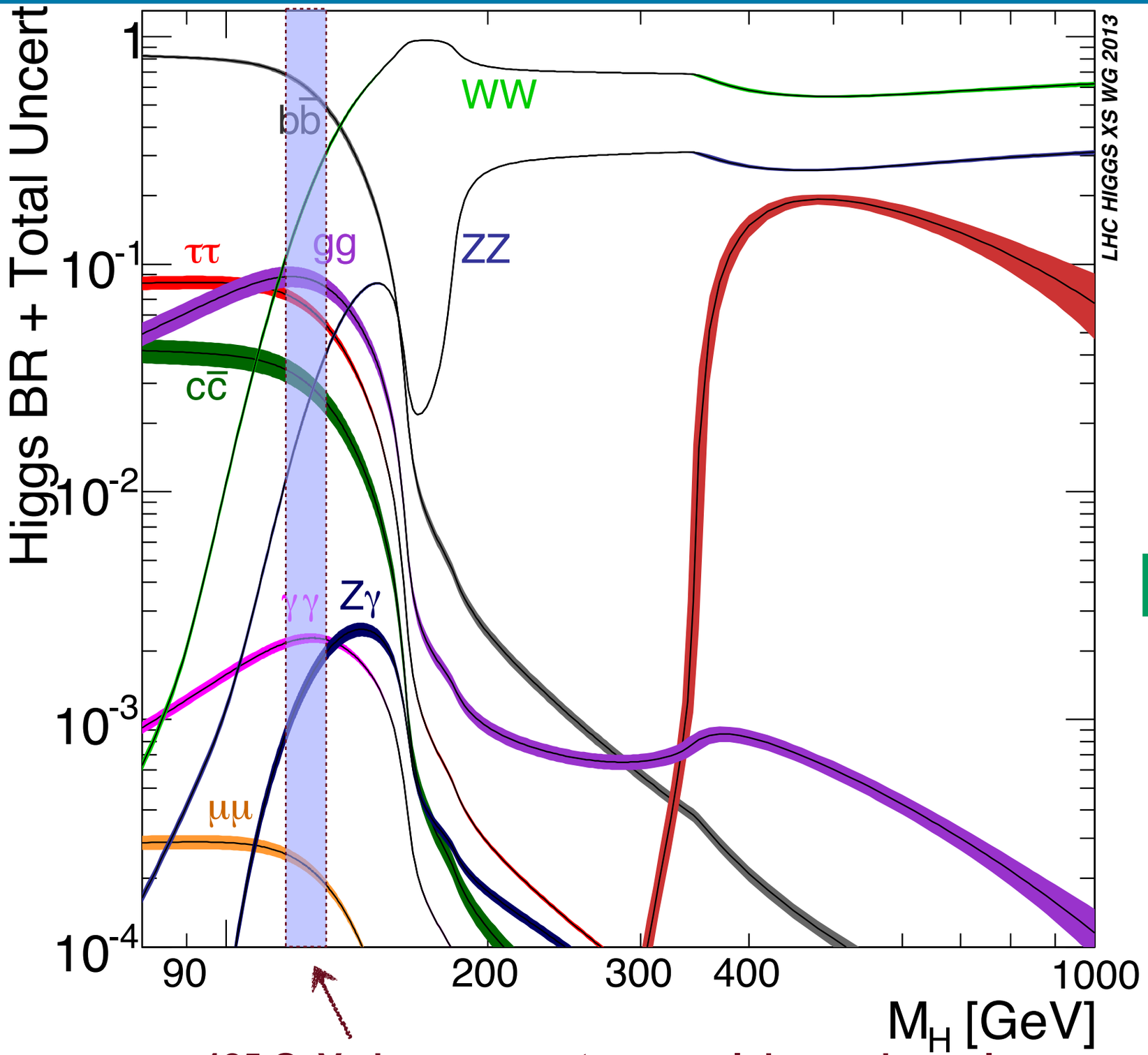

m_H~125 GeV gives access to several decay channels
Gauge bosons: γγ, ZZ*, WW*, Zγ
Fermions: bb, ττ, μμ

This talk will focus on bosonic decays

H→γγ

H→ZZ→4l

H→WW→lνlν

H→Zγ→llγ

with emphasis on most recent results

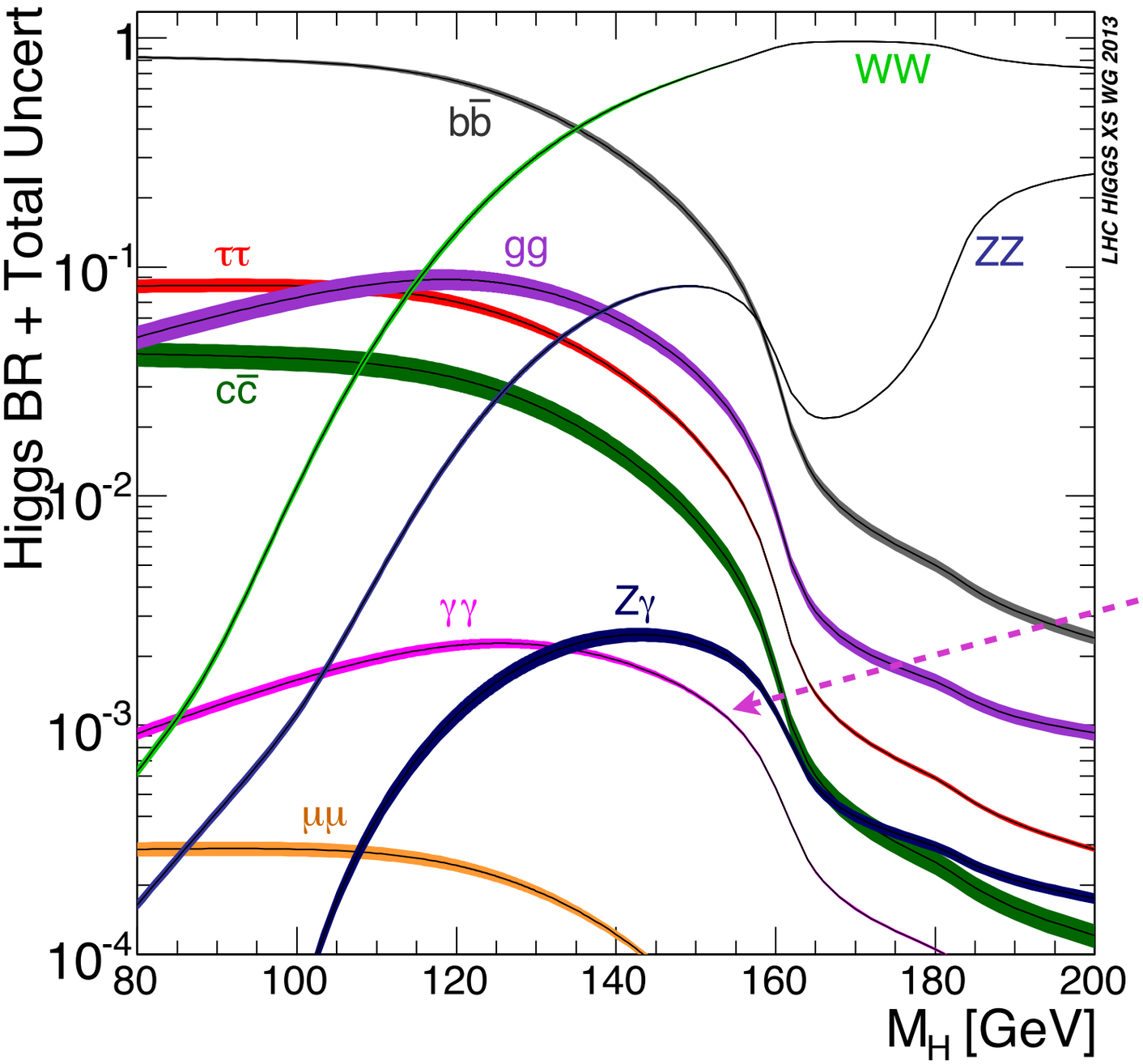

H→γγ

Mass Measurement: arXiv:1406.3827 accepted by PRD

Couplings: Phys. Lett. B726 (2013) 88/ATLAS-CONF-2013-012

Differential Cross-Sections: arXiv:1407.4222 submitted to JHEP

Spin/CP: Phys. Lett. B726 (2013) 120

H→γγ: Updated m_H Analysis

- Narrow peak in $m_{\gamma\gamma}$ spectrum
  - inclusive S/B ~ 3-4%
- Main Backgrounds:
  ~80% di-photon → $m_{\gamma\gamma}$ resolution [~1.7 GeV]
  ~20% γj and jj → photon-ID
- Background directly from data side-bands
- Event Selection:
  → Two isolated photons ($|\eta|<2.47$) with $E_T>0.35(0.25)*m_{\gamma\gamma}$
- m_H optimized categories [min expected δm_H for SM Higgs inc. systematics]
  → New e/γ calibration (~10% resolution imrpovement)
  → Photon quality, detector region and p_{Tt}
  → 10 exclusive categories

NEW!

Updated coupling analysis to appear

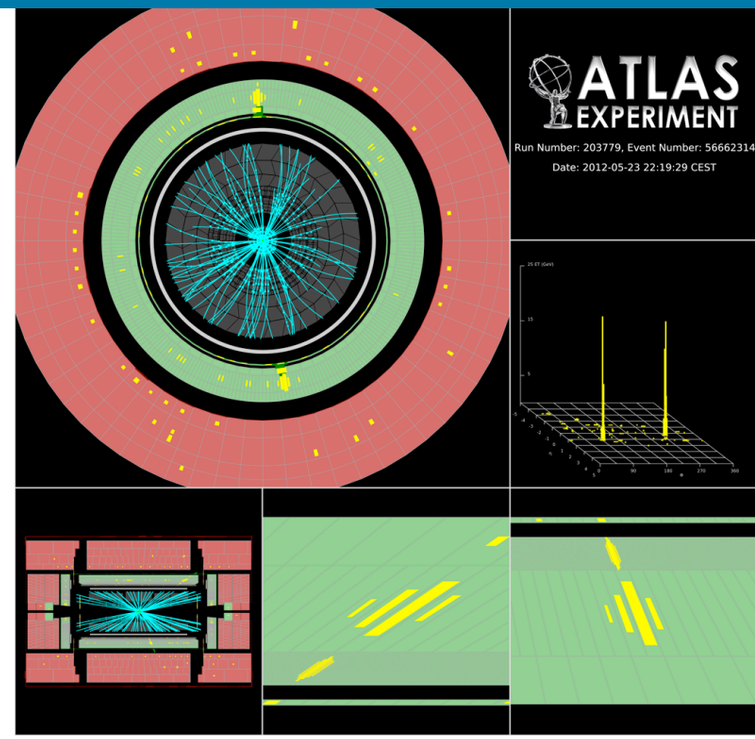

See Cyril's talk

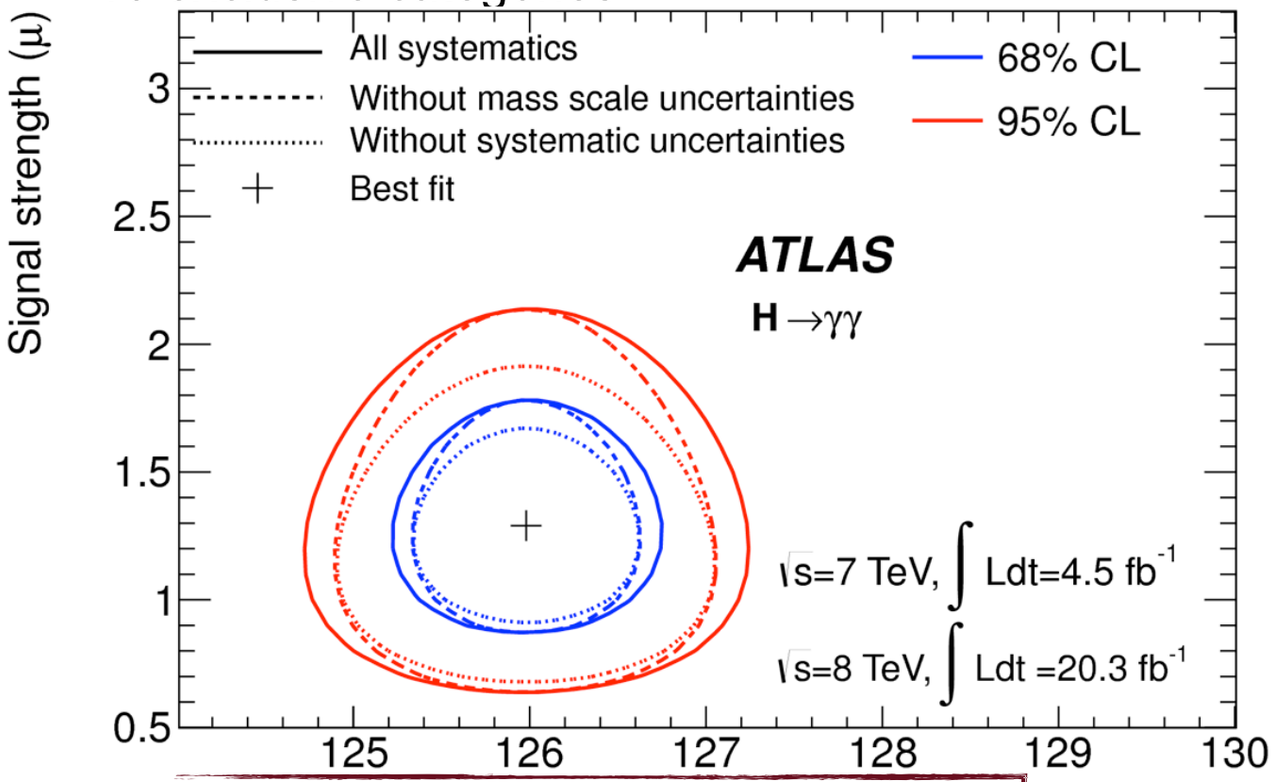

m_H=125.98 ± 0.42(stat) ± 0.28(syst) GeV
μ = 1.29 ± 0.30

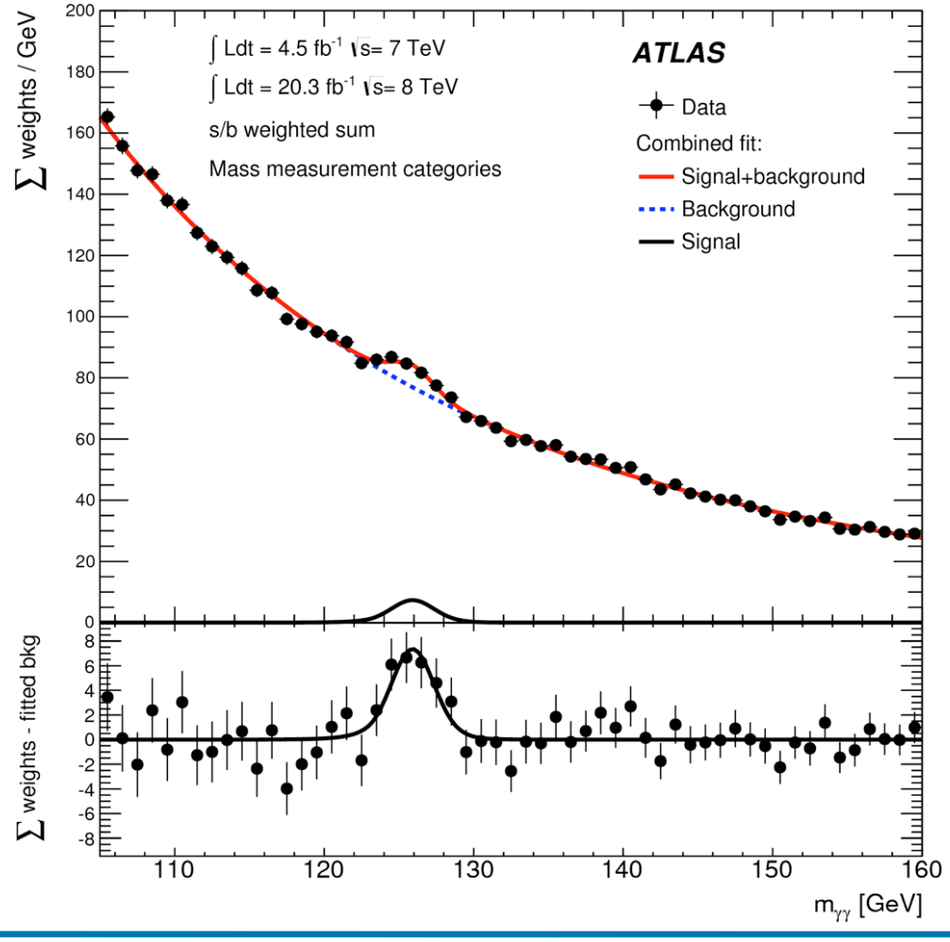

H→γγ: Fiducial/Differential cross sections

5 measurements + 2 upper limits on fiducial cross sections

NEW!

12 differential cross sections
a) kinematics ($pT_{\gamma\gamma}$,$|y_{\gamma\gamma}|$)
b) associated jet activity (Nj, $|y_j|$, ...)
c) spin-CP-sensitive ($|\cos\theta^*|$, ...)
d) VBF-sensitive ($|\Delta y_{jj}|$,...)

Procedure:
- $m_{\gamma\gamma}$ ML fit simultaneously in bins of variable of interest
- bin-by-bin unfolding (A, ε, resolution)

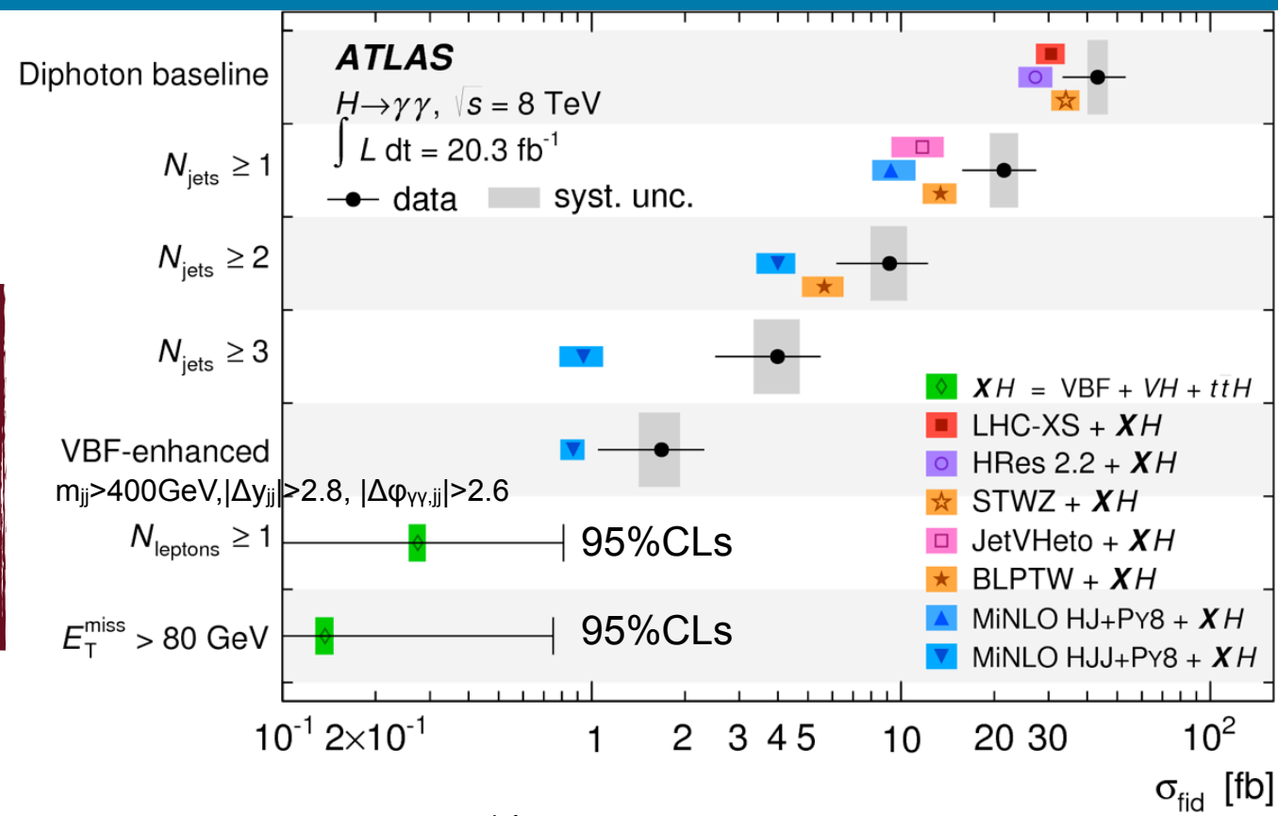

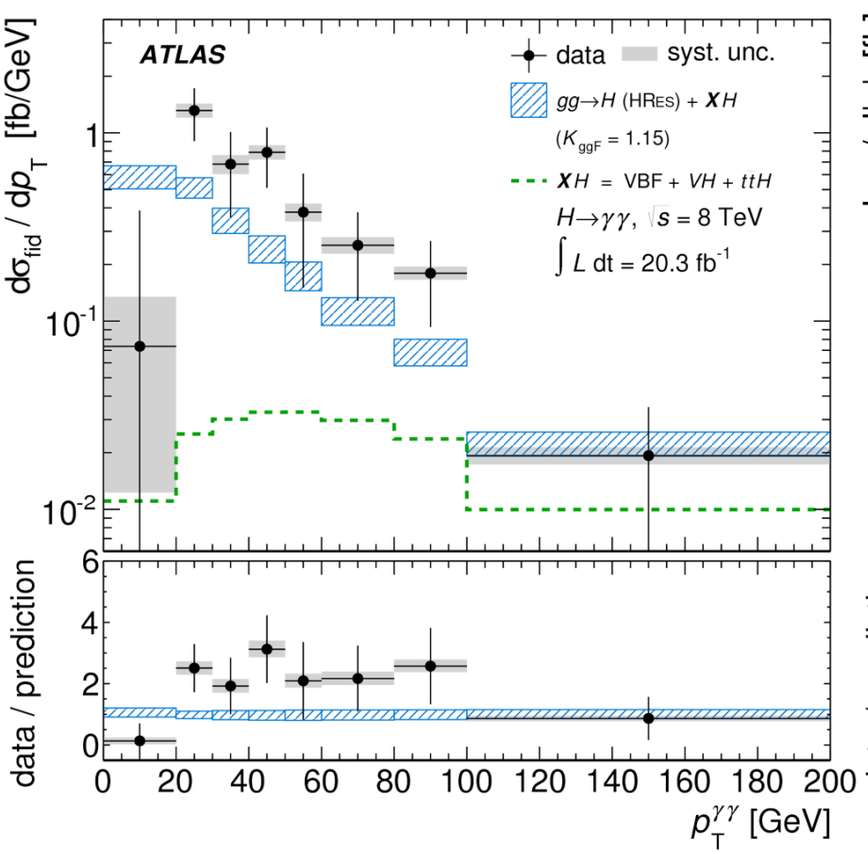

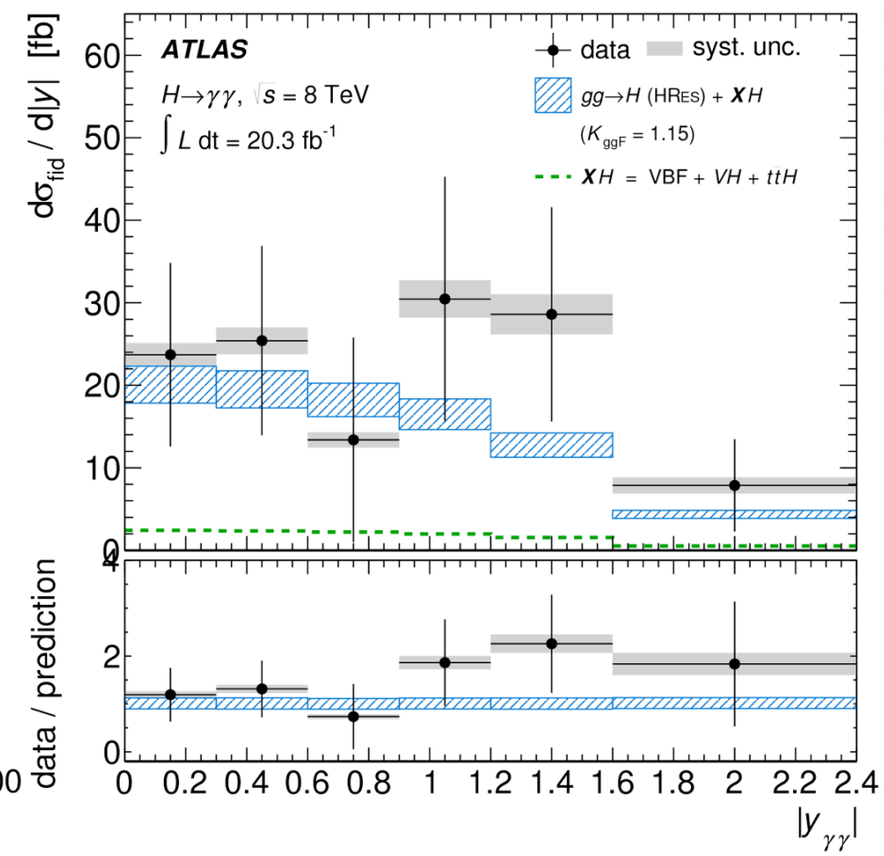

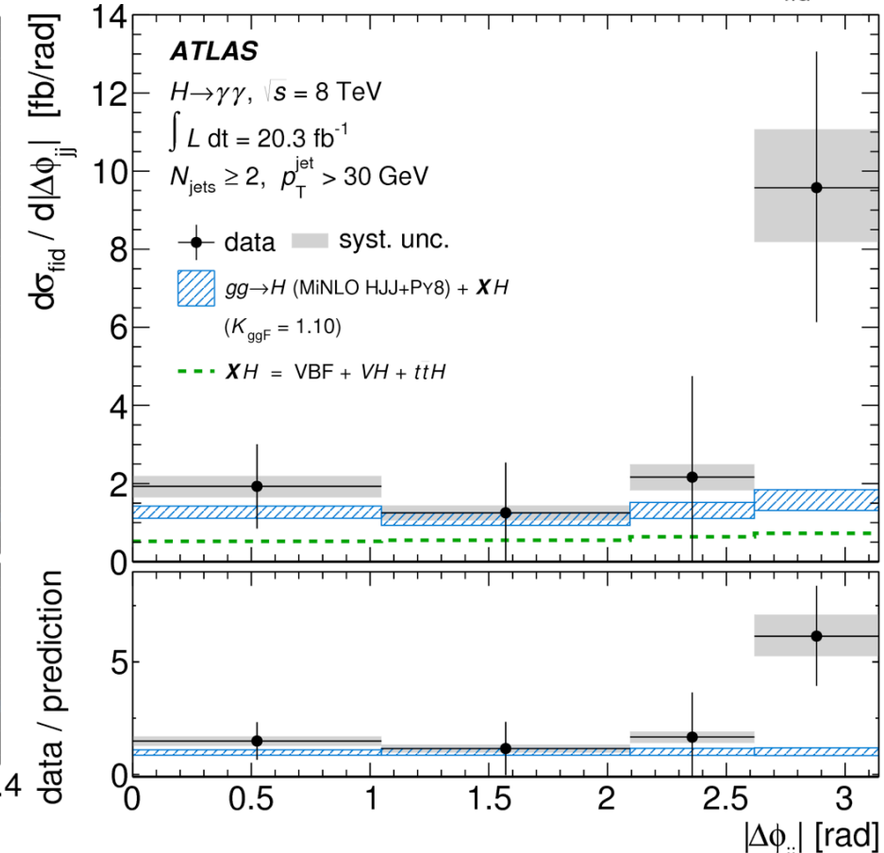

H→γγ: Fiducial/Differential cross sections

NEW!

Overall good data/ theory agreement
Somewhat higher jet activity data

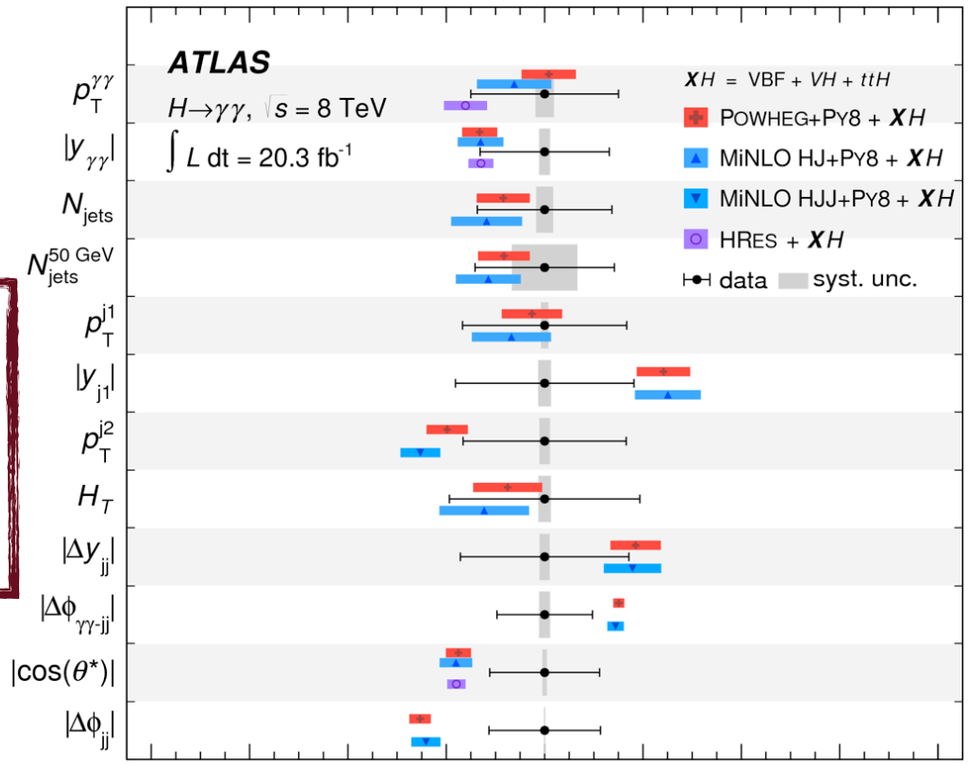

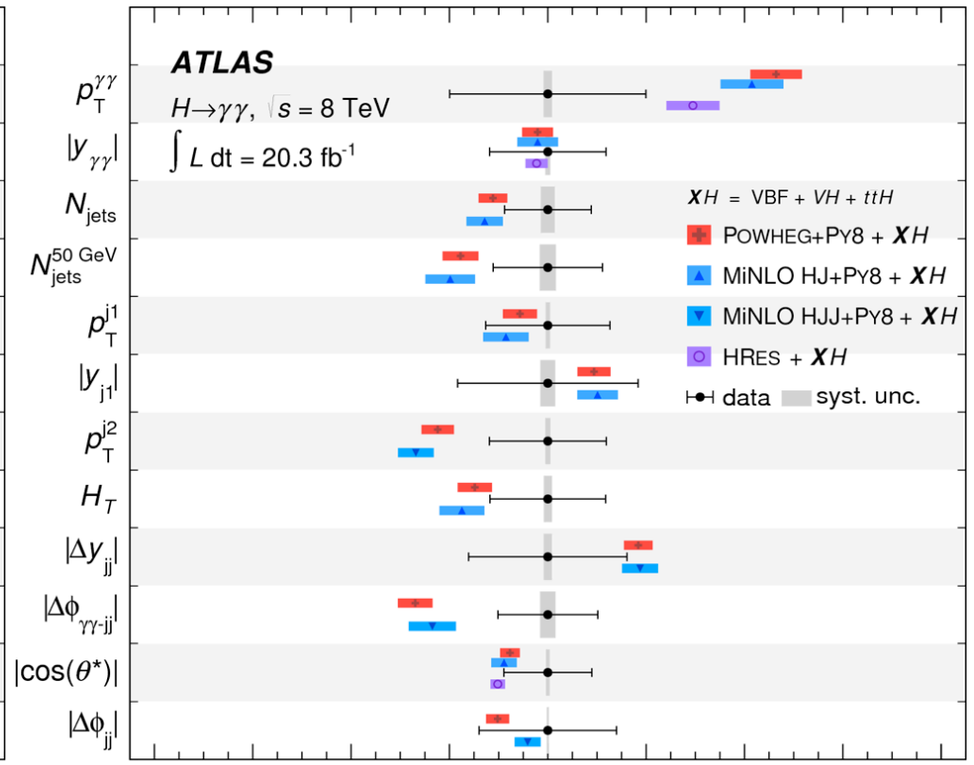

Variable	POWHEG	MINLO HJ	MINLO HJJ	HRES
$p_{\mathrm{T}}^{\gamma\gamma}$	0.12	0.10	0.09	0.12
$\lvert y_{\gamma\gamma}\rvert$	0.81	0.83	0.83	0.80
$\lvert\cos\theta^*\rvert$	0.59	0.57	0.58	0.56
N_{jets}	0.42	0.36	0.30	-
$N_{\mathrm{jets}}^{50\ \mathrm{GeV}}$	0.33	0.33	0.30	-
H_{T}	0.43	0.39	0.34	-
$p_{\mathrm{T}}^{j_1}$	0.84	0.82	0.79	-
$\lvert y_{j_1}\rvert$	0.64	0.58	0.51	-
$p_{\mathrm{T}}^{j_2}$	0.34	0.29	0.23	-
$\lvert\Delta\phi_{jj}\rvert$	0.21	0.28	0.24	-
$\lvert\Delta y_{jj}\rvert$	0.64	0.58	0.49	-
$\lvert\Delta\phi_{\gamma\gamma,jj}\rvert$	0.45	0.46	0.42	-

H→γγ a swiss army knife for Higgs boson studies:
- Search for associated top-H(→γγ) production.
- Search for FCNC Higgs boson decays.
See talk by Austin Basye
- Search for additional γγ resonances.
See talk by Ilya Tsukerman

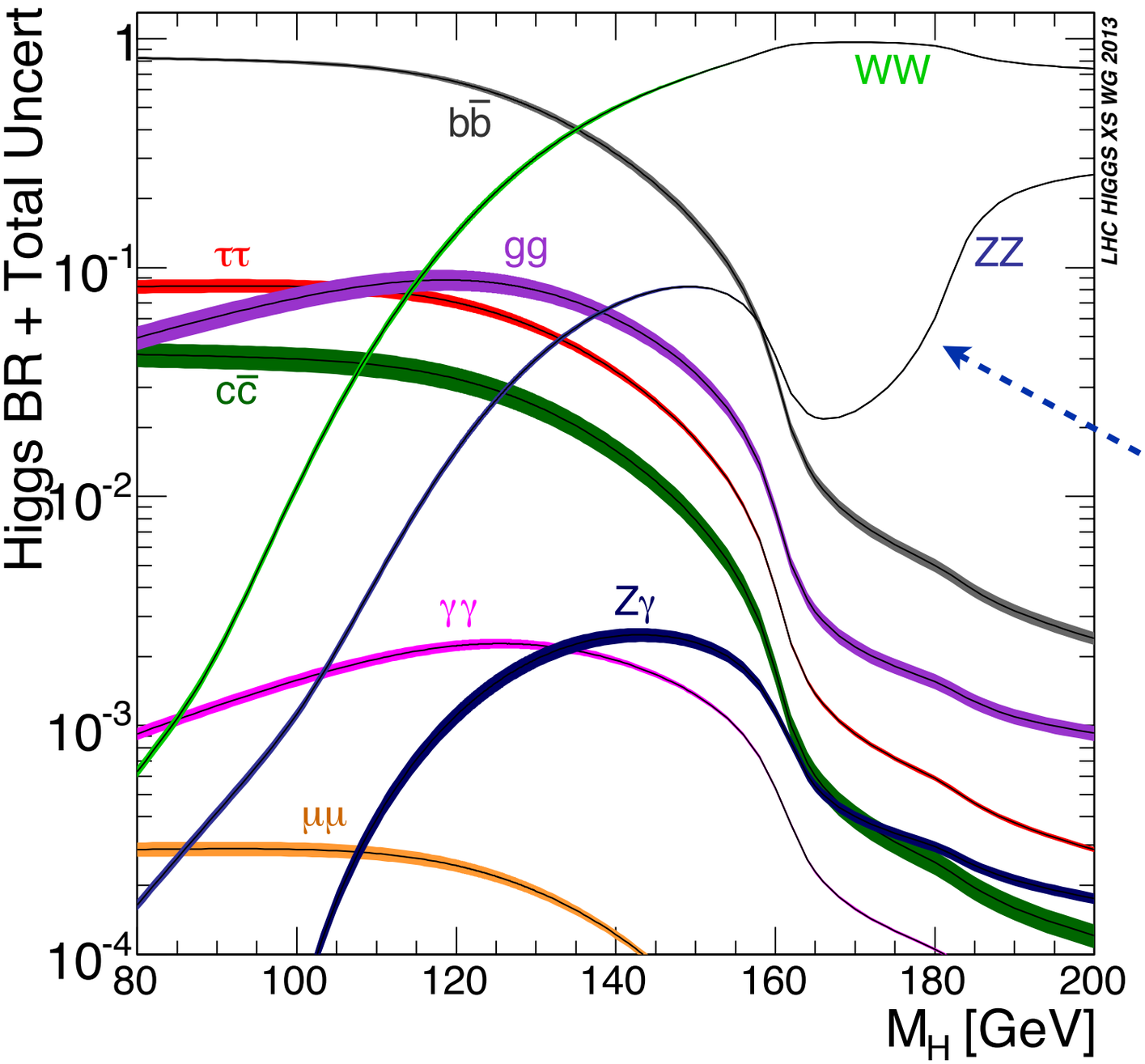

H→ZZ→4l

Mass Measurement: arXiv:1406.3827 accepted by PRD

Couplings: to be submitted to PRD

Differential Cross-Sections: ATLAS-CONF-2014-044

Spin/CP: Phys. Lett. B726 (2013) 120

Indirect Γ_H measurement: ATLAS-CONF-2014-042

$H \to ZZ^{(*)} \to 4l$: Updated Analysis

Search for peak in m_{4l} spectrum:
- S/B~1.4 - 1.7 @ m_H=125 GeV
- Mass resolution ~1.6-2.2 GeV

Backgrounds: $ZZ^{(*)} \to 4l$, Z+jets and ttbar

Event Selection
- Same-flavor opposite-sign isolated di-leptons (e/μ)
- Requirements on lepton pT, vertexing and m_{ll}

	Signal	$ZZ^{(*)}$	Other BKG	Observed	S/B
4μ	6.20±0.61	2.82±0.14	0.79±0.13	14	~1.7
2μ2e	3.15±0.32	1.38±0.08	0.72±0.12	6	~1.5
2e2μ	4.04±0.40	1.99±0.10	0.69±0.11	9	~1.5
4e	2.77±0.29	1.22±0.08	0.76±0.11	8	~1.4

120-130 GeV

New improved (MVA) electron identification! See Christopher's talk

New improved muon/electron calibration! See Cyril's talk

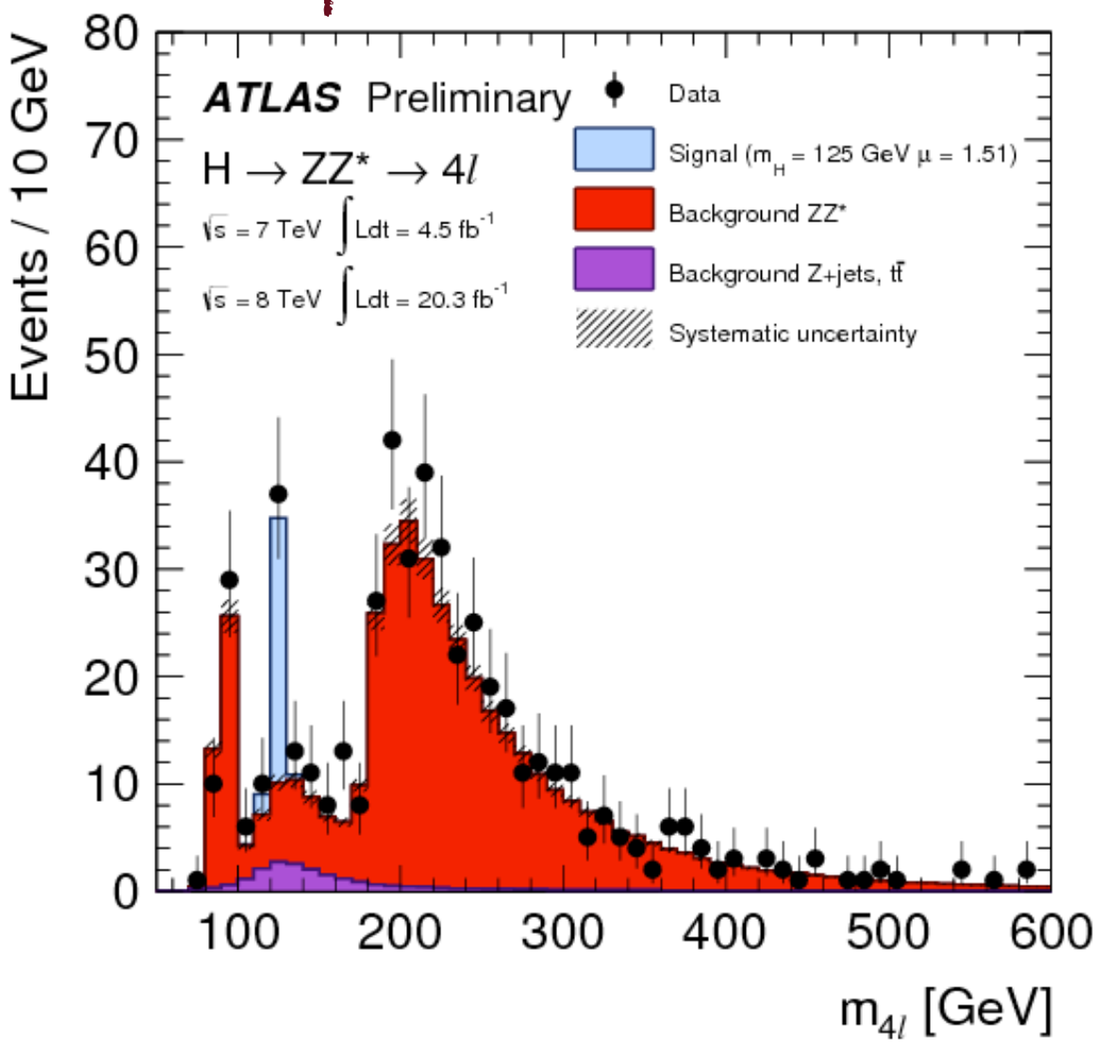

NEW!

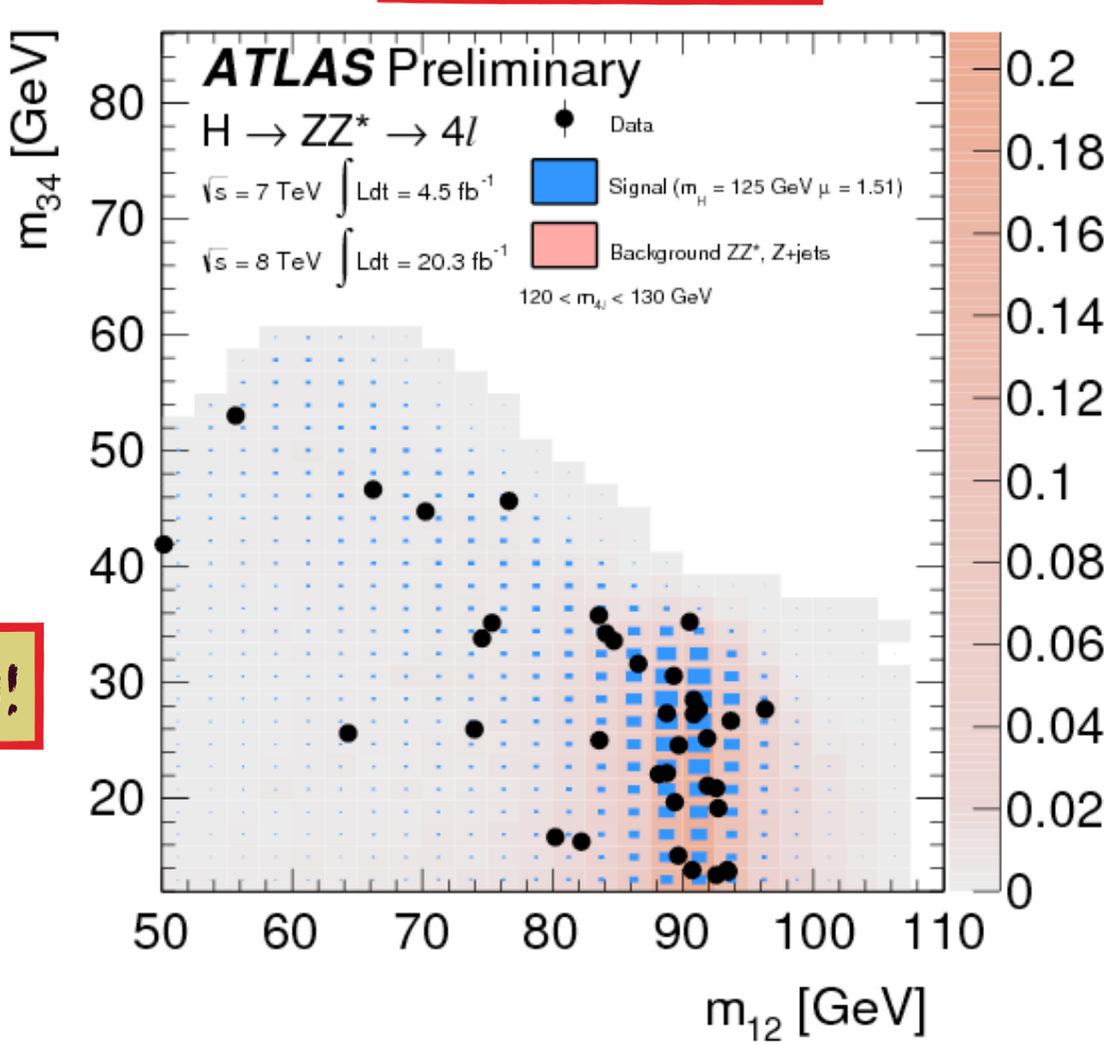

$H \to ZZ^{(*)} \to 4l$: ZZ* suppression

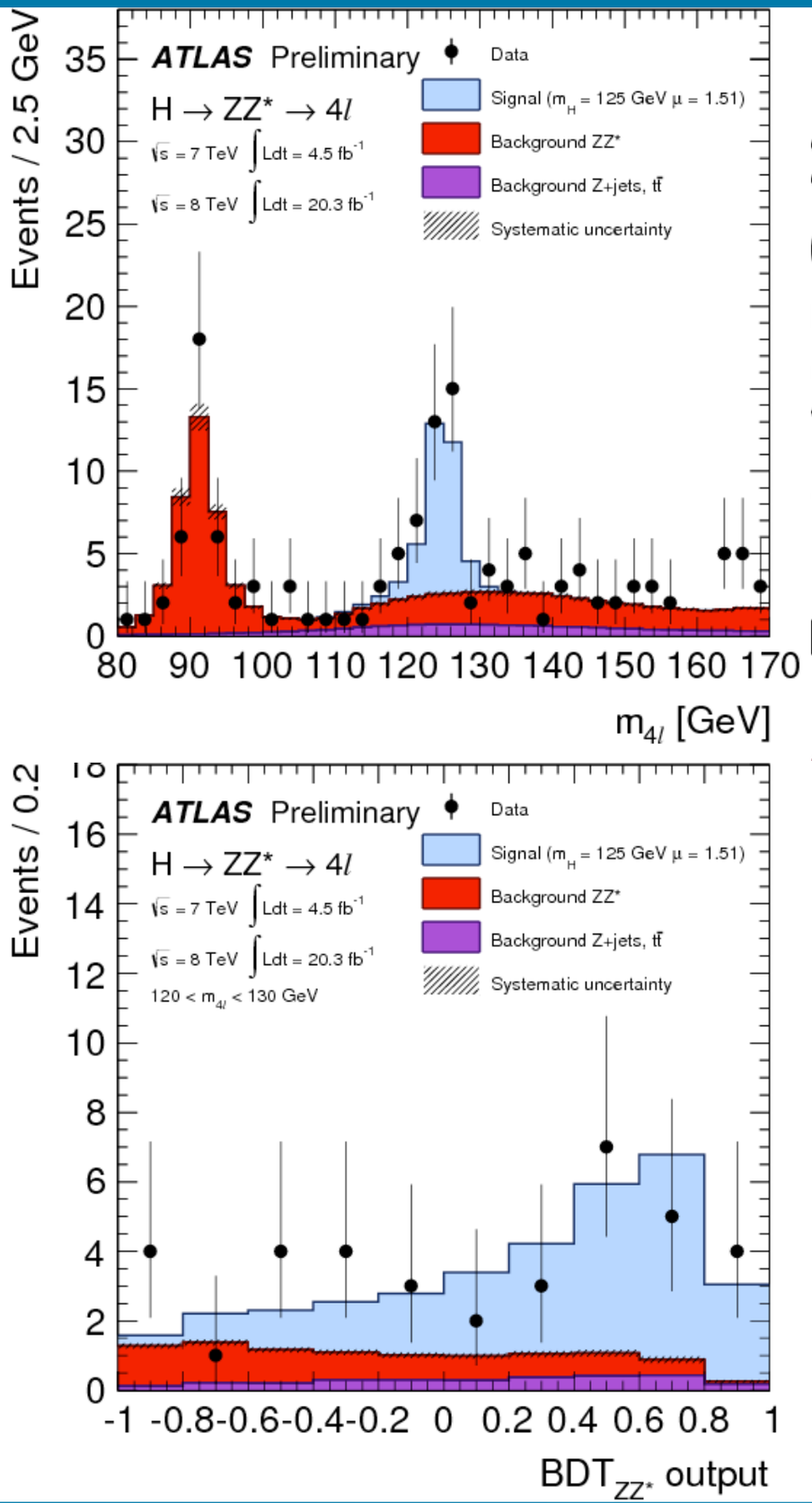

Introduced BDT discriminant to suppress ZZ* contribution

using Matrix Element Kinematic Discriminant, pT_{4l}, η_{4l}

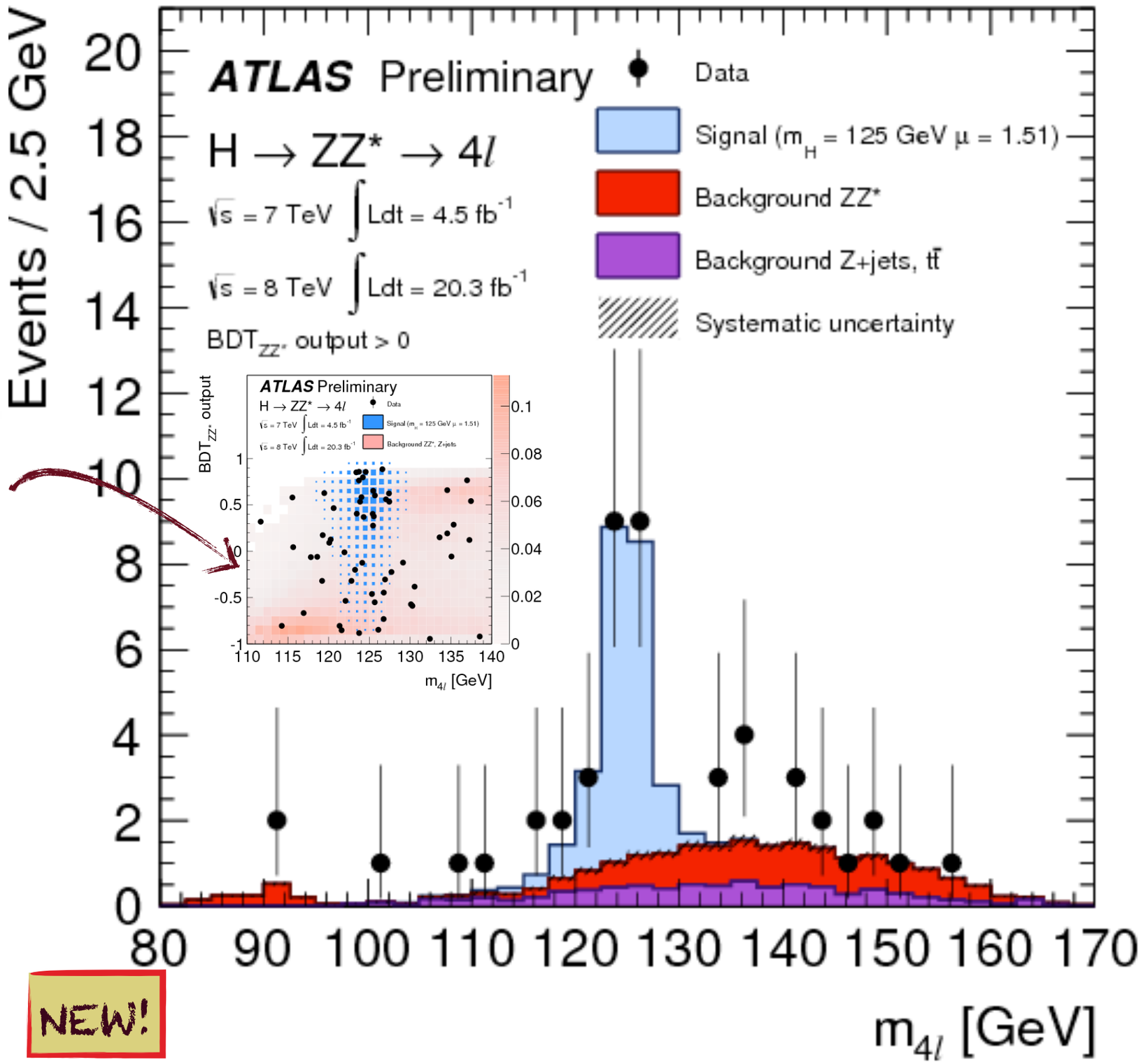

NEW!

$H \to ZZ^{(*)} \to 4l$: Inclusive Results

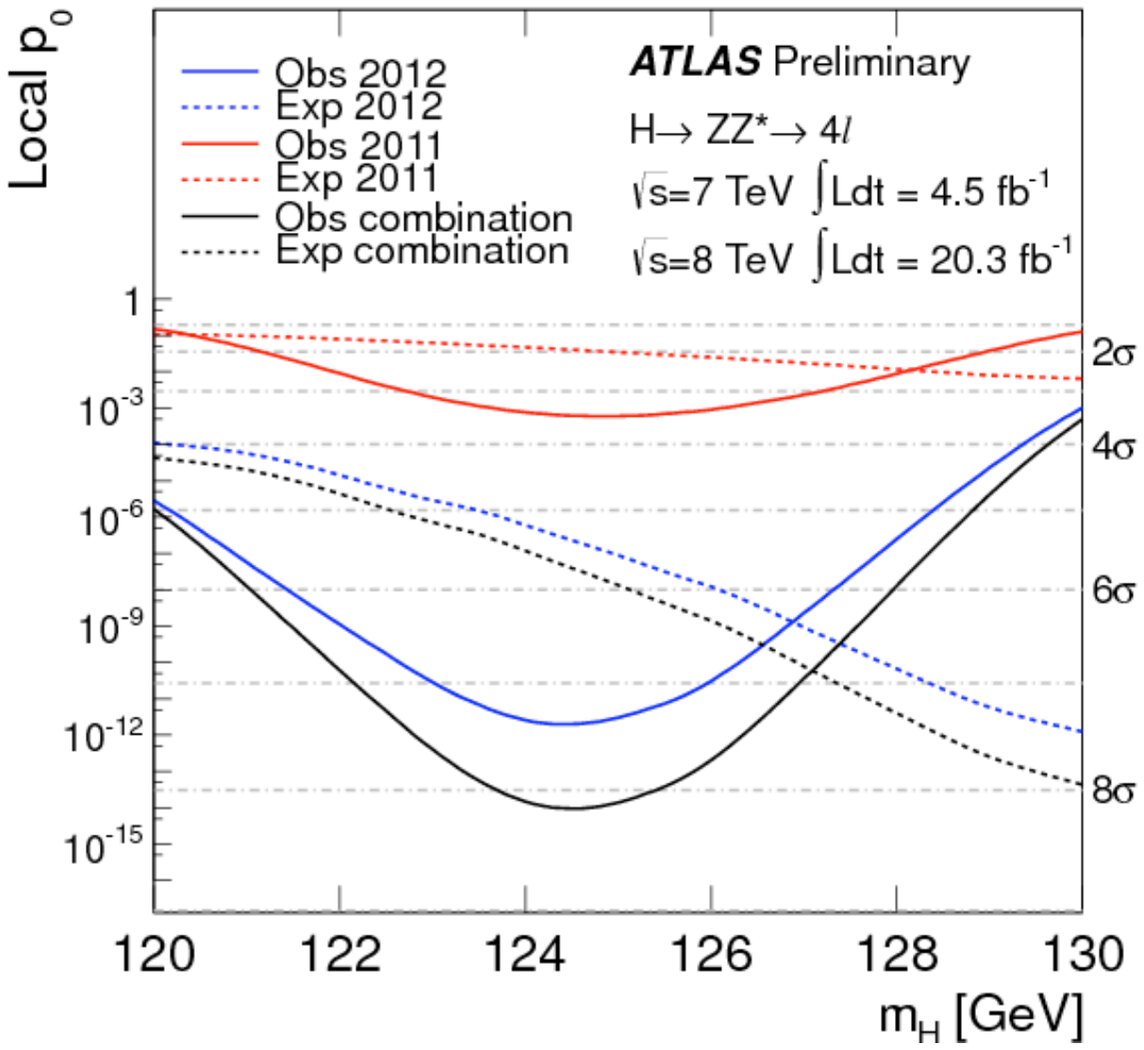

NEW!

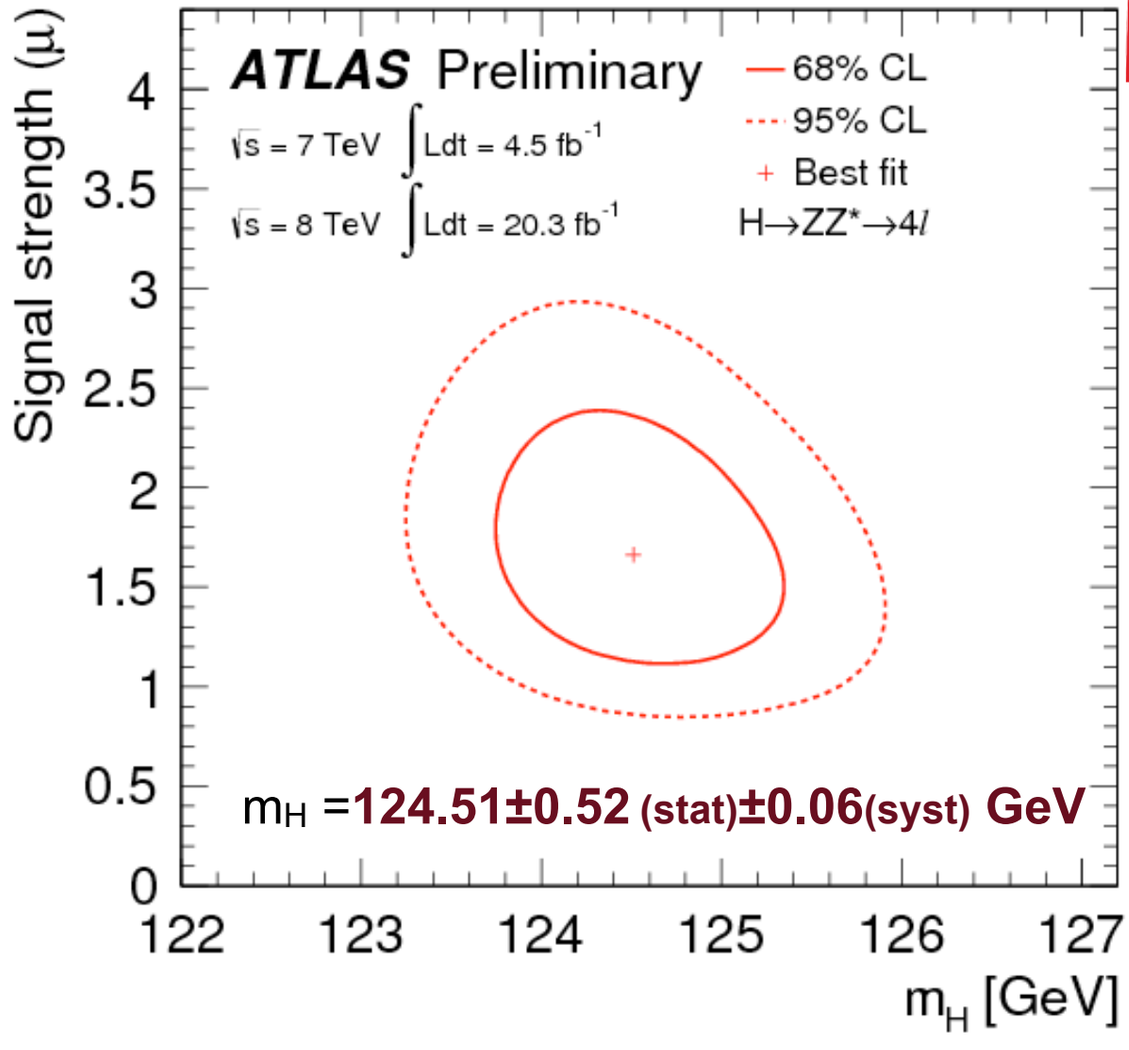

Maximum local significance: **8.2σ** (5.8σ)@ m_H=124.5GeV

For m_H = 125.36GeV

local significance: **8.1σ** (6.2σ)

and inclusive rate with respect to SM: **1.5 ± 0.4**

$H \to ZZ^{(*)} \to 4l$: Event Categorization

Event Categorization
-> probe production mechanisms

2D fit: (m_{4l},BDT_{VBF})

1D fit: m_{4l}
[selection using BDT_{VH}]

1D fit: m_{4l}

2D fit: (m_{4l},BDT_{ZZ})

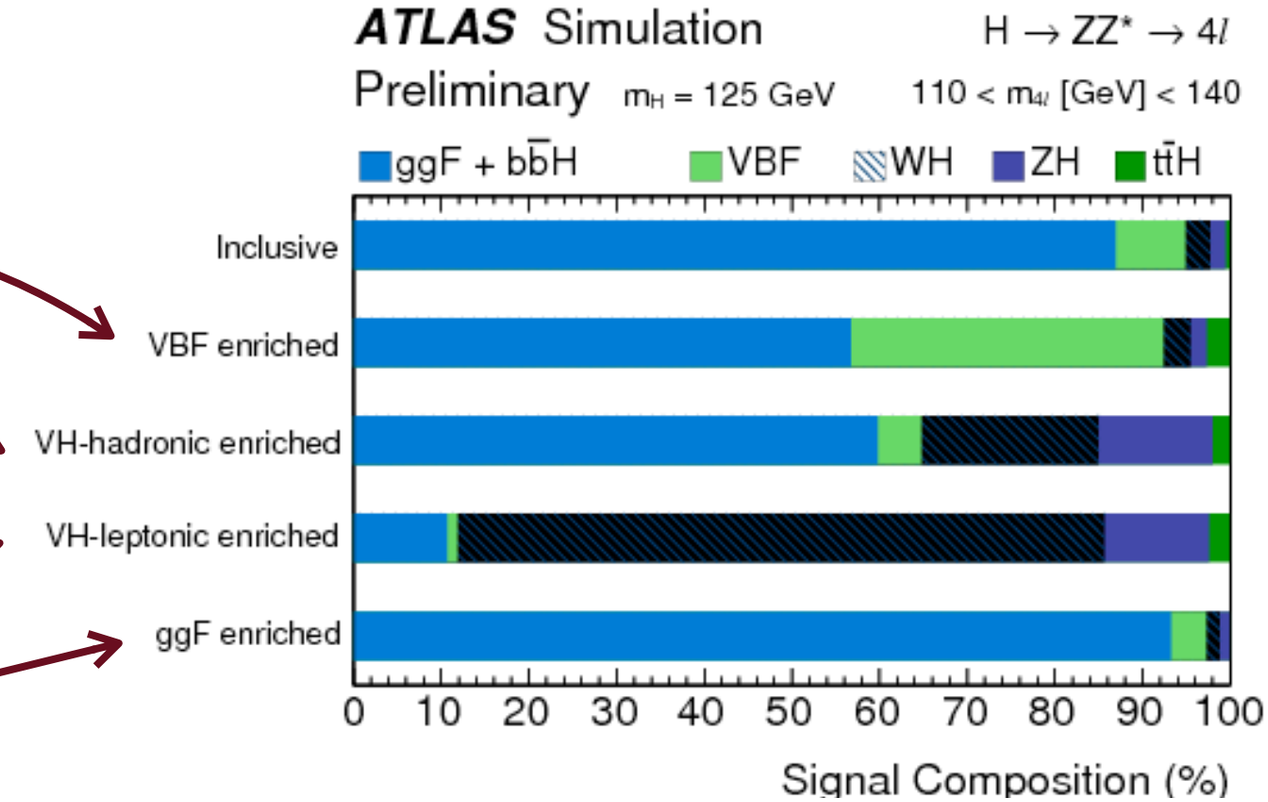

NEW!

$110 < m_{4l} < 140$ GeV
event yields
VBF-enriched: 5
VH-hadronic: 0
VH-leptonic: 0

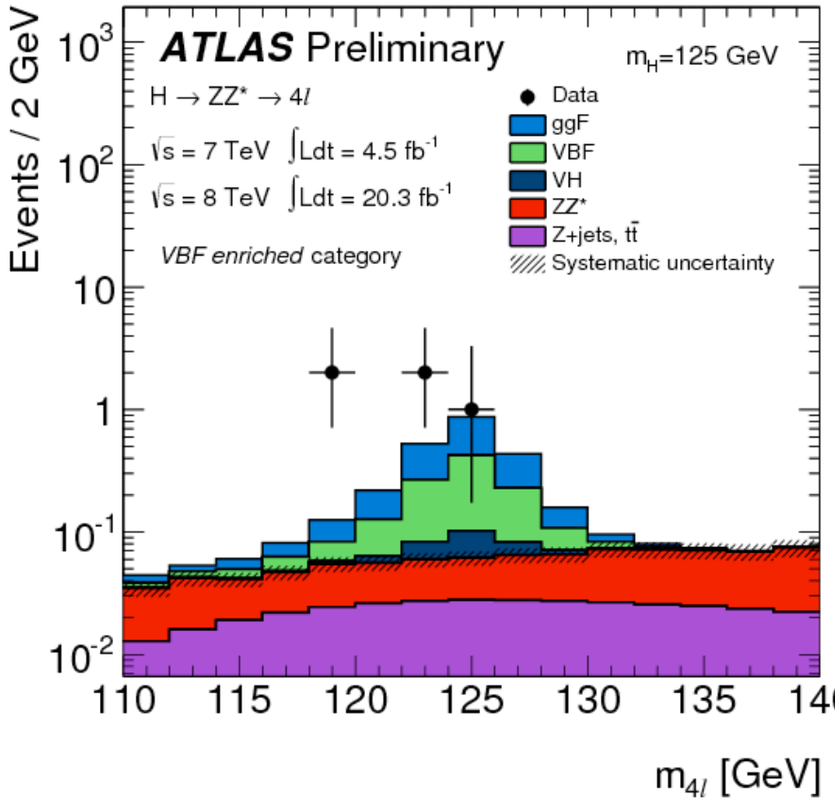

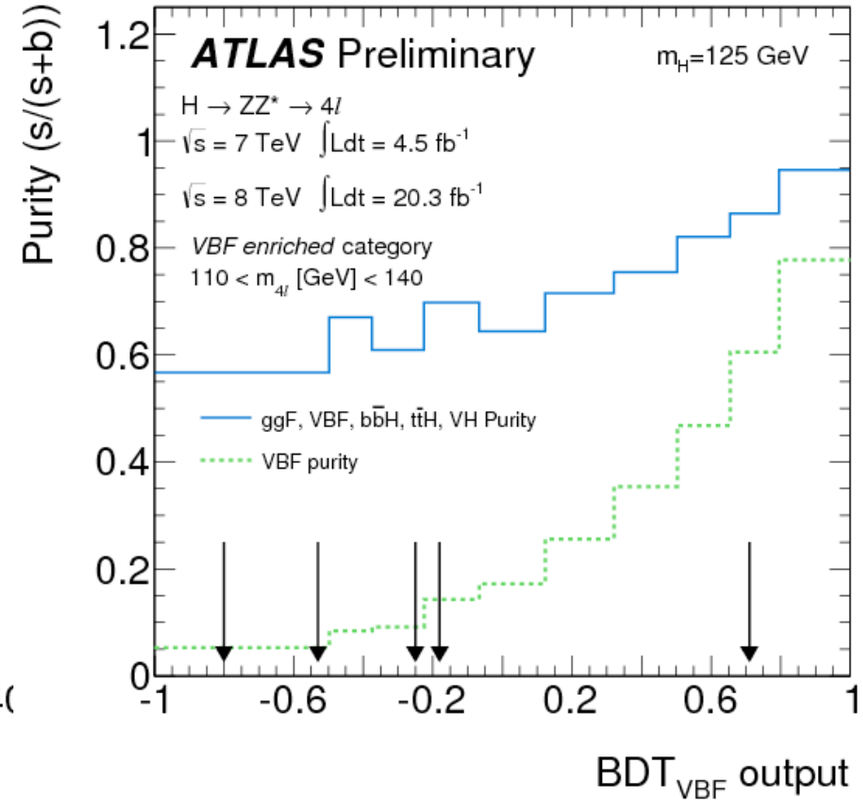

H→ZZ(*)→4l: Coupling Results

NEW!

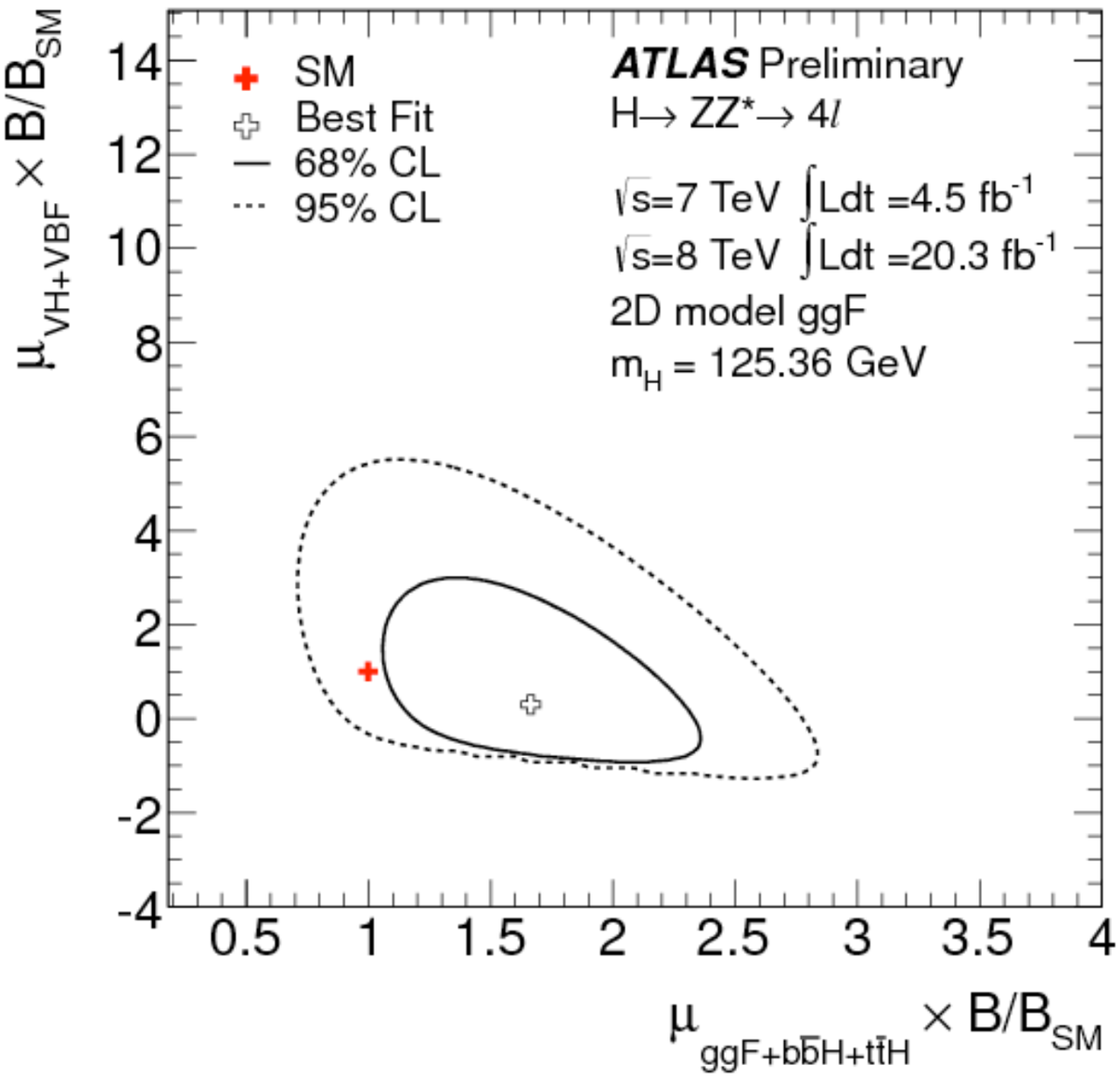

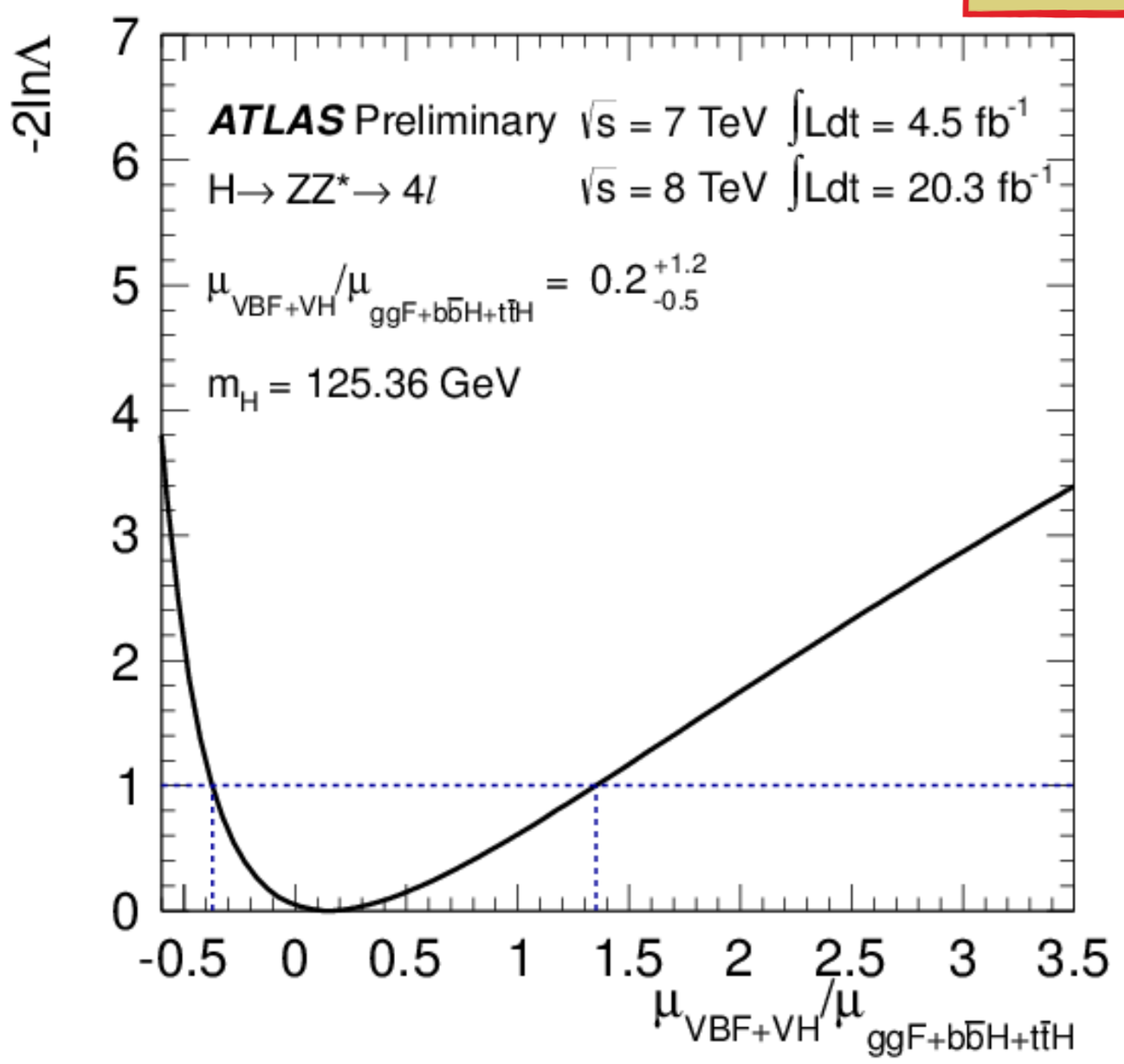

$\mu_{ggF+bbH+ttH} = 1.66^{+0.45}_{-0.41}(stat)^{+0.25}_{-0.15}(syst)$

$\mu_{VBF+VH} = 0.26^{+1.60}_{-0.91}(stat)^{+0.36}_{-0.23}(syst)$

$\mu_{VBF+VH}/\mu_{ggF+bbH+ttH} = 0.2^{+1.2}_{-0.5}$

$H \to ZZ^{(*)} \to 4l$: Fiducial/Differential cross sections

fiducial cross-section

6 differential cross sections

$$\sigma_{\text{tot}}^{\text{fid}} = 2.11^{+0.53}_{-0.47}(\text{stat})^{+0.08}_{-0.08}(\text{syst})\ \text{fb}$$

SM prediction at 125.4GeV = 1.30 ± 0.13 fb

NEW!

Procedure ($120 < m_{4l} < 130$ GeV):
- expected background subtracted from observed events in bins of interesting variable
- bin-by-bin unfolding

	p-values		
Variable	POWHEG	MINLO	HRES2
$p_{T,H}$	0.30	0.23	0.16
$\lvert y_H \rvert$	0.37	0.45	0.36
m_{34}	0.48	0.60	-
$\lvert \cos\theta^* \rvert$	0.35	0.45	-
n_{jets}	0.37	0.28	-
$p_{\text{T}}^{\text{jet}}$	0.33	0.26	-

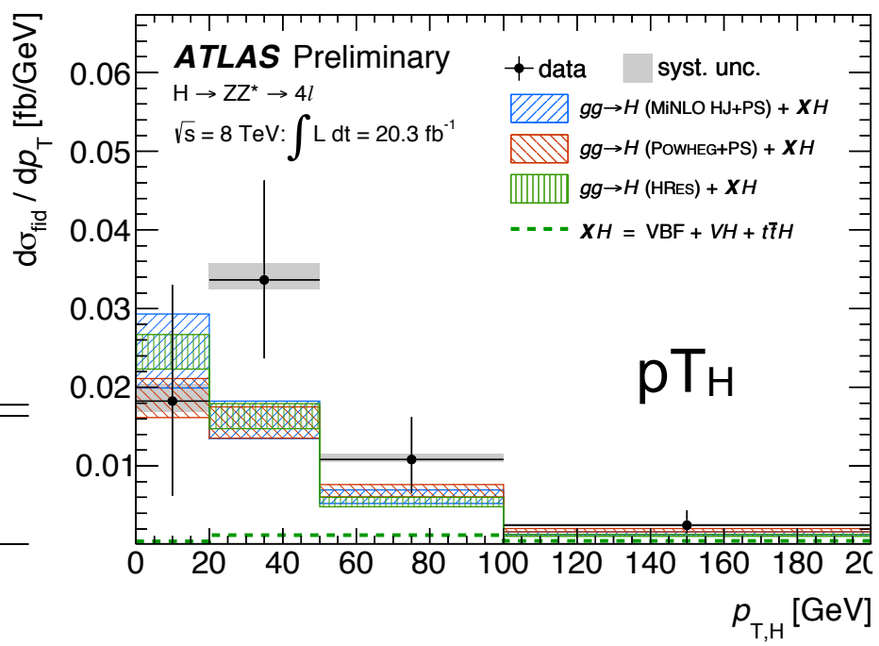

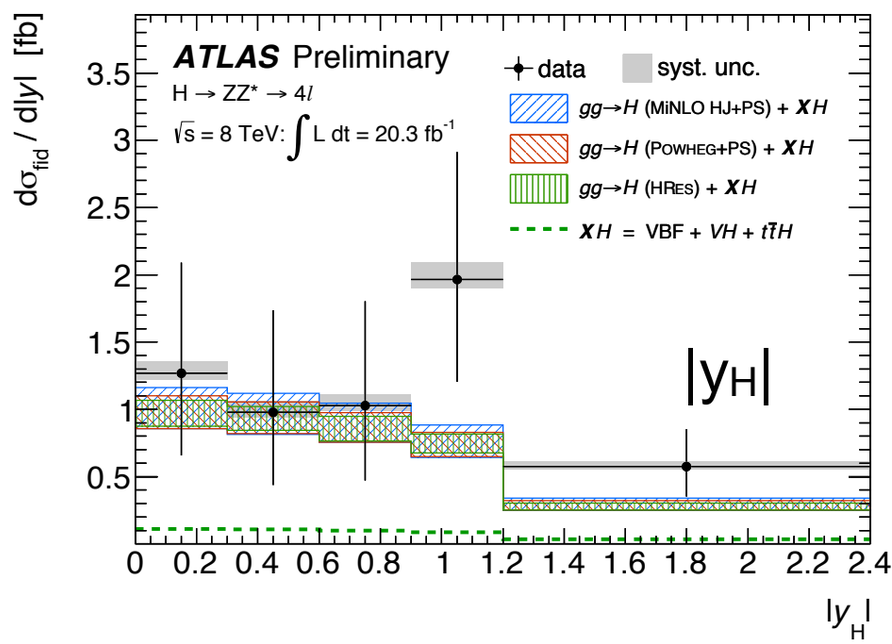

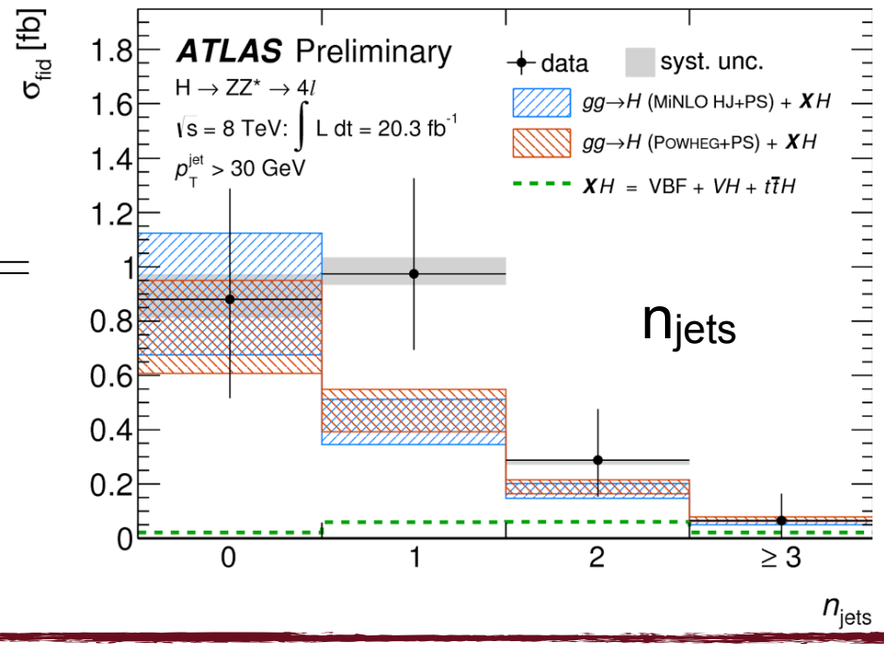

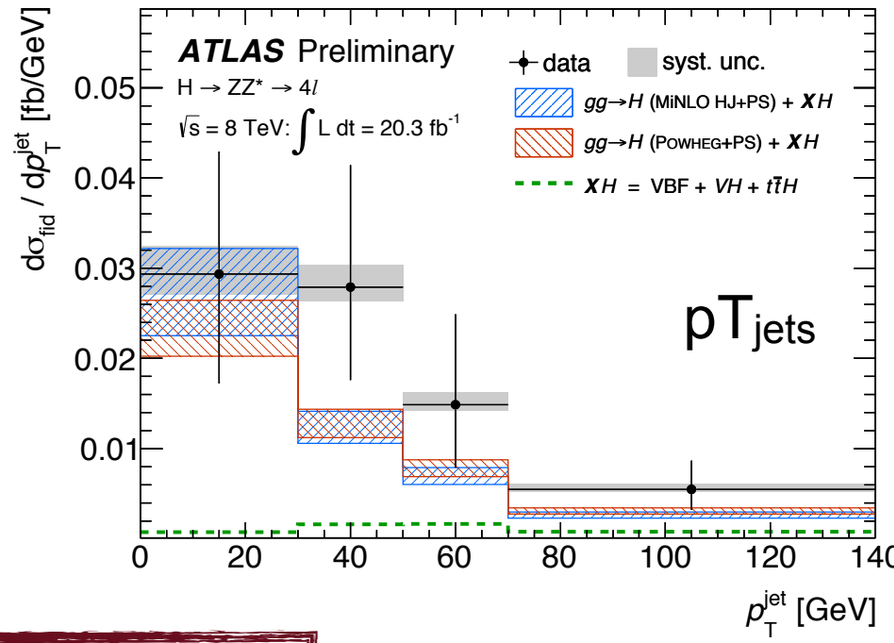

First result/statistics limited →No large surprise

$H\to ZZ^{(*)}\to 4l$/$H\to\gamma\gamma$: m_H and Γ_H measurement

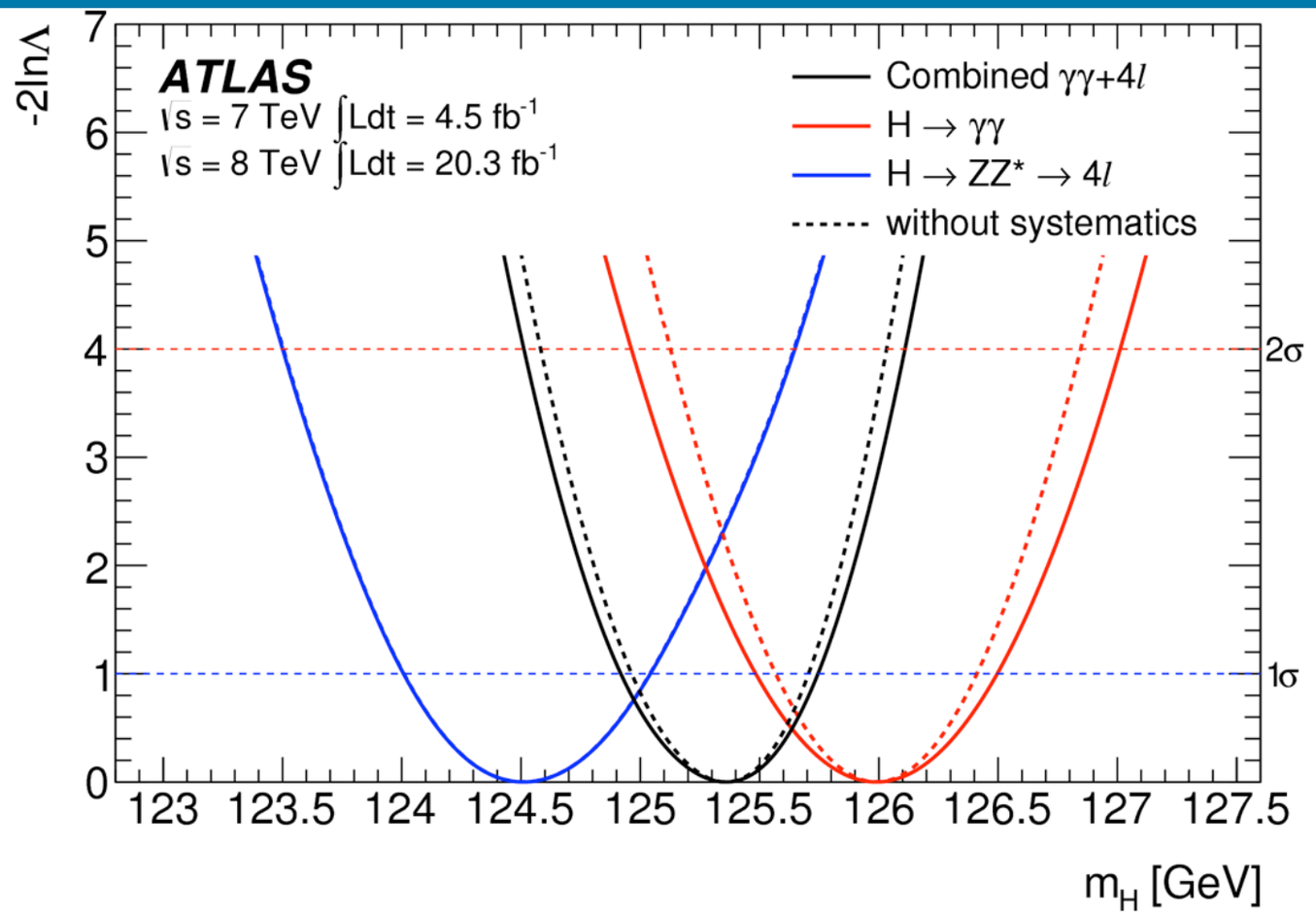

Channel	Mass measurement [GeV]
$H\to\gamma\gamma$	$125.98 \pm 0.42\,(\text{stat}) \pm 0.28\,(\text{syst}) = 125.98 \pm 0.50$
$H\to ZZ^*\to 4\ell$	$124.51 \pm 0.52\,(\text{stat}) \pm 0.06\,(\text{syst}) = 124.51 \pm 0.52$
Combined	$125.36 \pm 0.37\,(\text{stat}) \pm 0.18\,(\text{syst}) = 125.36 \pm 0.41$

H→4l/H→γγ compatibility: **1.97σ**
- fixing rates to SM expectation →1.6σ
- γ systematics as box →1.8σ

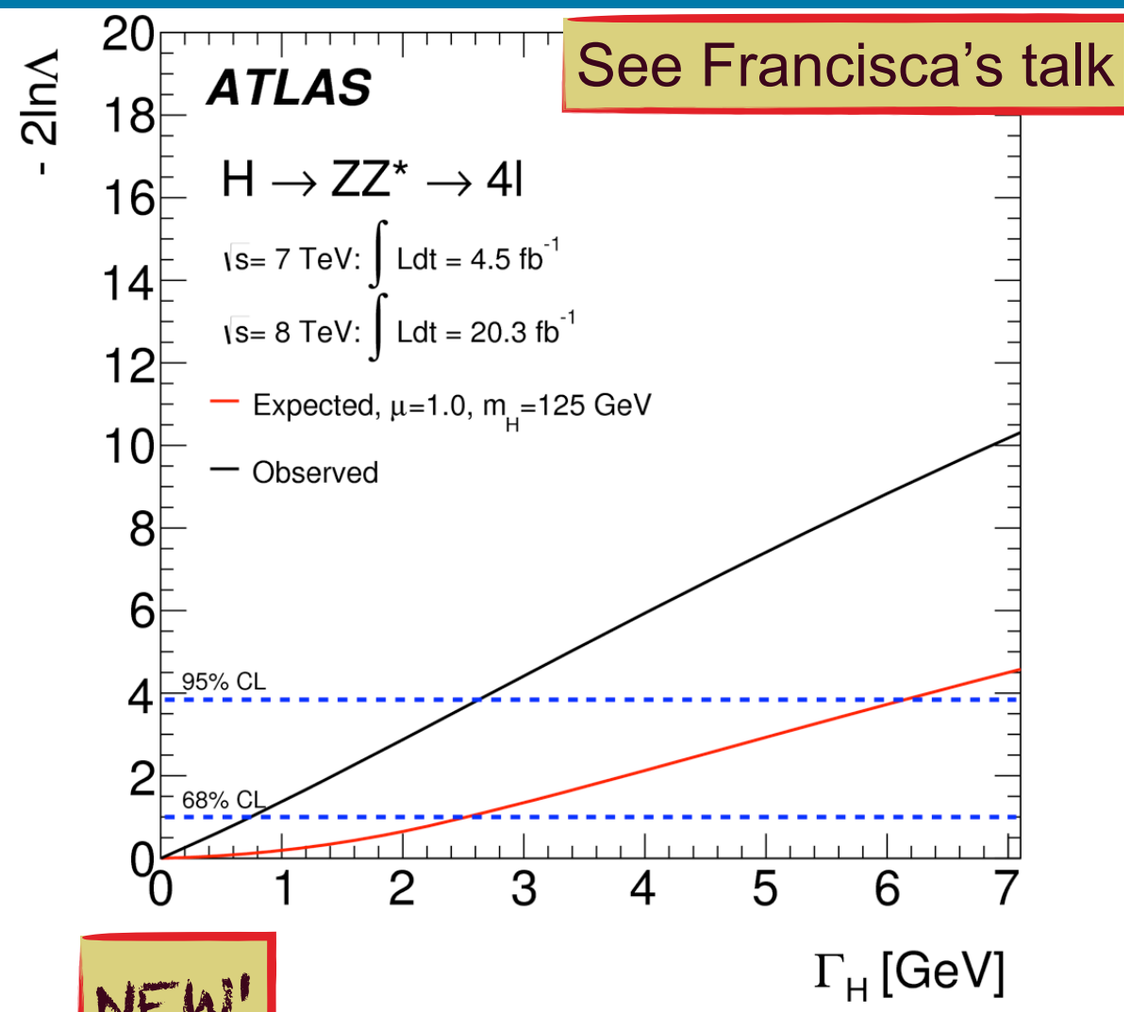

NEW!

H→ZZ→4l
- Event-by-event (detector response)⊗(H line-shape)
- Γ_H<2.6 (6.2@SM rate) GeV @ 95% CLs

H→γγ
- Non-relativistic Breit-Wigner ⊗ detector resolution
- Γ_H<5.0 (6.2@SM rate) GeV @ 95% CLs

Indirect Γ_H measurement: Introduction

Off-shell production of Higgs boson provides indirect constraint to Γ_H

$$\frac{\sigma^{gg\to H\to ZZ}_{\text{on-shell}}}{\sigma^{gg\to H\to ZZ}_{\text{on-shell, SM}}} = \mu_{\text{on-shell}} = \frac{\kappa^2_{g,\text{on-shell}} \cdot \kappa^2_{V,\text{on-shell}}}{\Gamma_H/\Gamma_H^{\text{SM}}}$$

$$\frac{\sigma^{gg\to H^*\to ZZ}_{\text{off-shell}}}{\sigma^{gg\to H^*\to ZZ}_{\text{off-shell, SM}}} = \mu_{\text{off-shell}} = \kappa^2_{g,\text{off-shell}} \cdot \kappa^2_{V,\text{off-shell}}$$

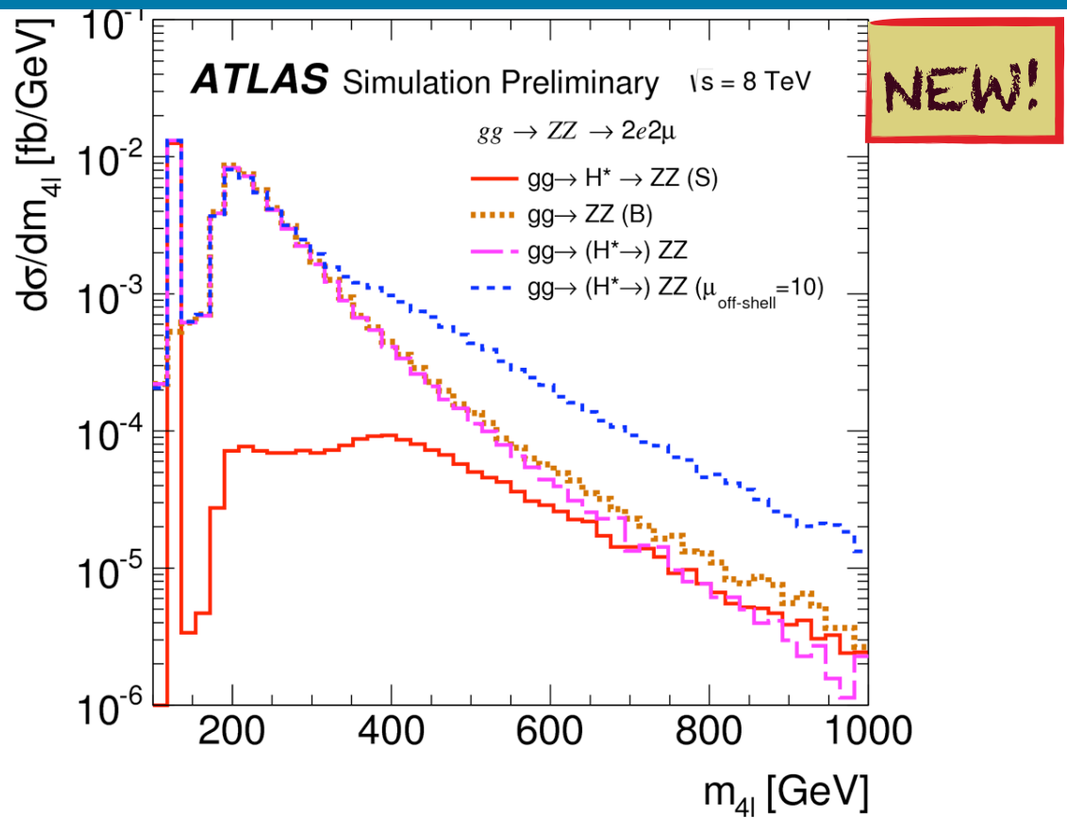

Implemented with H→ZZ with the following assumptions:

→ Backgrounds insensitive to new physics modifying off-shell couplings

→ Running of couplings similar for on-shell/off-shell region

→ Use inclusive selections [where HO corrections available]

→ gg→ZZ K-factors in off-shell region unknown

[for signal known to NNLO, gg→WW at NLO indicates that K-factors may be of similar magnitude, see later]

Similar assumptions to the one used for the coupling studies with the κ-factor framework

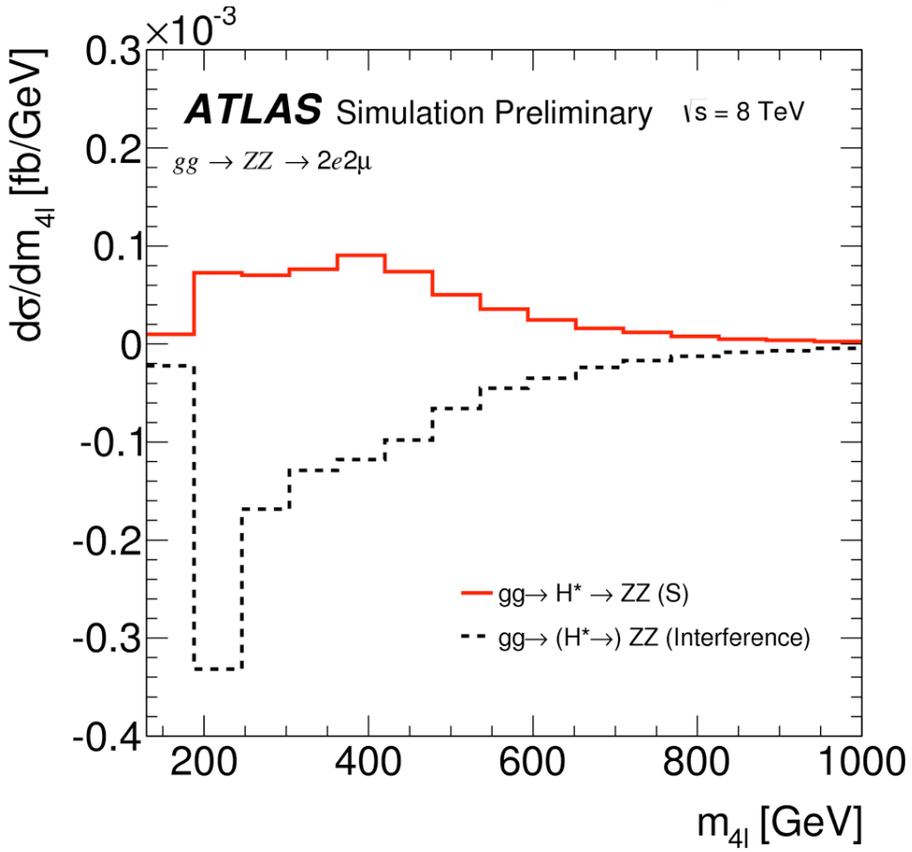

Indirect Γ_H measurement: Analysis

ZZ→4l
- Off-peak region [220 GeV, 1TeV]
- Matrix Element Kinematic Discriminant to separate gg→H*→ZZ→4l from qq→ZZ→4l/ gg→(H*)→ZZ→4l
- Limit on off-shell rate based on fit on MEKD shape

NEW!

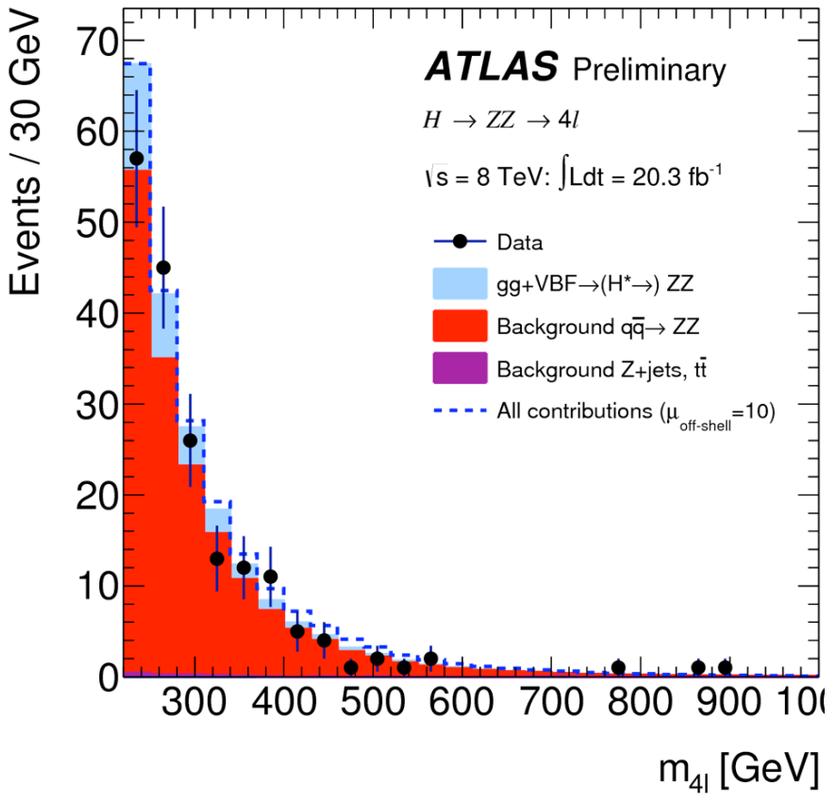

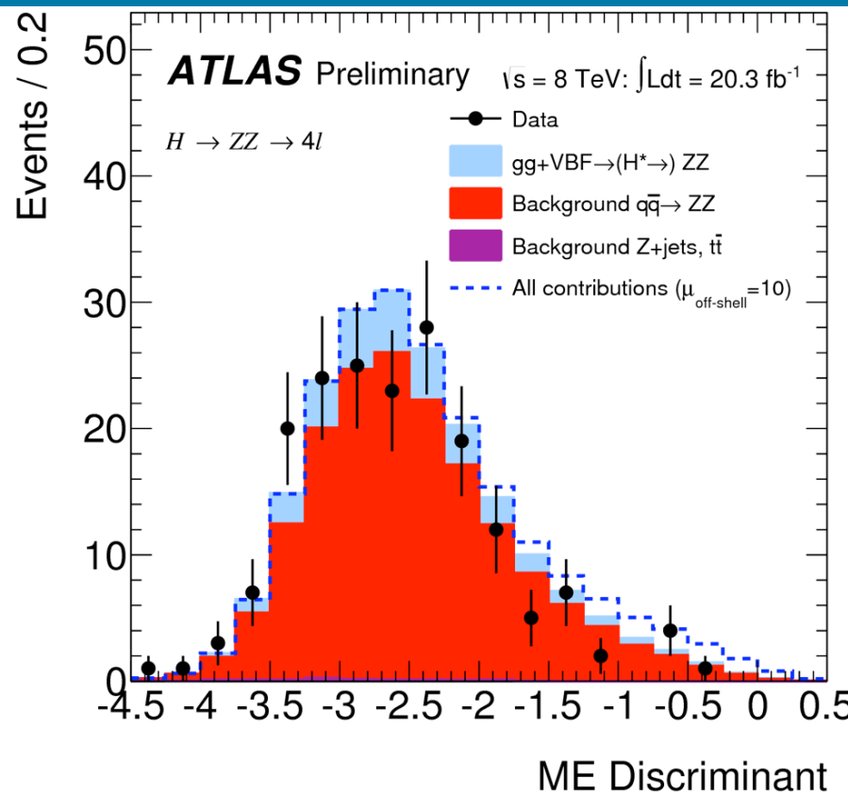

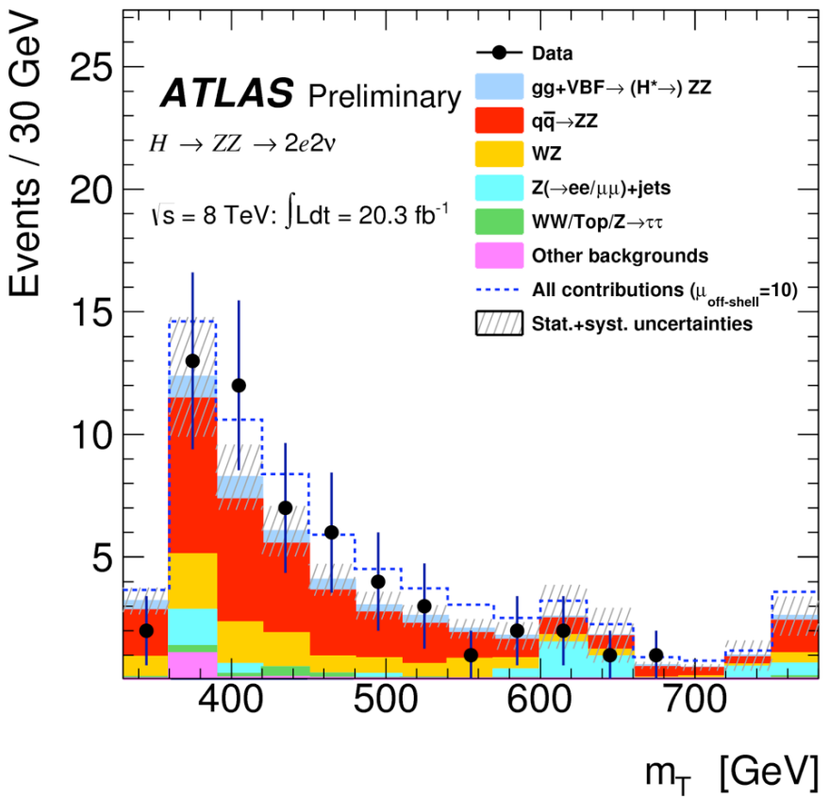

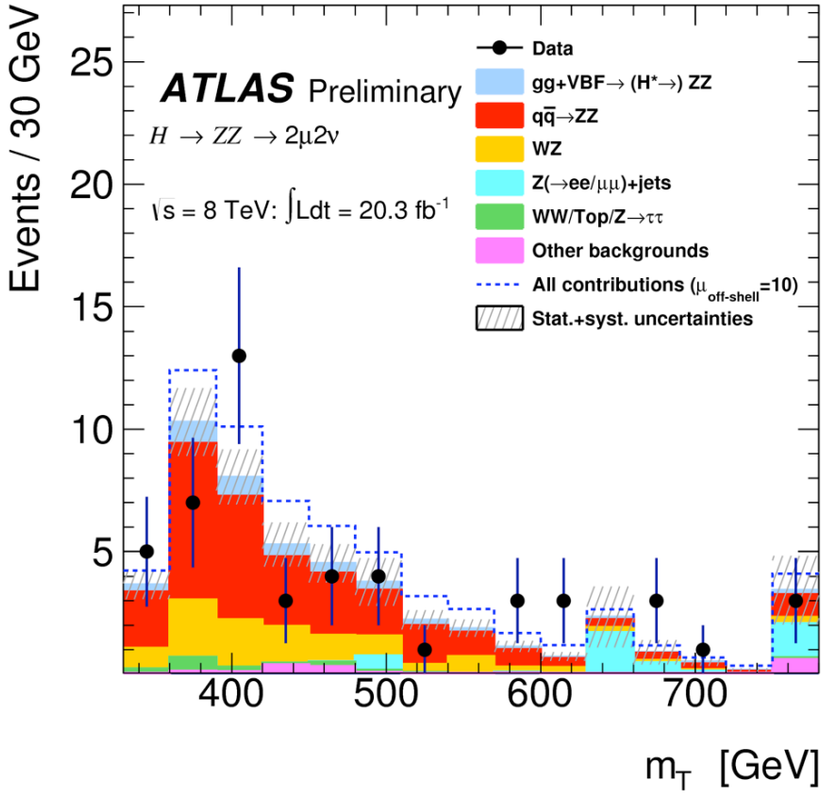

ZZ→llνν
- ETmiss>150 GeV and 76 GeV<m_{ll}<106
- Main backgrounds: qq→ZZ and WZ/WW, Z+jets and top
- Off-peak region m_{TZZ}>350 GeV
- Limit on off-shell rate based on event counting

Indirect Γ_H measurement: Results

NEW!

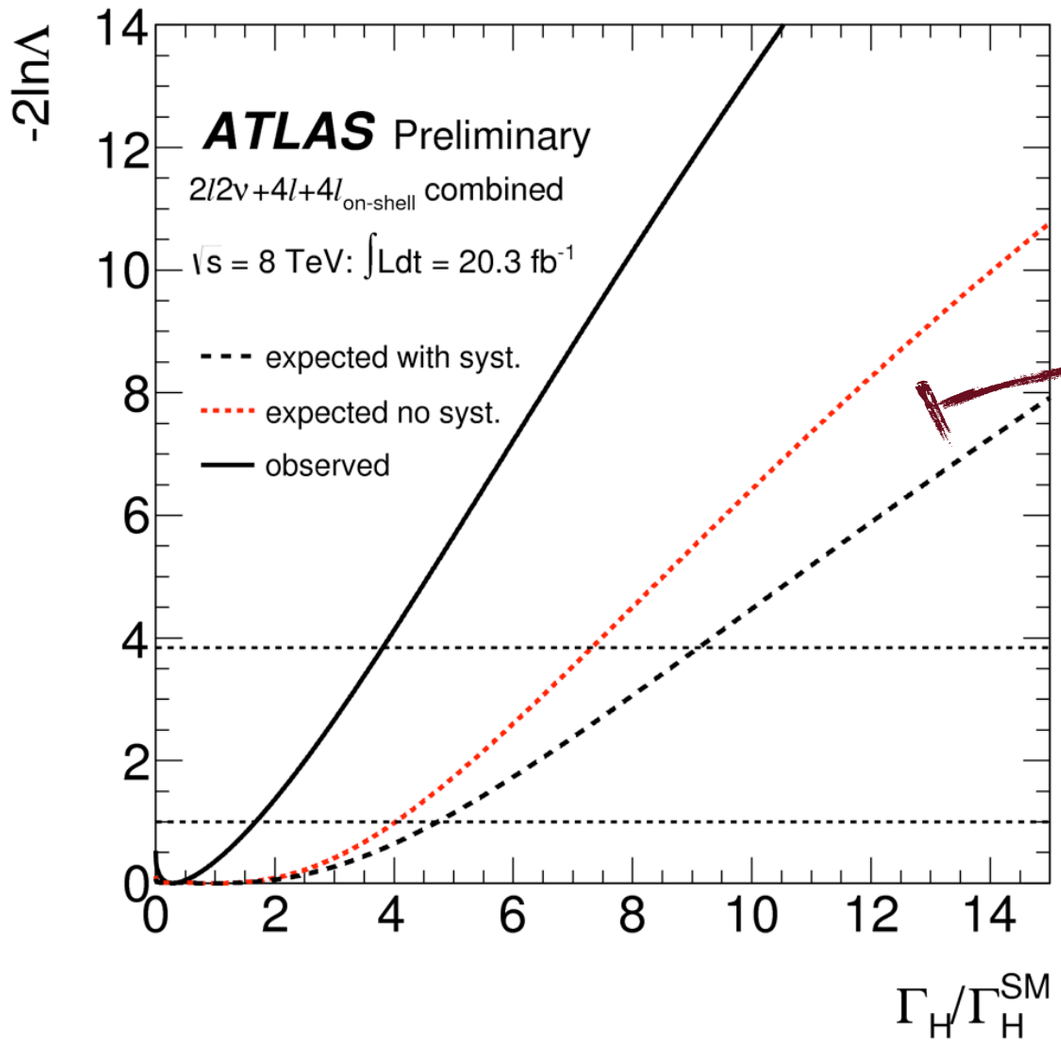

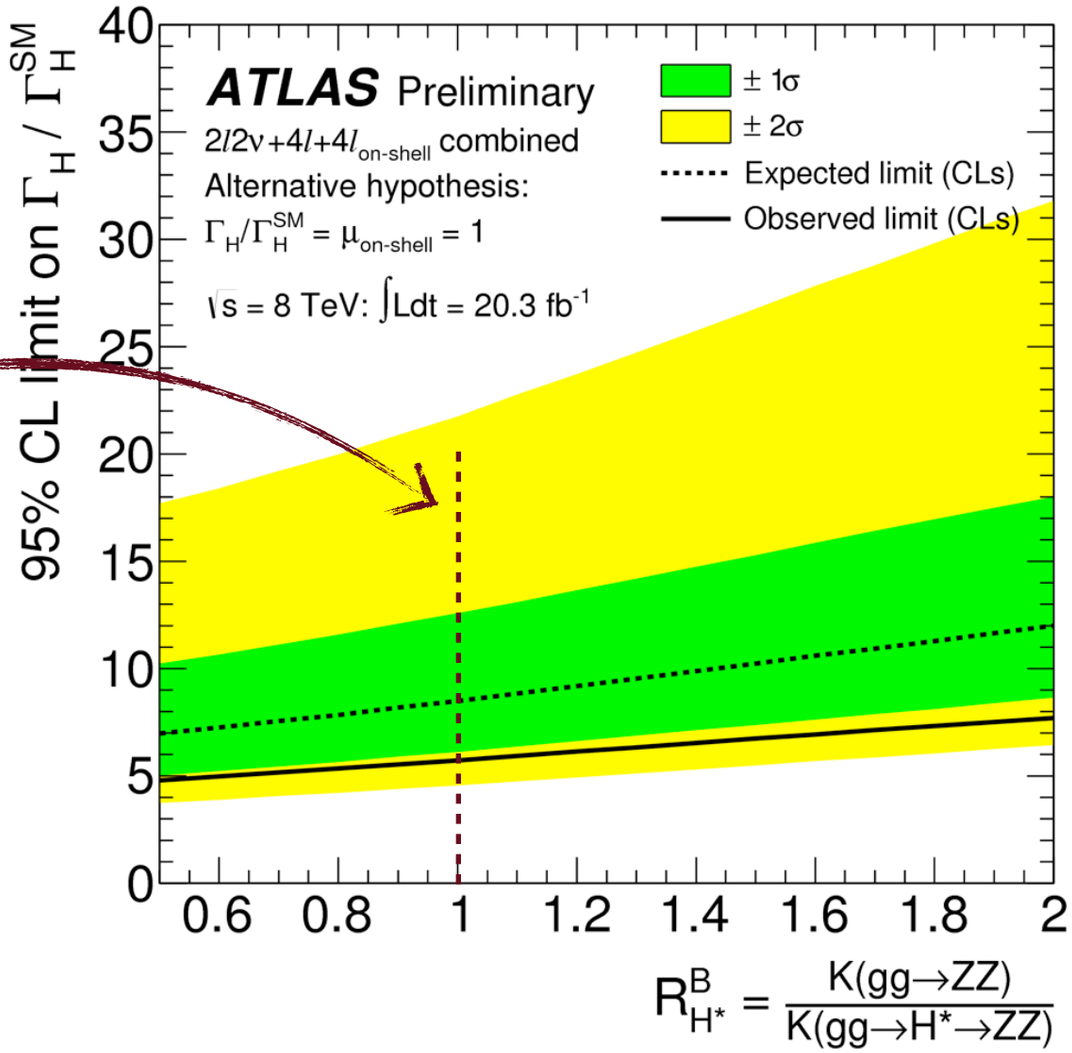

Results are expressed as a function of the unknown K-factor for the gg→ZZ background.

Assuming background K-factors same as for signal:

- $\Gamma_H/\Gamma_{SM} < 4.8$ (5.8) at 95% CLs with alternative hypothesis $R^B_{H^*}=1$, $\Gamma_H/\Gamma_{SM}=1$ and $\mu_{on\text{-}shell}=1.51$
- $\Gamma_H/\Gamma_{SM} < 5.7$ (8.5) at 95% CLs with alternative hypothesis $R^B_{H^*}=1$, $\Gamma_H/\Gamma_{SM}=1$ and $\mu_{on\text{-}shell}=1.00$

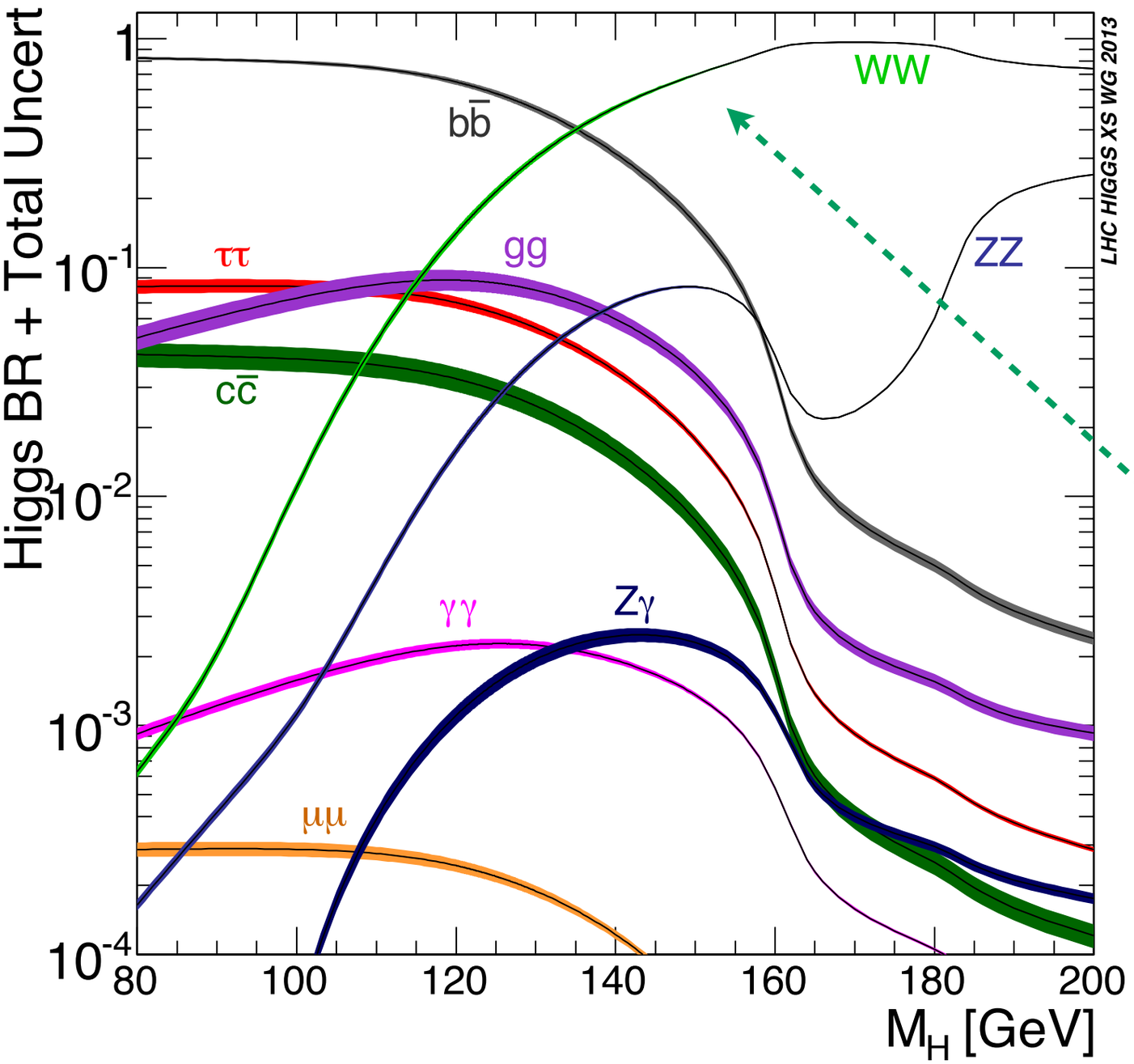

H→WW→lνlν

Couplings: Phys. Lett. B726 (2013) 88/ATLAS-CONF-2013-030
Spin/CP: Phys. Lett. B726 (2013) 120
VH(→WW): ATLAS-CONF-2013-075

H→WW(*)→lνlν

- Complex final state without mass peak
- Signature: l^+l^- + MET
- Observable:

$$m_{\mathrm{T}} = \sqrt{(E_{\mathrm{T}}^{\ell\ell} + E_{\mathrm{T}}^{\mathrm{miss}})^2 - (\mathbf{P}_{\mathrm{T}}^{\ell\ell} + \mathbf{P}_{\mathrm{T}}^{\mathrm{miss}})^2}$$

- Backgrounds: WW, top, W/Z+jets
- Categories: m_{ll}, di-lepton flavor, Njet

For m_H=125 GeV

Local significance: 3.8σ (3.7σ)

μ=1.01 ± 0.31 @ m_H=125 GeV

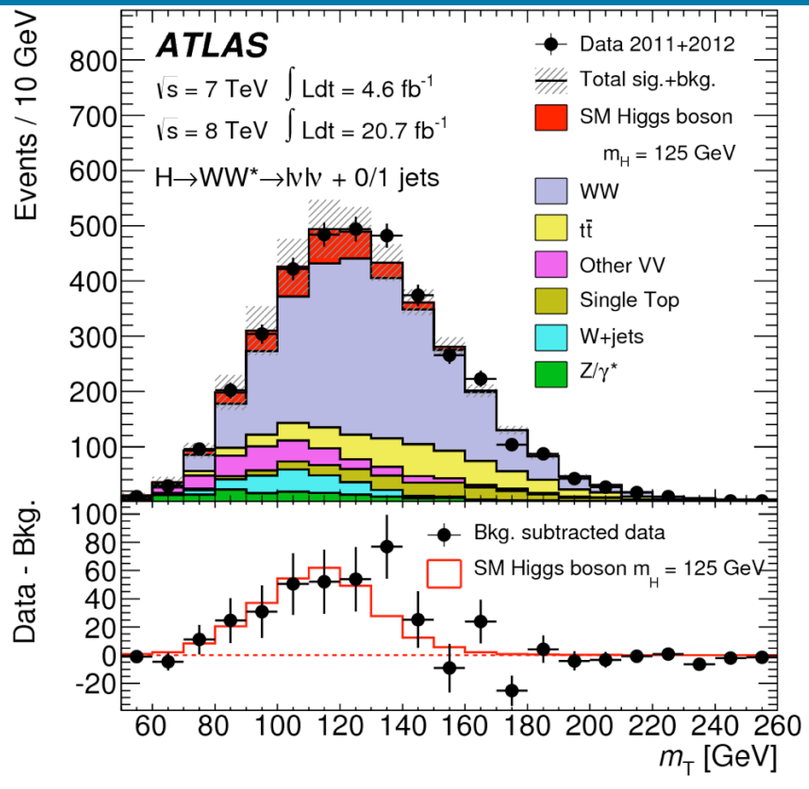

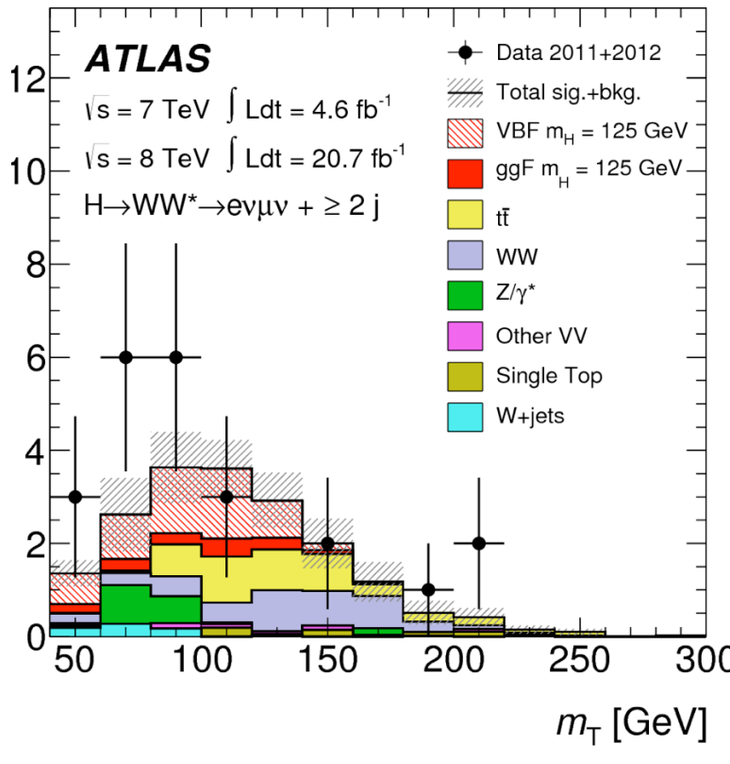

Towards more exclusive final states...

Analysis designed to select VH(→WW)

3-lepton final state

- WH→WWW→lνlνlν
- 3 leptons, |ΣQ|=1, 0 b-tags, m_{ll},MET, $\Delta\varphi_{ll}$

4-lepton final state

- ZH→ZWW→lllνlν
- 4 leptons, MET, 0 b-tags, m_{ll}

- Remove overlap with H→WW→lνlν analysis
- 95% CL upper limit on ttH production @m_H=125 GeV: 7.2 (3.6)xSM

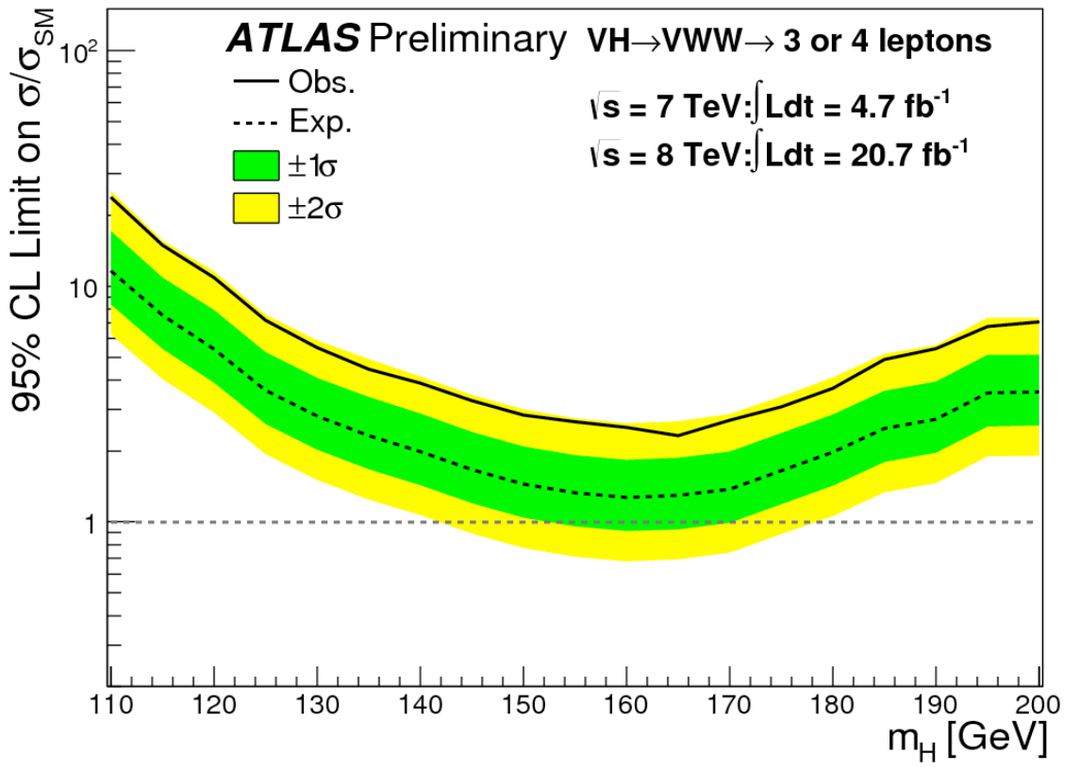

Spin/CP studies: Overview

	$H \to ZZ^{(*)} \to 4\ell$	$H \to WW^{(*)} \to \ell\nu\ell\nu$	$H \to \gamma\gamma$
0^-	✓	-	-
1^+	✓	✓	-
1^-	✓	✓	-
2^+	✓	✓	✓

See talk by:
Petar Kevin Rados

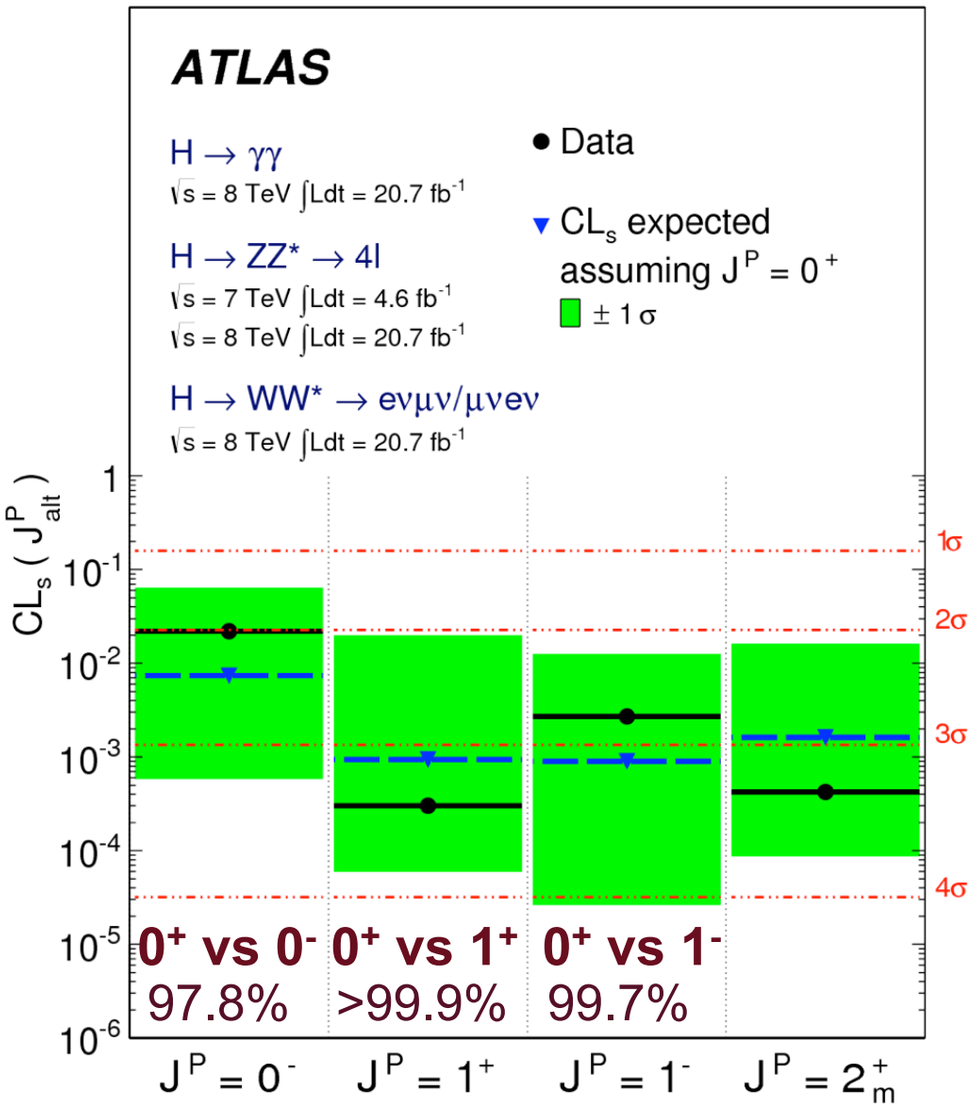

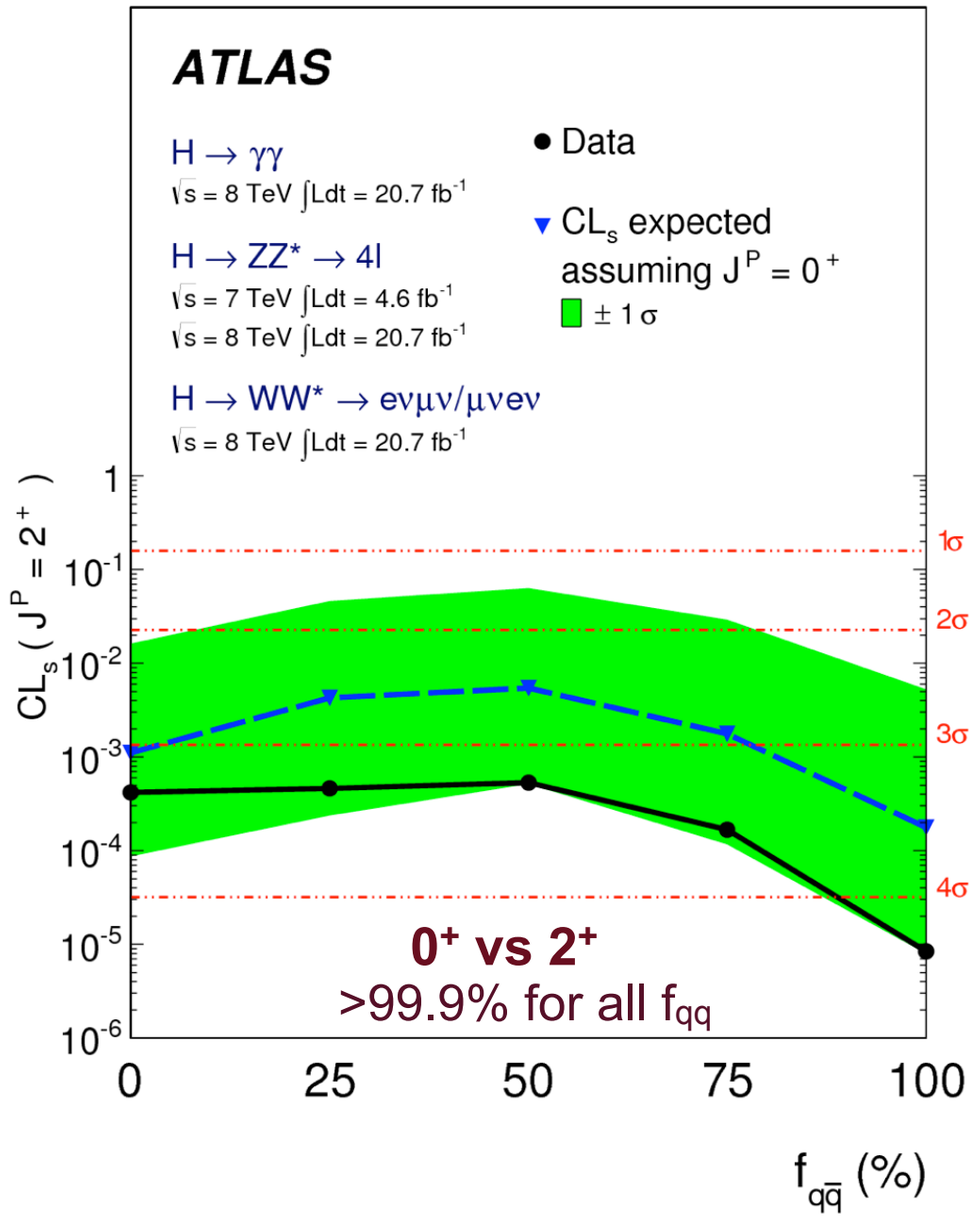

All studied alternative hypotheses are strongly disfavored with respect to the 0^+ hypothesis

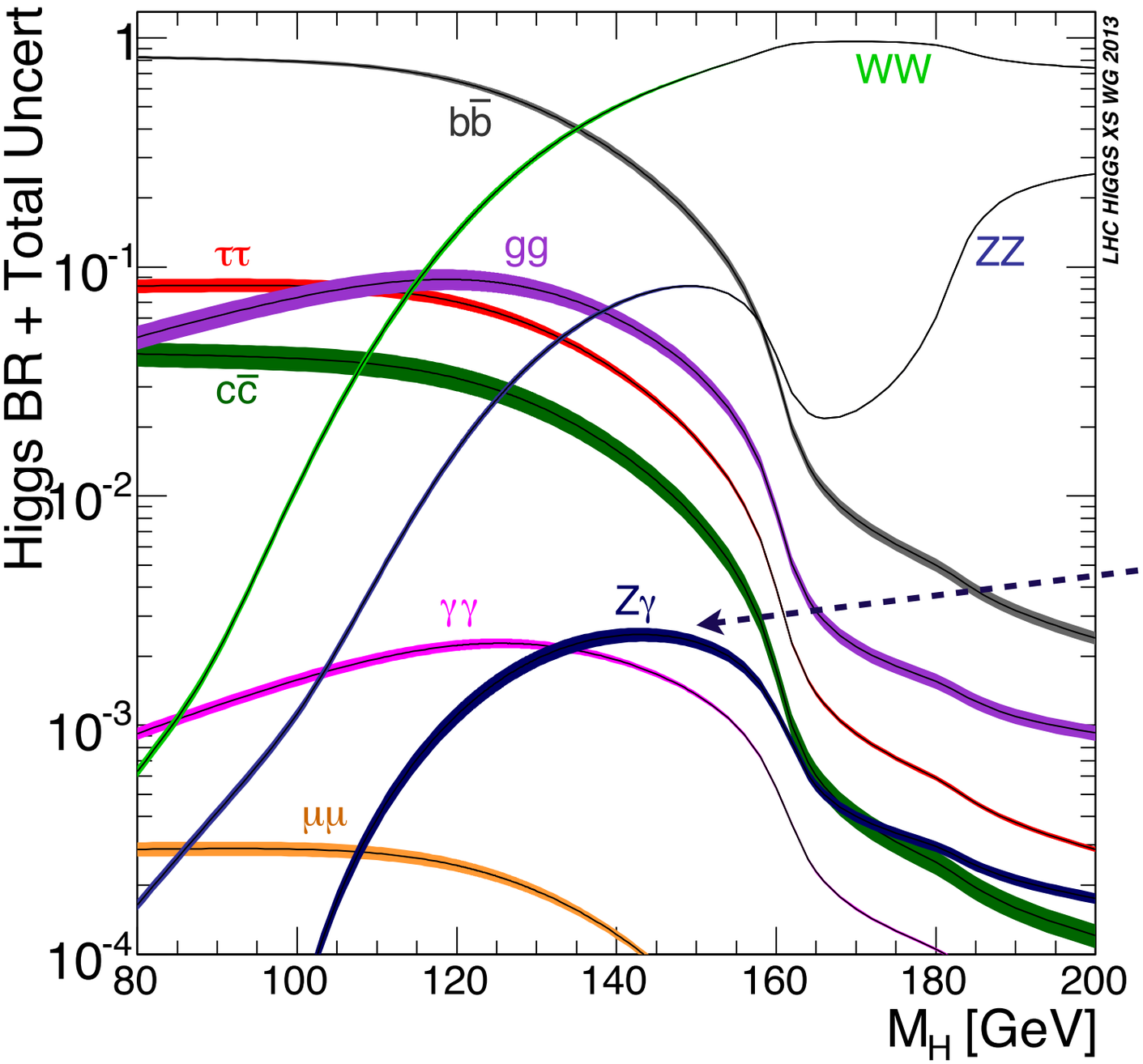

H→Zγ

Phys. Lett. B732 (2014) 8

H→Zγ

Loop mediated Higgs decay
→ BR~10-4(125GeV)
→ sensitive to new physics
(additional singlets, compositeness, etc)

Signature: $e^+e^-/\mu^+\mu^-+\gamma$
→ signal efficiency eeγ (μμγ):27% (33%)

Background
→ $Z\rightarrow ll\gamma_{FSR}$ an Z+γ continuum (82%)
→ Z+jets (17%)
→ ttbar, WZ (~1%)

Event categories
→ $\Delta\eta_{\gamma Z}, p_{Tt}$
→ S/B~3-13%

$\sqrt{s}$ [TeV]	ℓ	Category	N_S	N_B	N_D	$\frac{N_S}{\sqrt{N_B}}$	FWHM [GeV]
8	μ	high p_{Tt}	2.3	310	324	0.13	3.8
8	μ	low p_{Tt}, low $\Delta\eta$	3.7	1600	1587	0.09	3.8
8	μ	low p_{Tt}, high $\Delta\eta$	0.8	600	602	0.03	4.1
8	e	high p_{Tt}	1.9	260	270	0.12	3.9
8	e	low p_{Tt}, low $\Delta\eta$	2.9	1300	1304	0.08	4.2
8	e	low p_{Tt}, high $\Delta\eta$	0.6	430	421	0.03	4.5
7	μ	high p_{Tt}	0.4	40	40	0.06	3.9
7	μ	low p_{Tt}	0.6	340	335	0.03	3.9
7	e	high p_{Tt}	0.3	25	21	0.06	3.9
7	e	low p_{Tt}	0.5	240	234	0.03	4.0

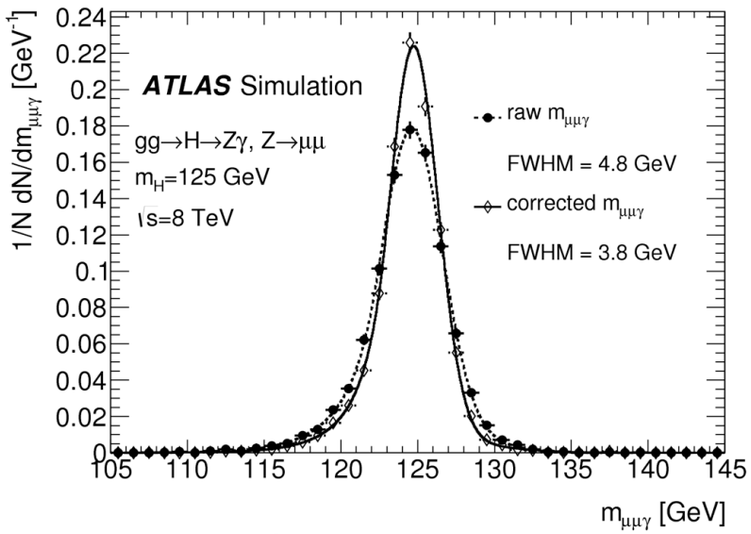

corrections: photon vertex, μ-collinear FSR and m_Z constraint

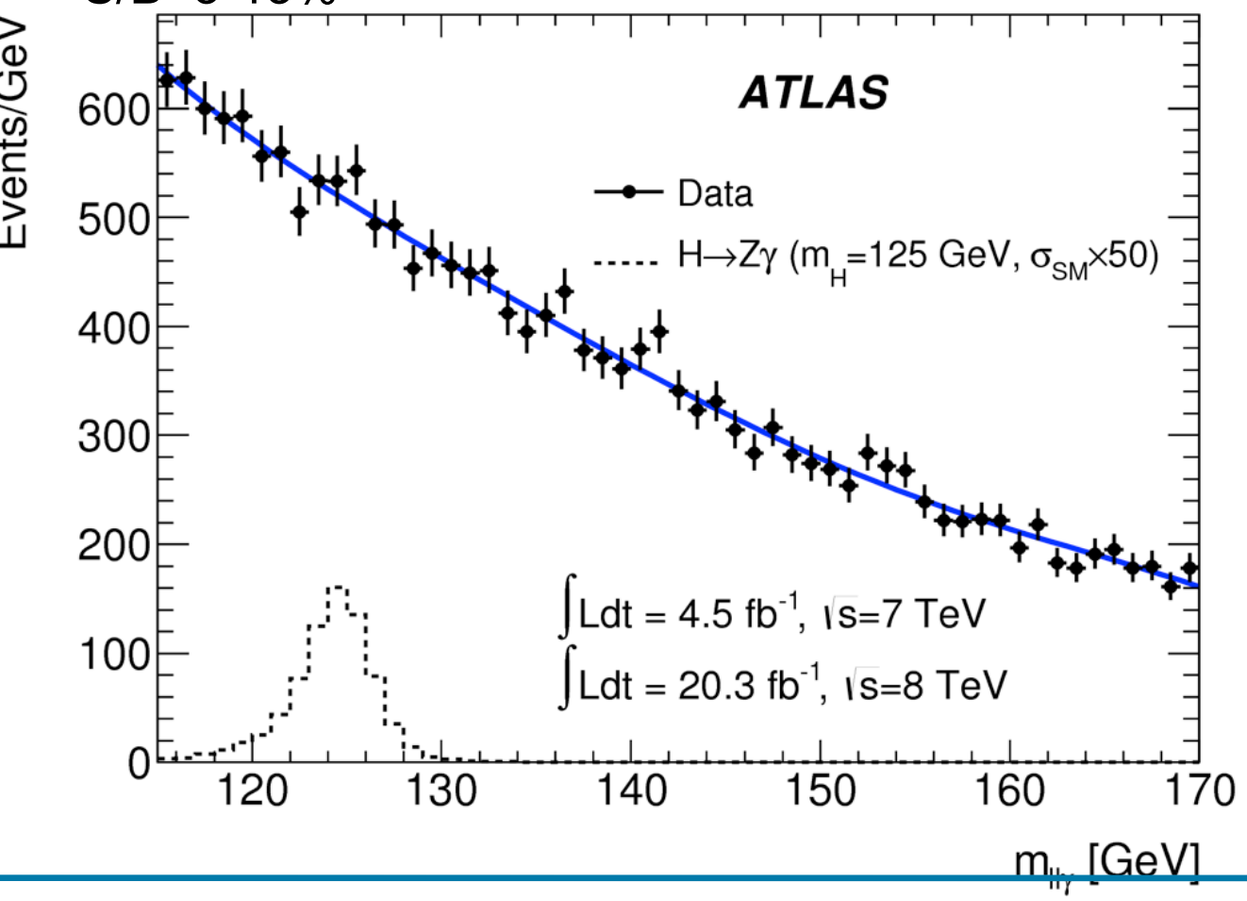

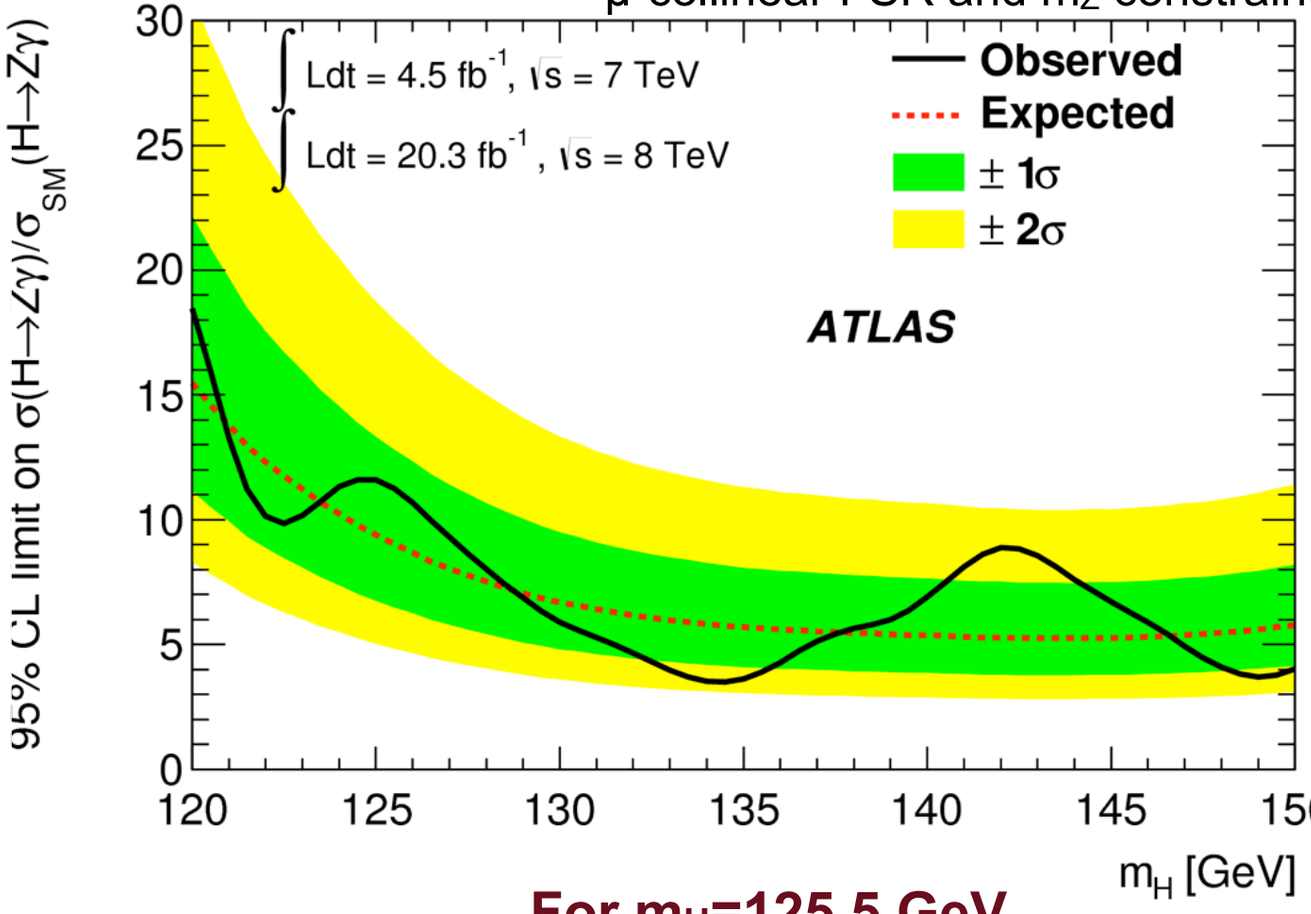

For m_H=125.5 GeV,
95% CLs upper limit: 11 (9) x SM

Summary

Two years after the observation of the Higgs-like boson, it is by now a SM-like Higgs boson!

m_H=125.36 ± 0.37 (stat) ± 0.18 GeV

Production rates in γγ, ZZ and WW in agreement with SM expectations,

fiducial and differential cross sections appear, data compatible with the 0^+ hypothesis,

physics reach of LHC extended in the Γ_H front following fruitful dialogue with theory community

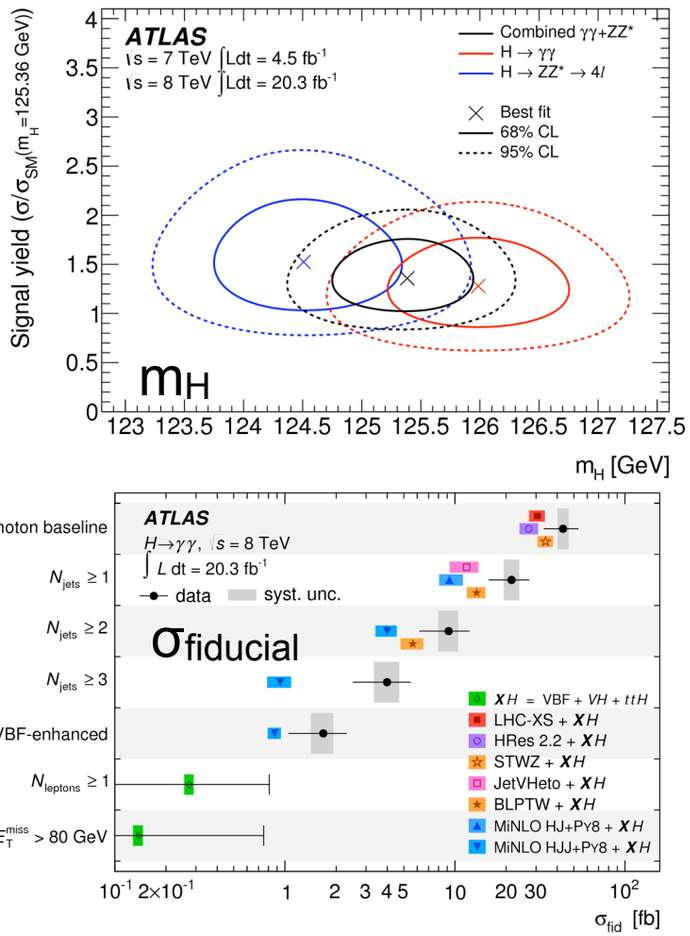

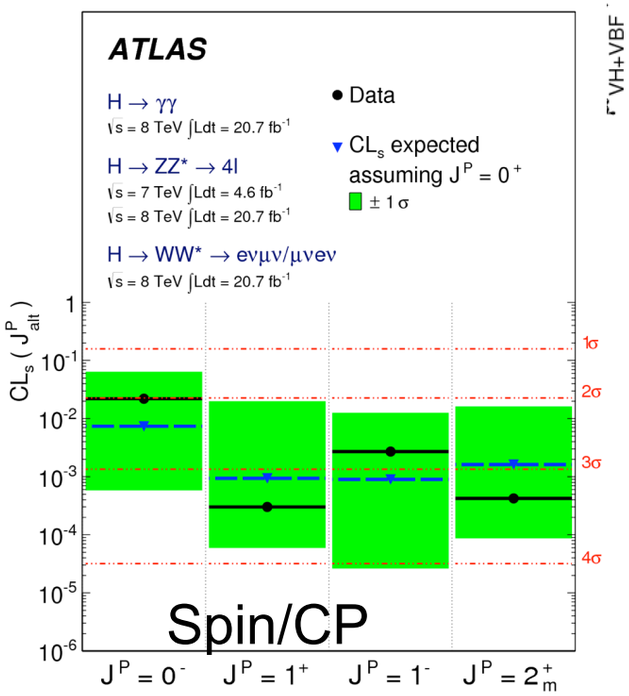

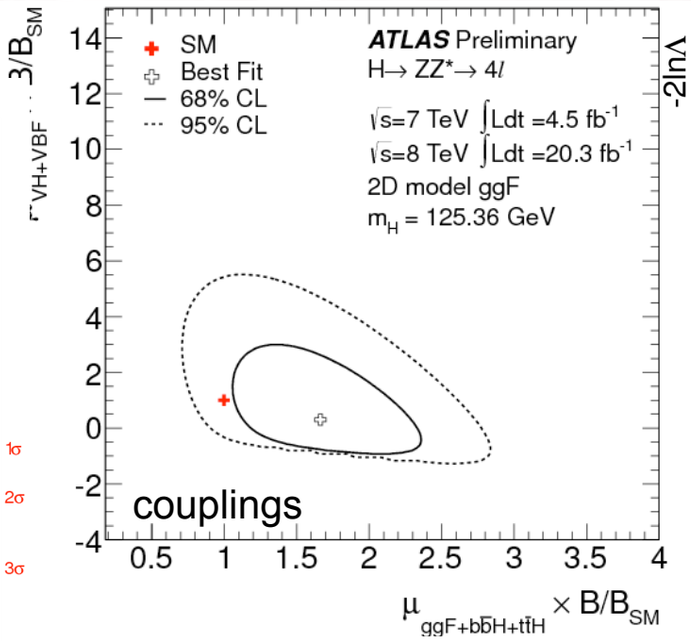

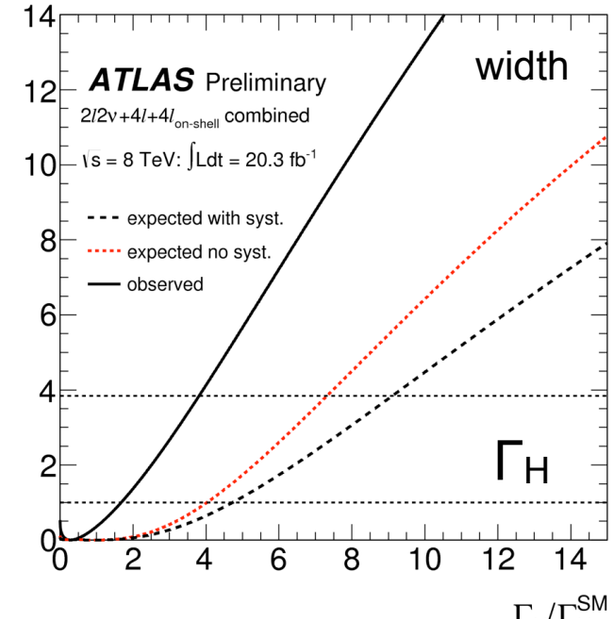

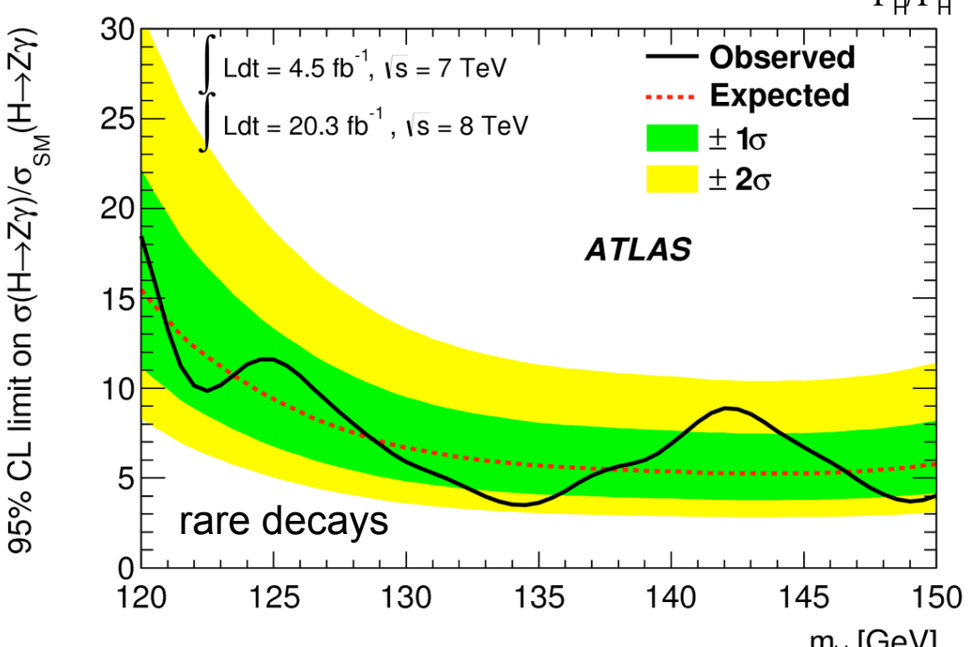

Final Run 1 results already out for several H→VV channels/measurements, remaining analyses to follow suit!

Looking forward to x10 more Higgs bosons in Run II

Additional Slides

A Toroidal LHC ApparatuS

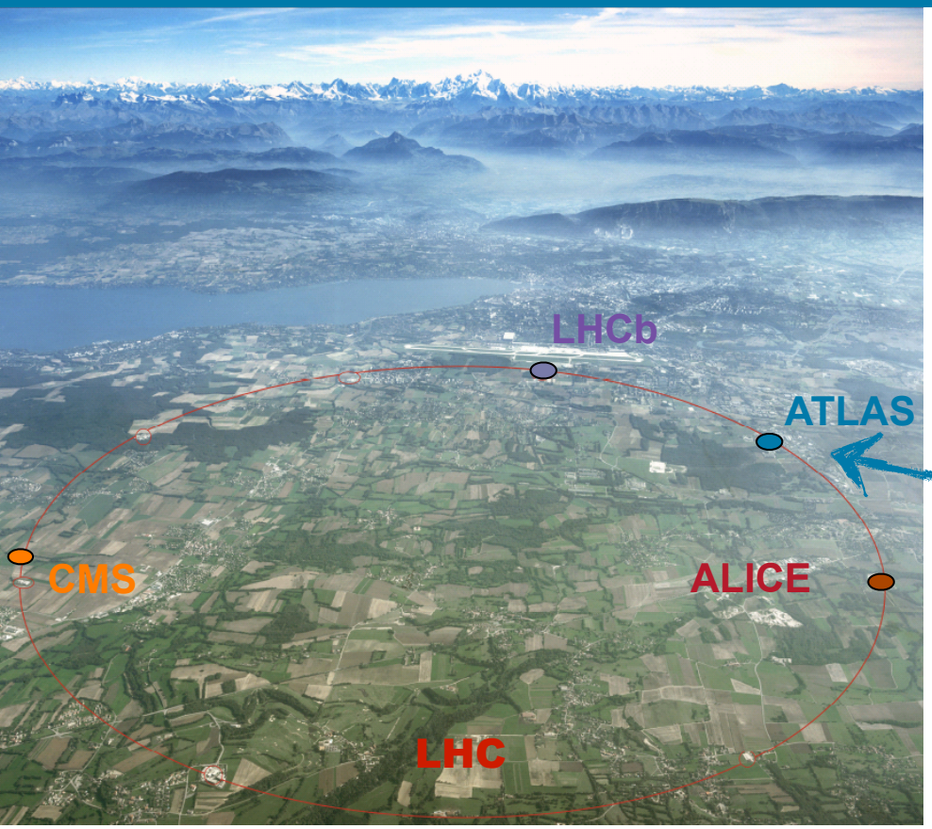

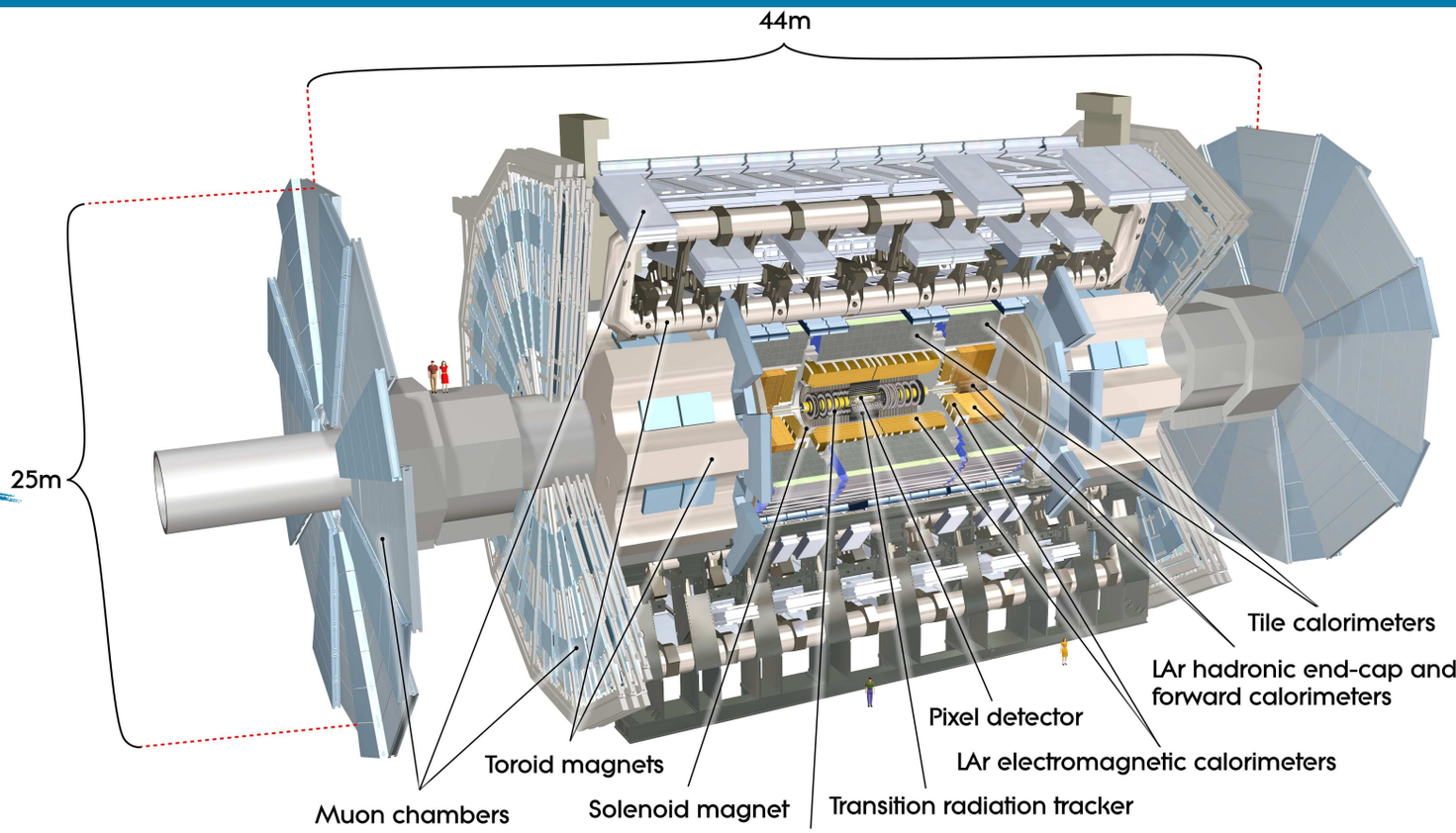

→ Multi-purpose detector designed for the harsh LHC environment

→ High data-taking efficiency and very good data-quality

ATLAS p-p run: April-December 2012										
Inner Tracker			Calorimeters		Muon Spectrometer				Magnets	
Pixel	SCT	TRT	LAr	Tile	MDT	RPC	CSC	TGC	Solenoid	Toroid
99.9	99.4	99.8	99.1	99.6	99.6	99.8	100.	99.6	99.8	99.5
All good for physics: 95.8%										

Luminosity weighted relative detector uptime and good quality data delivery during 2012 stable beams in pp collisions at $\sqrt{s}$=8 TeV between April 4th and December 6th (in %) – corresponding to 21.6 fb^{-1} of recorded data.

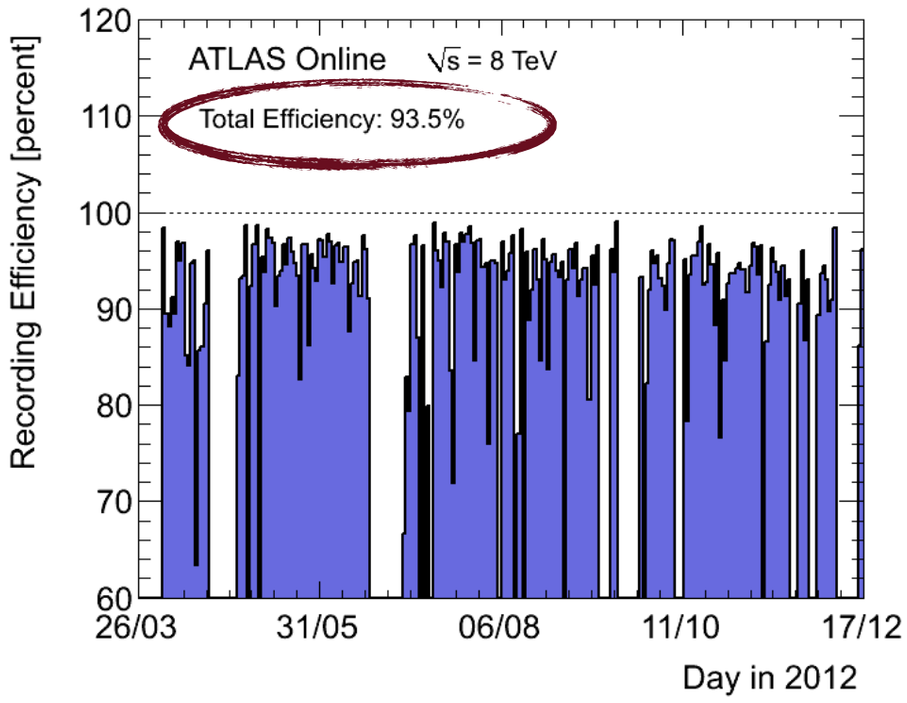

The LHC Run I dataset

Excellent LHC performance during Run I :
4.8 fb^{-1} at 7 TeV and 20.7 fb^{-1} at 8 TeV

Pile-up exceeding detector design specifications
→ Maintain performance through improved algorithms
→ Proper modeling of experimental conditions essential

Peak Luminosity [$cm^{-2}s^{-1}$]

2.07×10^{32} 3.65×10^{33} $7.73\times10^{33} cm^{-2}s^{-1}$

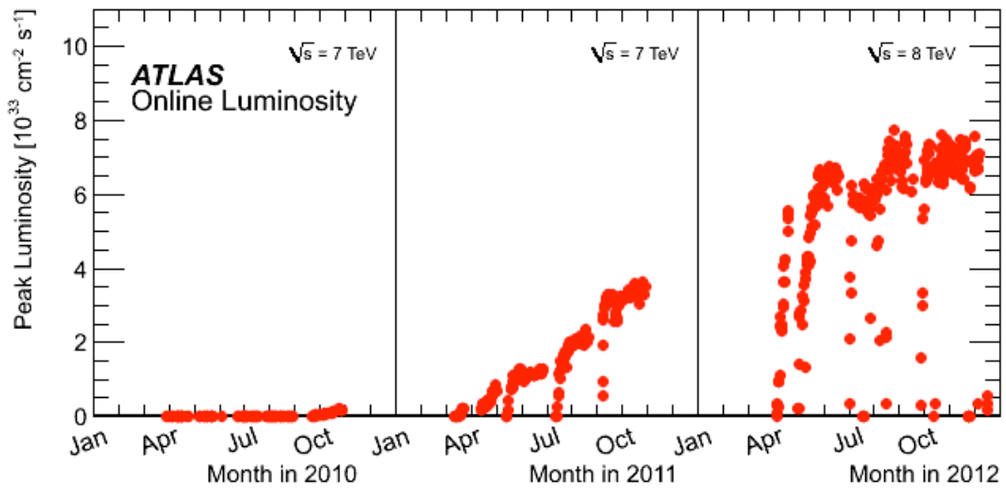

"Observation" dataset

Final LHC Run 1 dataset

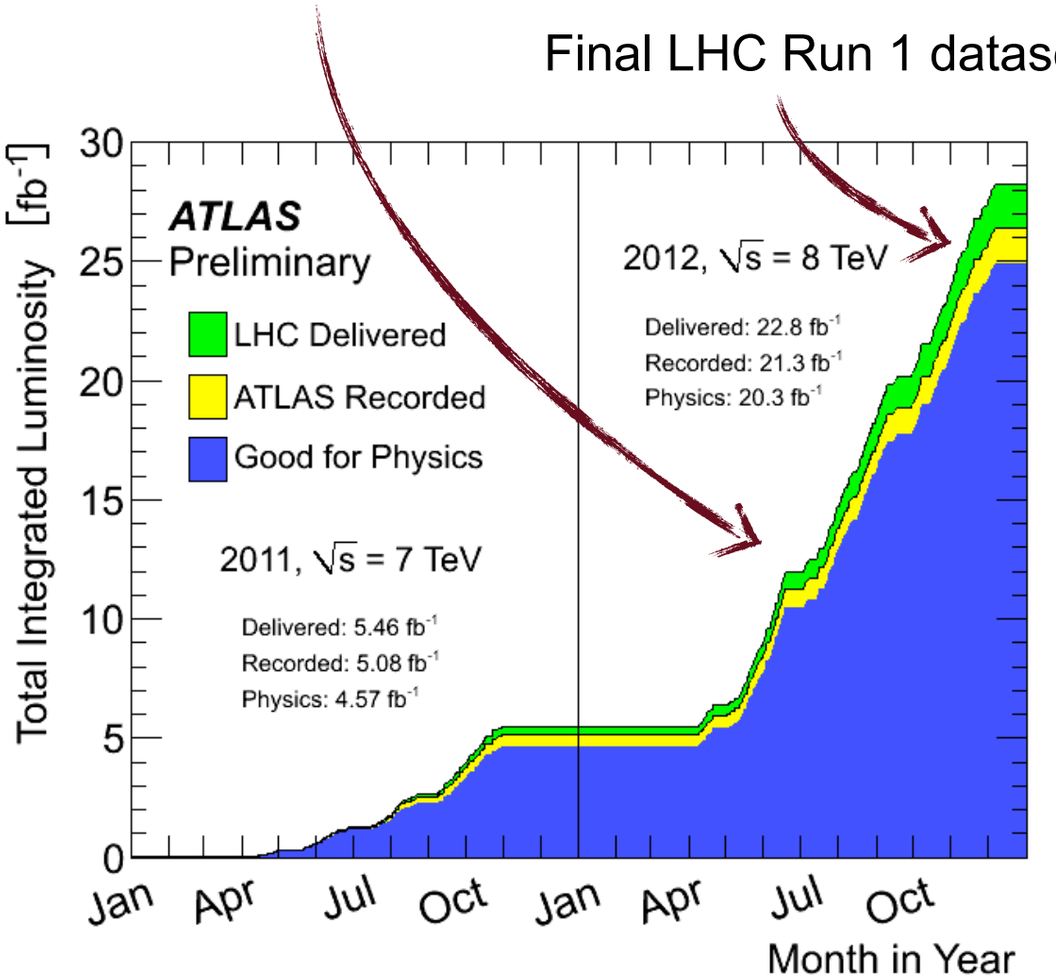

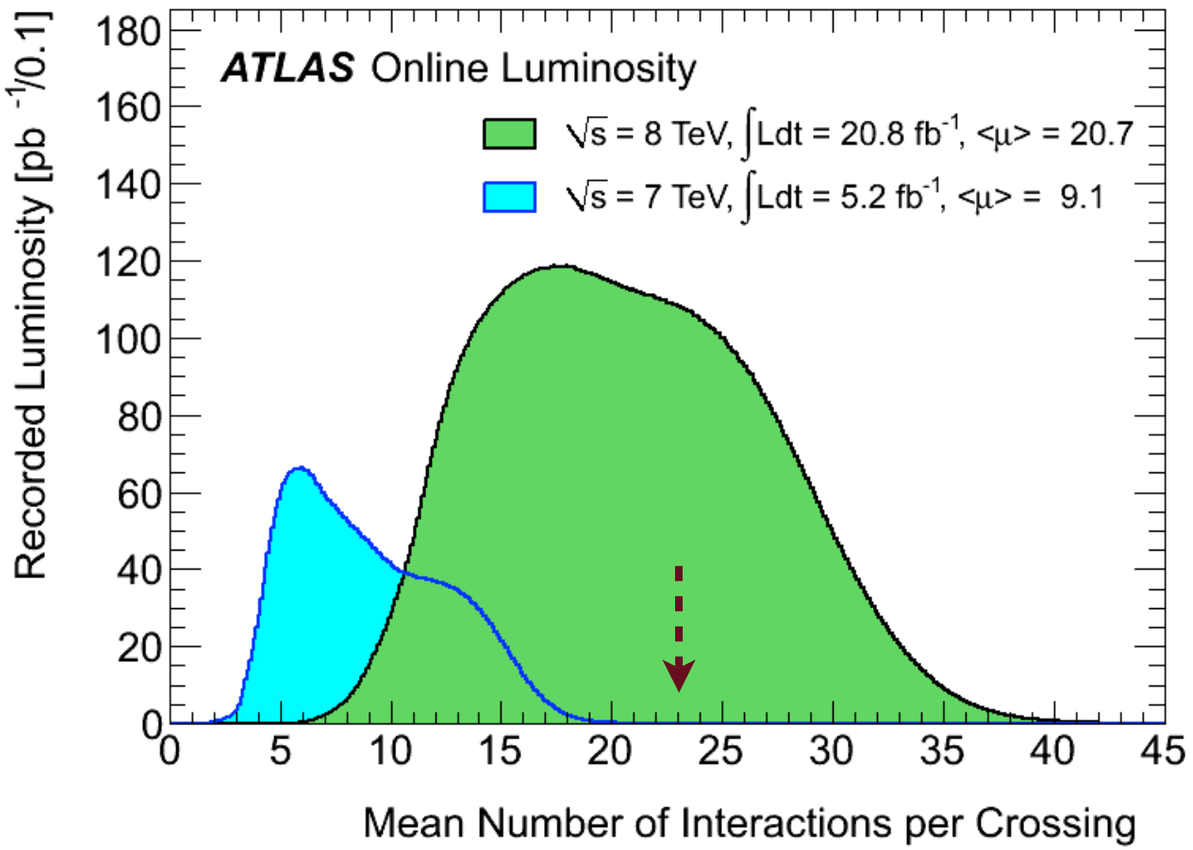

H→γγ: Updated m_H Analysis Categories

Table 1: Summary of the expected number of signal events in the 105–160 GeV mass range n_{sig}, the FWHM of mass resolution, σ_{eff} (half of the smallest range containing 68% of the signal events), number of background events b in the smallest mass window containing 90% of the signal (σ_{eff90}), and the ratio s/b and $s/\sqrt{b}$ with s the expected number of signal events in the window containing 90% of signal events, for the $H \to \gamma\gamma$ channel. b is derived from the fit of the data in the 105–160 GeV mass range. The value of m_H is taken to be 126 GeV and the signal yield is assumed to be the expected Standard Model value. The estimates are shown separately for the 7 TeV and 8 TeV datasets and for the inclusive sample as well as for each of the categories used in the analysis.

(90% signal window)

Category	n_{sig}	FWHM [GeV]	σ_{eff} [GeV]	b in $\pm\sigma_{eff90}$	s/b [%]	$s/\sqrt{b}$
			$\sqrt{s}$=8 TeV			
Inclusive	402.	3.69	1.67	10670	3.39	3.50
Unconv. central low p_{Tt}	59.3	3.13	1.35	801	6.66	1.88
Unconv. central high p_{Tt}	7.1	2.81	1.21	26.0	24.6	1.26
Unconv. rest low p_{Tt}	96.2	3.49	1.53	2624	3.30	1.69
Unconv. rest high p_{Tt}	10.4	3.11	1.36	93.9	9.95	0.96
Unconv. transition	26.0	4.24	1.86	910	2.57	0.78
Conv. central low p_{Tt}	37.2	3.47	1.52	589	5.69	1.38
Conv. central high p_{Tt}	4.5	3.07	1.35	20.9	19.4	0.88
Conv. rest low p_{Tt}	107.2	4.23	1.88	3834	2.52	1.56
Conv. rest high p_{Tt}	11.9	3.71	1.64	144.2	7.44	0.89
Conv. transition	42.1	5.31	2.41	1977	1.92	0.85
			$\sqrt{s}$=7 TeV			
Inclusive	73.9	3.38	1.54	1752	3.80	1.59
Unconv. central low p_{Tt}	10.8	2.89	1.24	128	7.55	0.85
Unconv. central high p_{Tt}	1.2	2.59	1.11	3.7	30.0	0.58
Unconv. rest low p_{Tt}	16.5	3.09	1.35	363	4.08	0.78
Unconv. rest high p_{Tt}	1.8	2.78	1.21	13.6	11.6	0.43
Unconv. transition	4.5	3.65	1.61	125	3.21	0.36
Conv. central low p_{Tt}	7.1	3.28	1.44	105	6.06	0.62
Conv. central high p_{Tt}	0.8	2.87	1.25	3.5	21.6	0.40
Conv. rest low p_{Tt}	21.0	3.93	1.75	695	2.72	0.72
Conv. rest high p_{Tt}	2.2	3.43	1.51	24.7	7.98	0.40
Conv. transition	8.1	4.81	2.23	365	2.00	0.38

Signal Model: Crystal-Ball + wide Gaussian
Background Model: exponential (high pTt), second order polynomial (others)
m_H resolution differences: estimate of effective constant term from Z→ee events and from lower pile-up in 7 TeV

H→γγ: Updated m_H Analysis Systematics

Table 2: Summary of the relative systematic uncertainties (in %) on the $H \to \gamma\gamma$ mass measurement for the different categories described in the text. The first seven rows give the impact of the photon energy scale systematic uncertainties, grouped into seven classes.

	Unconverted					Converted				
	Central		Rest		Trans.	Central		Rest		Trans.
Class	low p_{Tt}	high p_{Tt}	low p_{Tt}	high p_{Tt}		low p_{Tt}	high p_{Tt}	low p_{Tt}	high p_{Tt}	
$Z \to e^+e^-$ calibration	0.02	0.03	0.04	0.04	0.11	0.02	0.02	0.05	0.05	0.11
LAr cell non-linearity	0.12	0.19	0.09	0.16	0.39	0.09	0.19	0.06	0.14	0.29
Layer calibration	0.13	0.16	0.11	0.13	0.13	0.07	0.10	0.05	0.07	0.07
ID material	0.06	0.06	0.08	0.08	0.10	0.05	0.05	0.06	0.06	0.06
Other material	0.07	0.08	0.14	0.15	0.35	0.04	0.04	0.07	0.08	0.20
Conversion reconstruction	0.02	0.02	0.03	0.03	0.05	0.03	0.02	0.05	0.04	0.06
Lateral shower shape	0.04	0.04	0.07	0.07	0.06	0.09	0.09	0.18	0.19	0.16
Background modeling	0.10	0.06	0.05	0.11	0.16	0.13	0.06	0.14	0.18	0.20
Vertex measurement	0.03									
Total	0.23	0.28	0.24	0.30	0.59	0.21	0.25	0.27	0.33	0.47

Finally, uncertainties on the predicted overall signal yield are estimated as follows [17]. The uncertainty on the predicted cross-section for Higgs boson production is about 10% for the dominant gluon fusion process. The uncertainty on the predicted branching ratio to two photons is 5%. The uncertainty from the photon identification efficiency is derived from studies using several control samples: a sample of radiative Z decays, a sample of $Z \to e^+e^-$ events, where the shower shapes of electrons are corrected to resemble the shower shapes of photons, and a sample of high E_{T} isolated prompt photons. The estimated photon identification uncertainty amounts to 1.0% for the 8 TeV dataset, after correcting for small residual differences between simulation and data, and 8.4% for the 7 TeV dataset. The uncertainty is larger for the 7 TeV dataset because of the stronger correlation of the neural network photon identification with the photon isolation, and because the neural network identification relies more strongly on the correlations between the individual shower shape variables, complicating the measurement and introducing larger uncertainties on the estimate of its performance in data. The uncertainty on the integrated luminosity is 2.8% for the 8 TeV dataset and 1.8% for the 7 TeV dataset [31]. The uncertainties on the isolation cut efficiency and on the trigger efficiency are less than 1% for both the 7 TeV and 8 TeV datasets. These uncertainties on the overall signal yield also have a negligible effect on the mass measurement.

H→γγ: Fiducial Regions yields

Fiducial region	N_{data}	$N_{\text{MC}}^{\text{sig}}$	ν_i^{sig}
Baseline	94627	403 ± 45	570 ± 130
$N_{\text{jets}} \geq 1$	34293	$178\,^{+31}_{-26}$	308 ± 79
$N_{\text{jets}} \geq 2$	10699	63 ± 11	141 ± 43
$N_{\text{jets}} \geq 3$	2840	17 ± 4	64 ± 22
VBF-enhanced	334	13 ± 2	24 ± 9
$N_{\text{leptons}} \geq 1$	168	3.5 ± 0.4	-3 ± 5
$E_{\text{T}}^{\text{miss}} > 80$ GeV	154	2.6 ± 0.4	-2 ± 4

Table 1. The total number of events selected in data in each fiducial region, N_{data}, the expected signal yield obtained from the simulation samples discussed in section 4, $N_{\text{MC}}^{\text{sig}}$, and the fitted yield obtained from data, ν_i^{sig}. The uncertainty on the fitted yield is the total uncertainty on the signal extraction, including the statistical and systematic uncertainties. The uncertainty on the expected yields include both the theoretical and experimental systematic uncertainties.

H→γγ: Fiducial cross sections

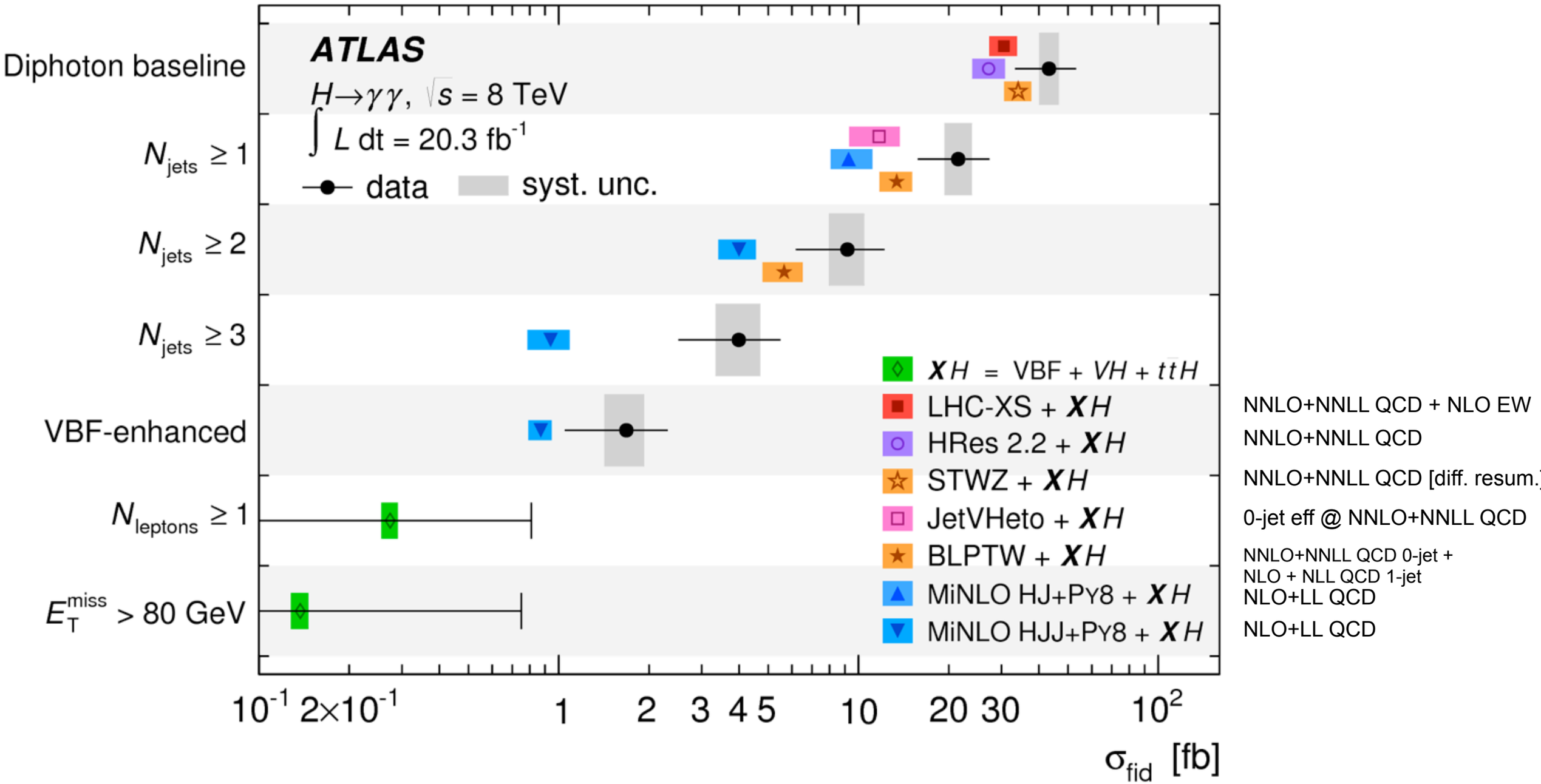

H→γγ: Fiducial cross sections

Fiducial region	Measured cross section (fb)
Baseline	$43.2 \pm 9.4\,(\text{stat.})\,^{+3.2}_{-2.9}\,(\text{syst.}) \pm 1.2\,(\text{lumi})$
$N_{\text{jets}} \geq 1$	$21.5 \pm 5.3\,(\text{stat.})\,^{+2.4}_{-2.2}\,(\text{syst.}) \pm 0.6\,(\text{lumi})$
$N_{\text{jets}} \geq 2$	$9.2 \pm 2.8\,(\text{stat.})^{+1.3}_{-1.2}\,(\text{syst.}) \pm 0.3\,(\text{lumi})$
$N_{\text{jets}} \geq 3$	$4.0 \pm 1.3\,(\text{stat.}) \pm 0.7\,(\text{syst.}) \pm 0.1\,(\text{lumi})$
VBF-enhanced	$1.68 \pm 0.58\,(\text{stat.})^{+0.24}_{-0.25}\,(\text{syst.}) \pm 0.05\,(\text{lumi})$
$N_{\text{leptons}} \geq 1$	< 0.80
$E_{\text{T}}^{\text{miss}} > 80$ GeV	< 0.74

Table 3. Measured cross sections in the baseline, $N_{\text{jets}} \geq 1$, $N_{\text{jets}} \geq 2$, $N_{\text{jets}} \geq 3$ and VBF-enhanced fiducial regions, and cross-section limits at 95% confidence level in the single-lepton and high-$E_{\text{T}}^{\text{miss}}$ fiducial regions. The seven phase space regions are defined in section 3.

Fiducial region	Theoretical prediction (fb)	Source
Baseline	30.5 ± 3.3	LHC-XS [56] + XH
	$34.1\,^{+3.6}_{-3.5}$	STWZ [98] + XH
	$27.2\,^{+3.6}_{-3.2}$	HRES [102] + XH
$N_{\text{jets}} \geq 1$	13.8 ± 1.7	BLPTW [105] + XH
	$11.7\,^{+2.0}_{-2.4}$	JetVHeto [106]+ XH
	$9.3\,^{+1.8}_{-1.2}$	MINLO HJ+ XH
$N_{\text{jets}} \geq 2$	5.65 ± 0.87	BLPTW + XH
	$3.99\,^{+0.56}_{-0.59}$	MINLO HJJ+ XH
$N_{\text{jets}} \geq 3$	0.94 ± 0.15	MINLO HJJ+ XH
VBF-enhanced	0.87 ± 0.08	MINLO HJJ+ XH
$N_{\text{leptons}} \geq 1$	0.27 ± 0.02	XH
$E_{\text{T}}^{\text{miss}} > 80$ GeV	0.14 ± 0.01	XH

Table 4. Theoretical predictions for the cross sections in the baseline, $N_{\text{jets}} \geq 1$, $N_{\text{jets}} \geq 2$, $N_{\text{jets}} \geq 3$, VBF-enhanced, single-lepton and high-$E_{\text{T}}^{\text{miss}}$ fiducial regions. The uncertainties on the cross-section predictions are discussed in detail in Section 8 and include the effect of scale and PDF variation as well as the uncertainties on the $H \to \gamma\gamma$ branching ratio and non-perturbative modelling factors. The seven phase space regions are defined in section 3. The 'XH' refers to the theoretical predictions for VBF, VH and $t\bar{t}H$ derived using the POWHEG-PYTHIA, and PYTHIA8 event generators discussed in section 4.

H→γγ: Differential cross sections bins

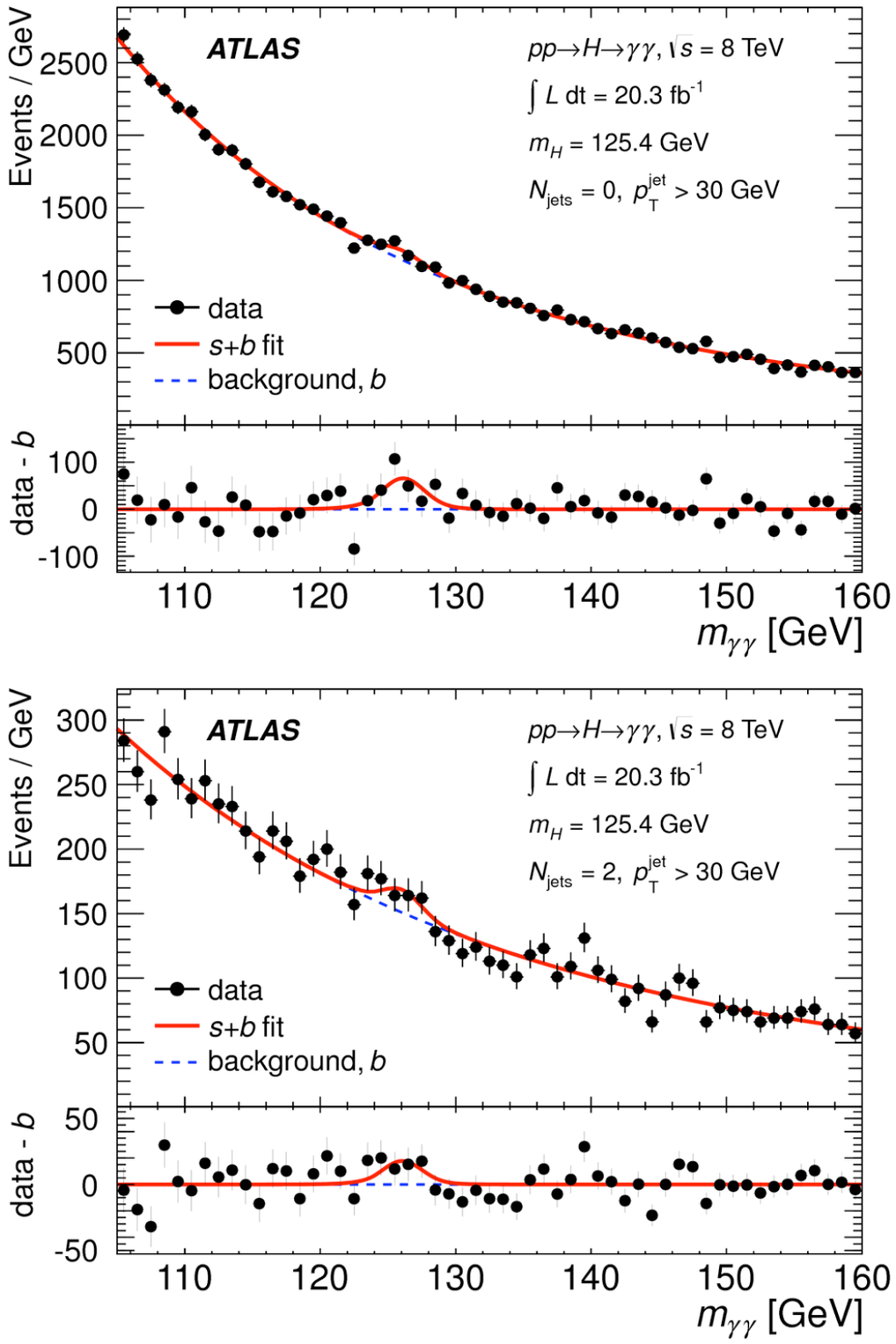

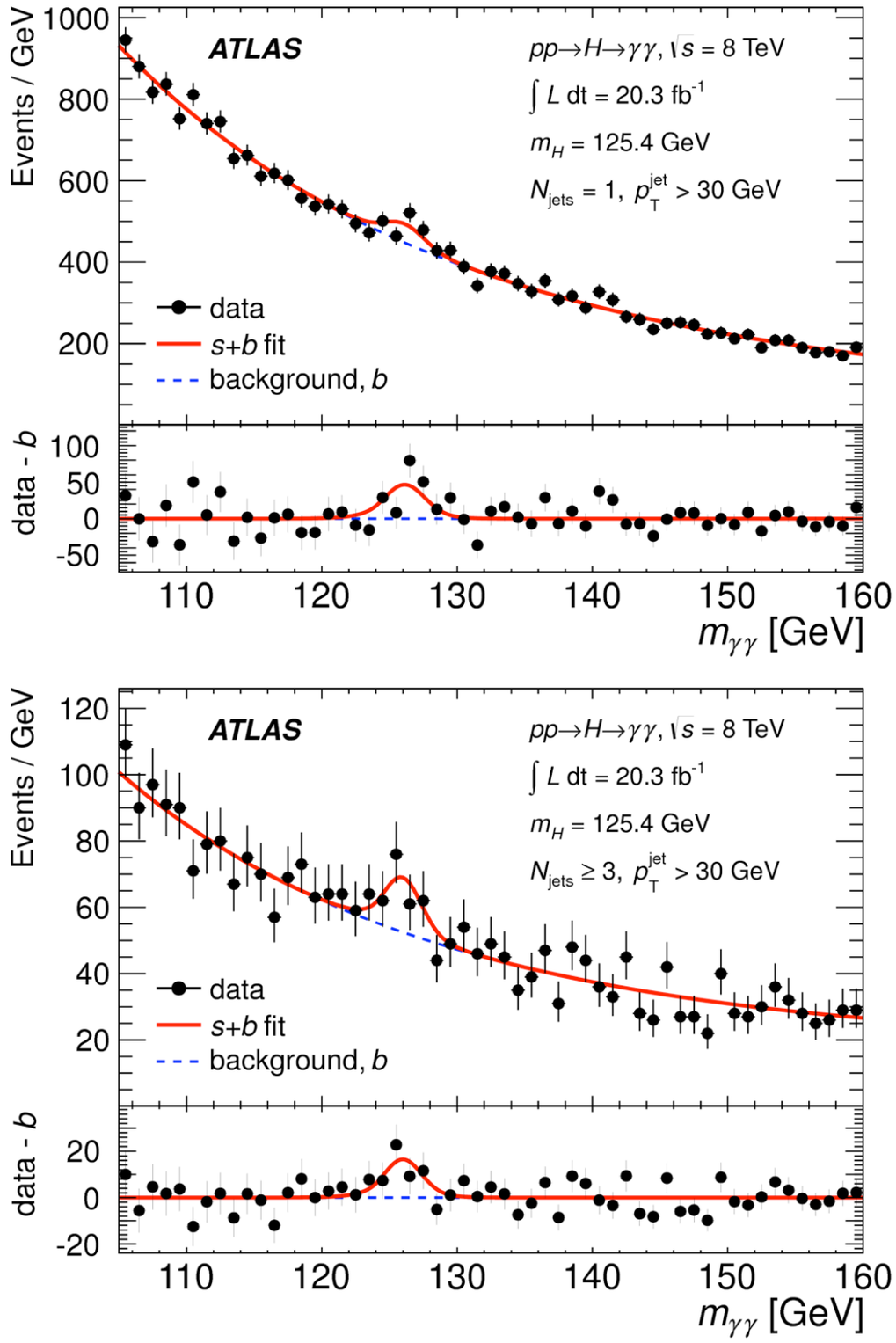

H→γγ: Differential cross sections systematics

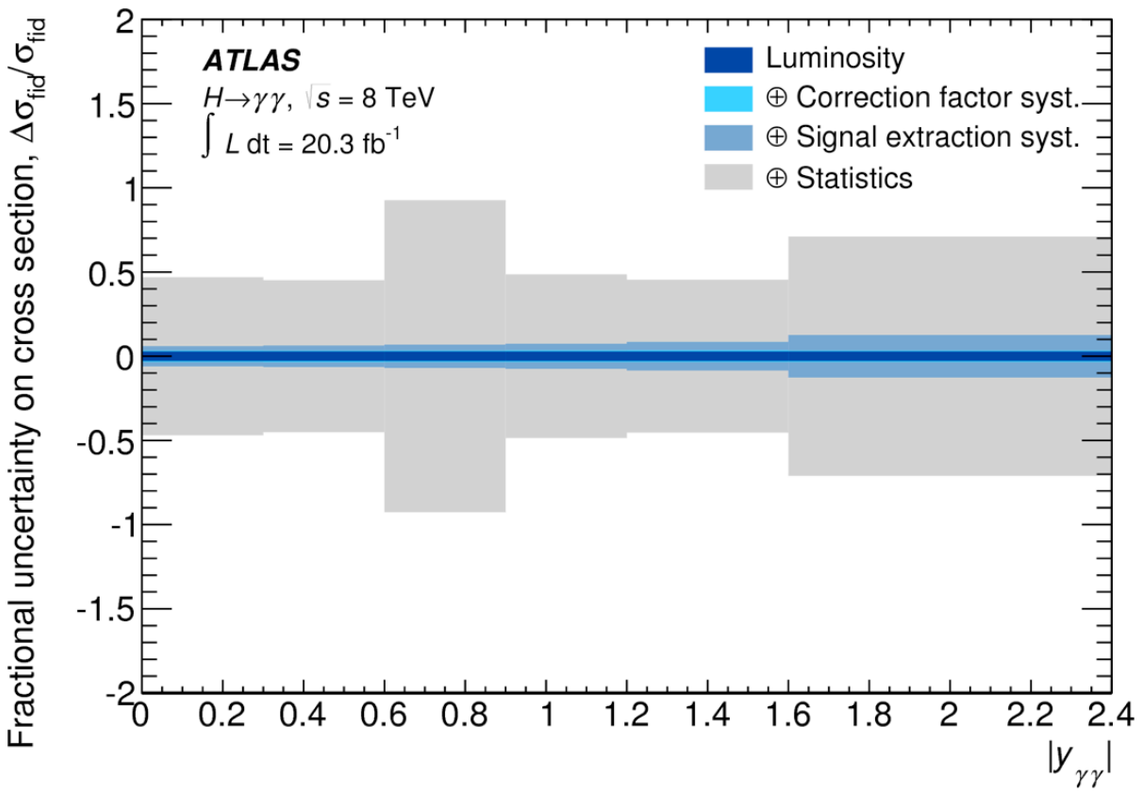

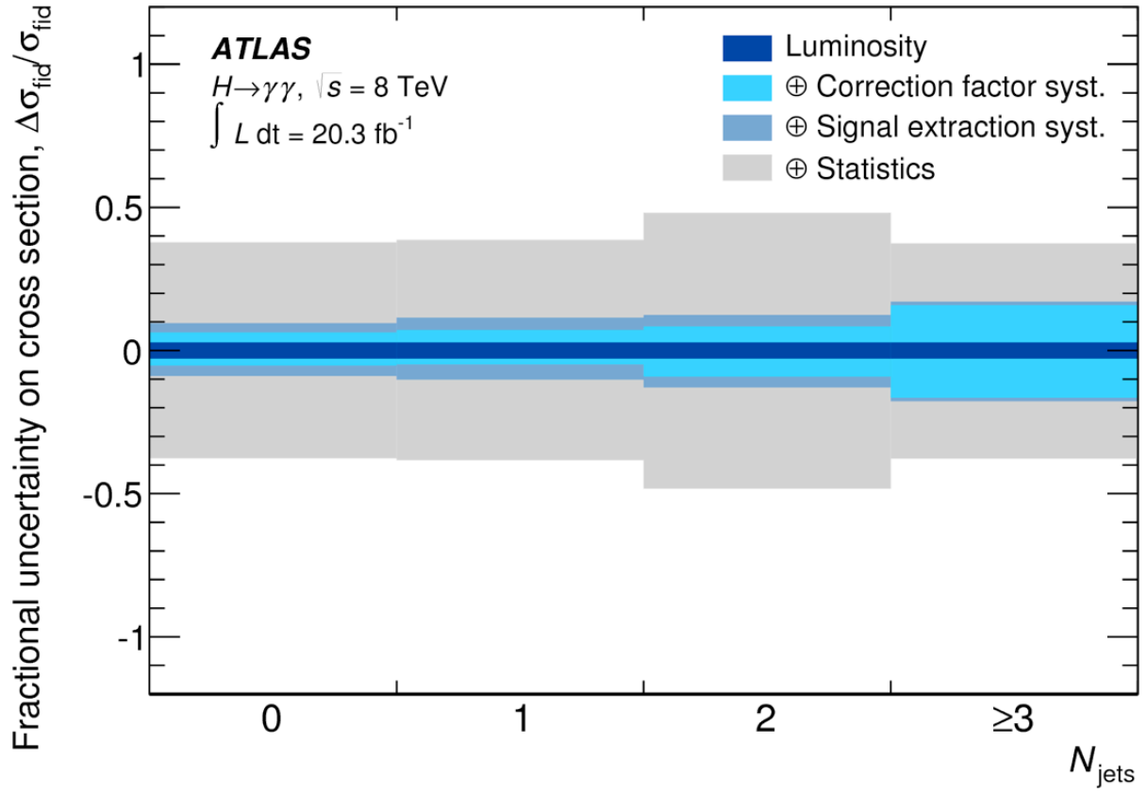

The binning of the differential variables is determined using two criteria. First, the purity of all bins is required to be larger than 60%, where the purity of a given bin is defined using simulation as the fraction of events at detector level that occupy the same bin at particle level. Second, the value of $s/\sqrt{b}$ in each bin is required to be larger than 1.5, where s is the expected number of signal events in a diphoton mass window of ± 4 GeV about the Higgs boson mass and b is the corresponding number of background events estimated from the data by linearly extrapolating the number of events observed outside of that window. In the rare case of the fit to data producing a negative yield in a differential distribution, the affected bin is merged with a neighbouring bin in order to ensure a positive yield (only one such case occurs).

$H\to\gamma\gamma/H\to ZZ^{(*)}\to 4l$: Fiducial region definition

In all cases, there is an effort to keep the fiducial near the analysis signal region. In the $H\to\gamma\gamma$ case, isolation is included in the fiducial region definition, in the $H\to ZZ(*)\to 4l$ case, it is not included.

the combined m_H is assumed. in $H\to\gamma\gamma$ [higher statistics] the effect of fixed or floating m_H was found to have negligible effect.

The measured fiducial cross section distributions are compared to three ggF theoretical calculations, POWHEG without the adjustments to the $p_{T,H}$ spectrum described above, POWHEG interfaced to MINLO (Multi-scale improved NLO) [53] and HRES2 (v.2.2) [18, 19]. POWHEG with MINLO provides predictions for jet-related variables at NLO for Higgs boson production in association with one jet. The HRES2 program computes fixed-order cross sections for ggF SM Higgs boson production up to NNLO. All-order resummation of soft-gluon effects at small transverse momenta is consistently included up to NNLL, using dynamic factorization and resummation scales. The program implements top- and bottom-quark mass dependence up to NLL+NLO. At NNLL+NNLO level only the top-quark contribution is considered. HRES2 does not perform showering, therefore no QED final state radiation effects are included.

H→ZZ(*)→4l: Backgrounds

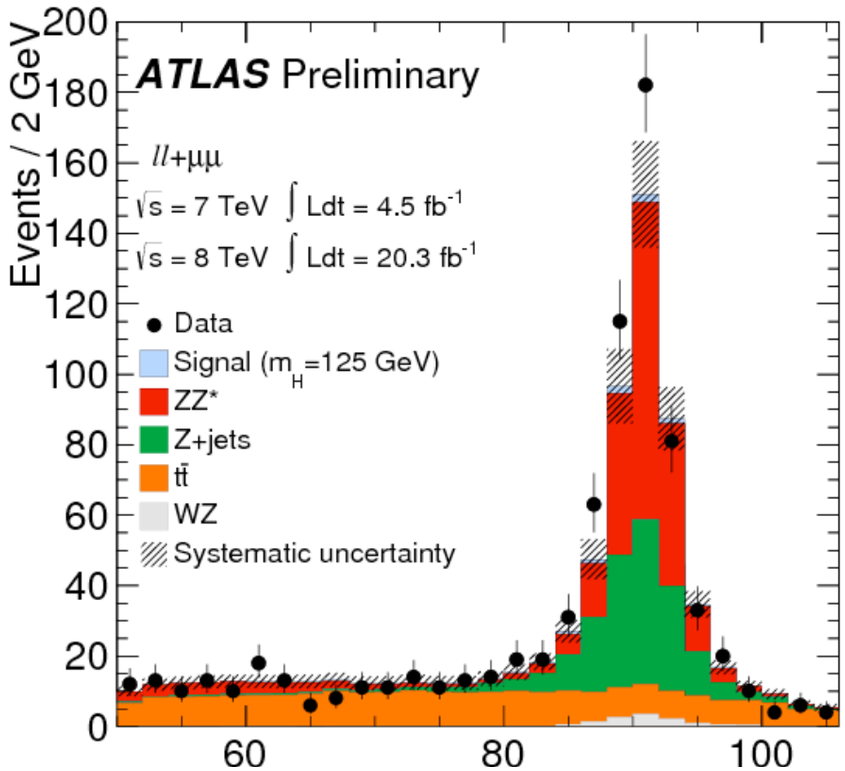

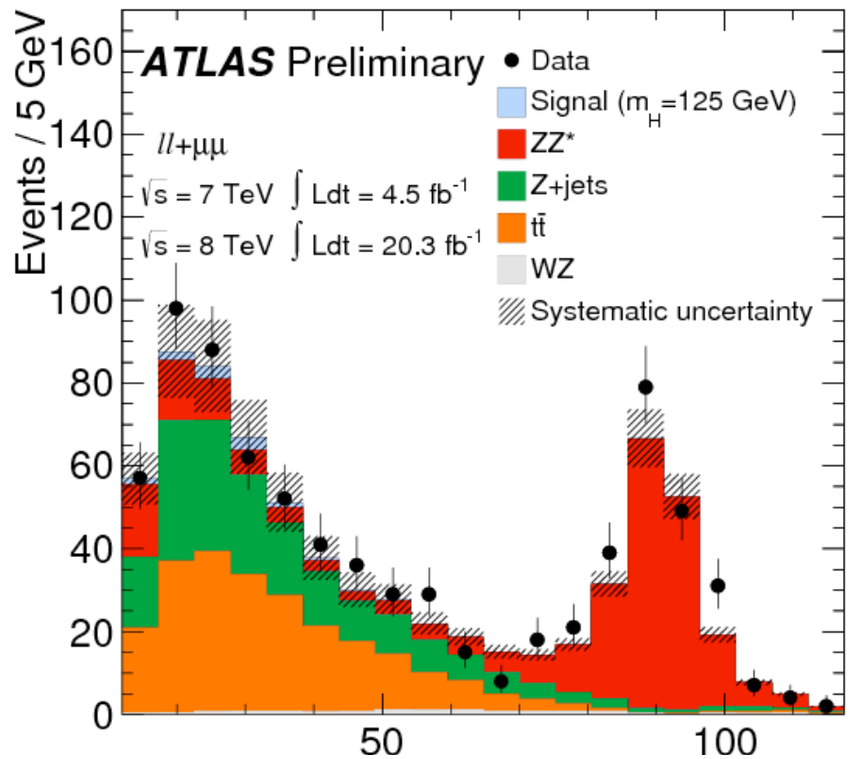

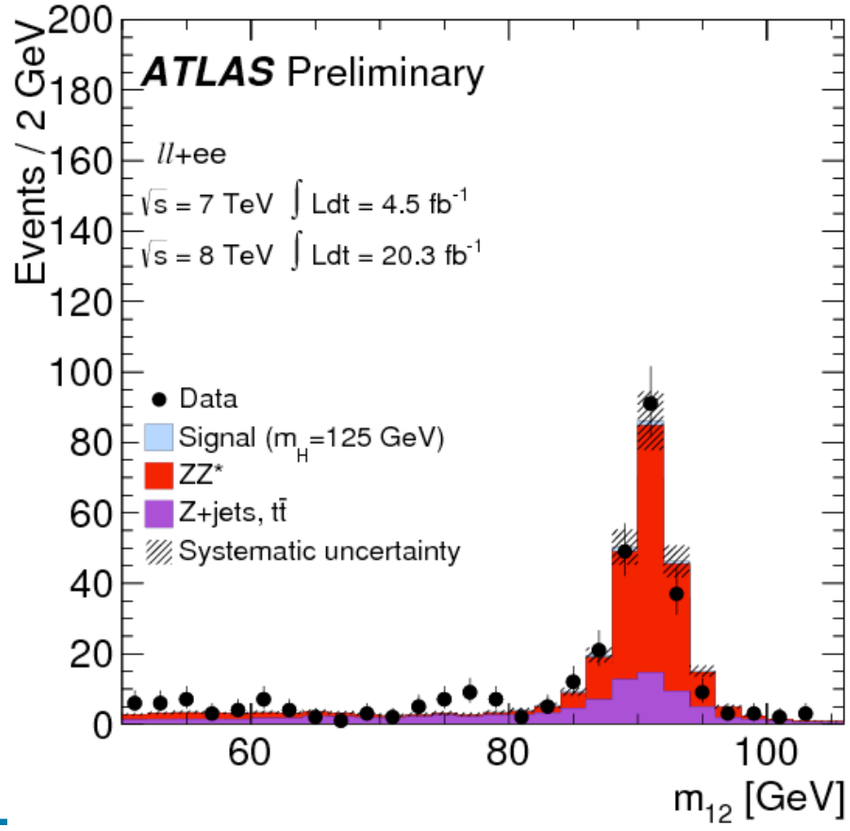

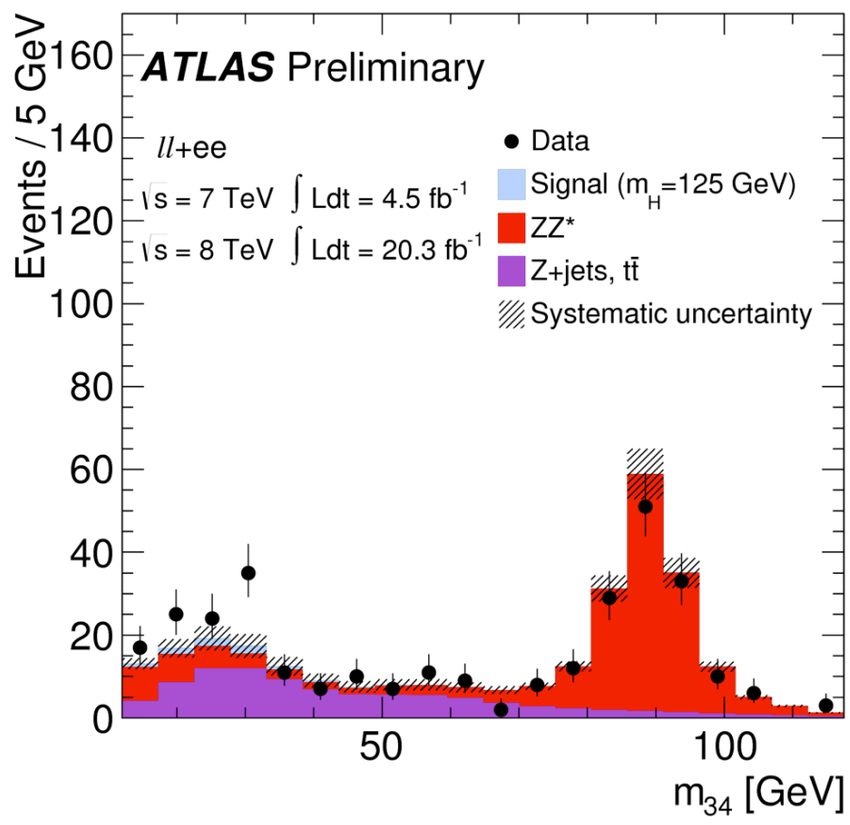

H→ZZ(*)→4l: SR plots

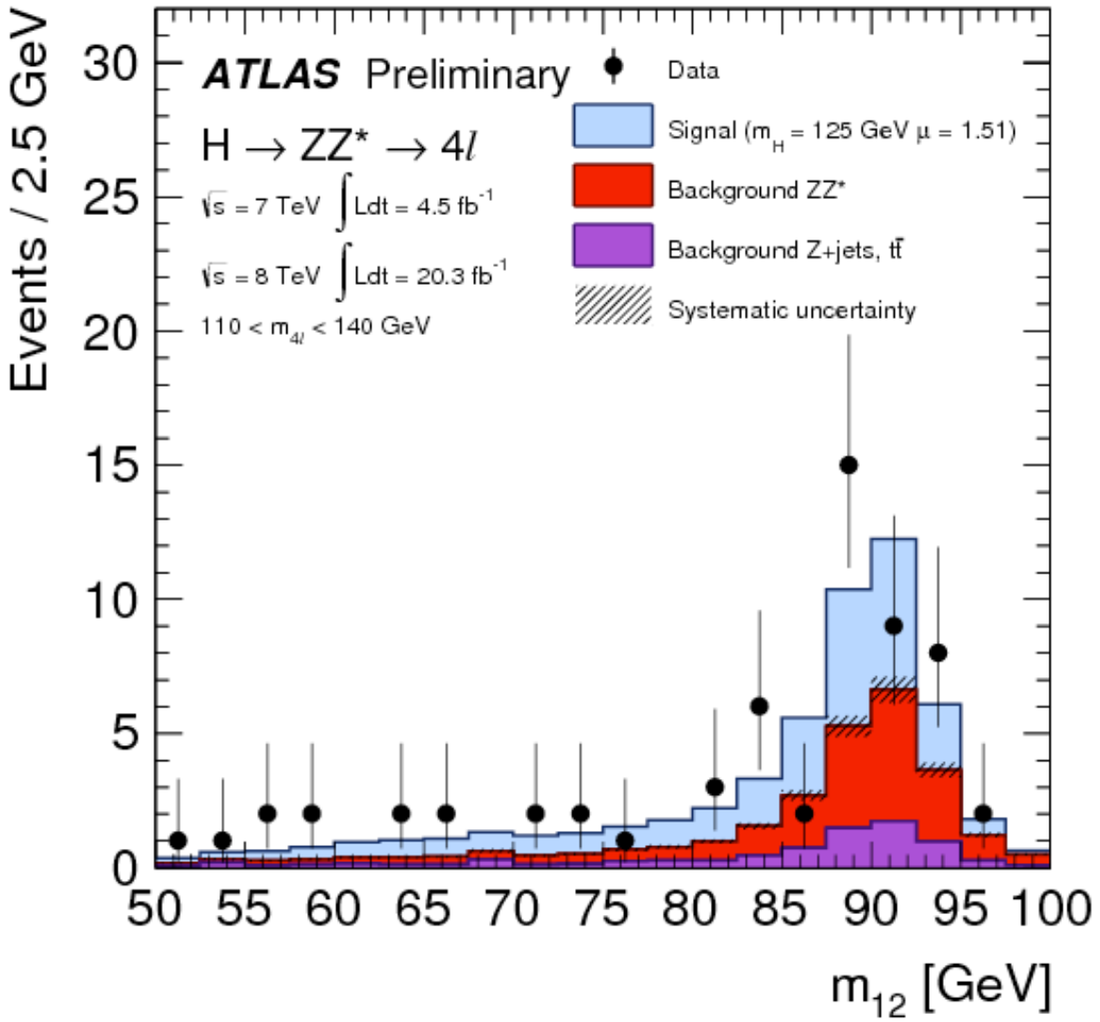

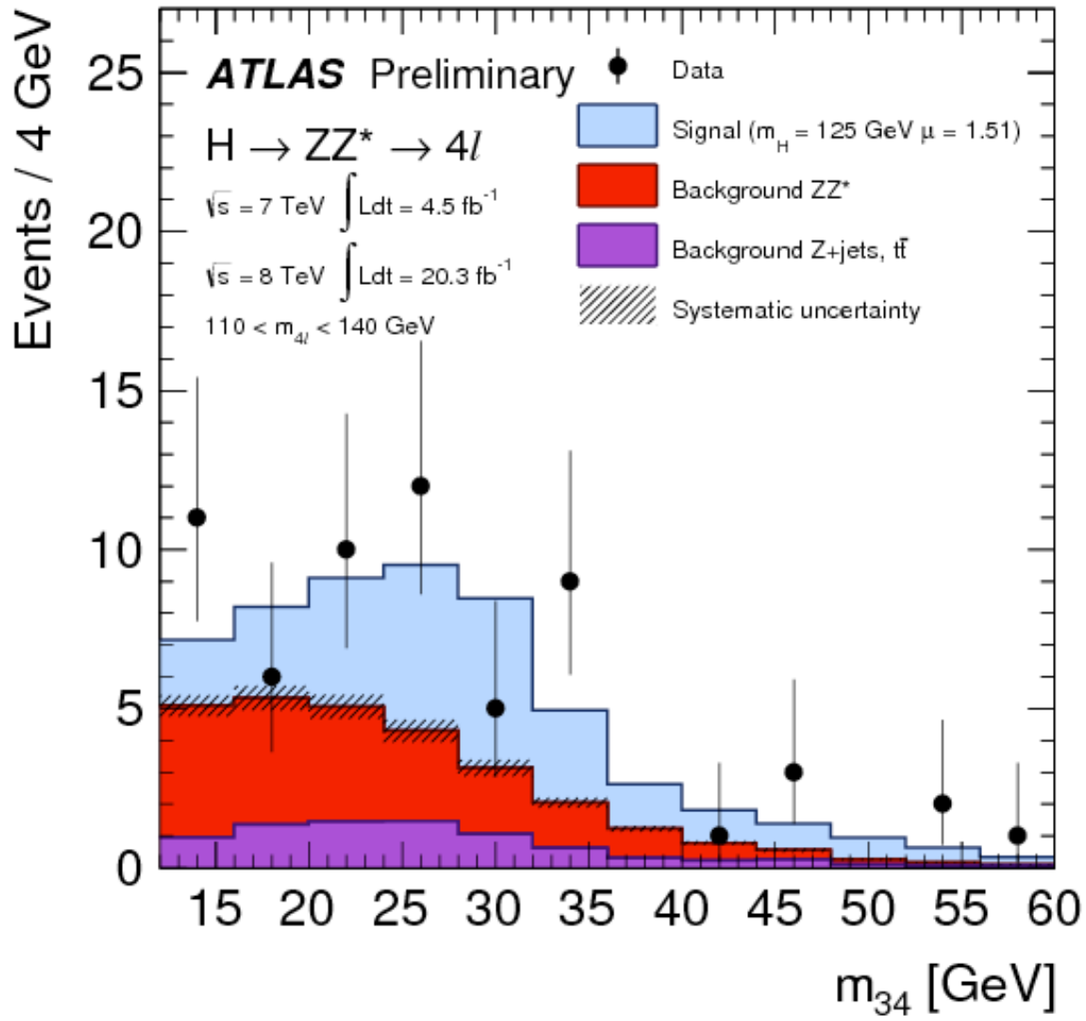

H→ZZ(*)→4l: Yields

	Signal	ZZ(*)	Other BKG	Observed	S/B
4μ	6.20±0.61	2.82±0.14	0.79±0.13	14	~1.7
2μ2e	3.15±0.32	1.38±0.08	0.72±0.12	6	~1.5
2e2μ	4.04±0.40	1.99±0.10	0.69±0.11	9	~1.5
4e	2.77±0.29	1.22±0.08	0.76±0.11	8	~1.4

120-130 GeV

120-130 GeV

	Signal	ZZ(*)	Other Backgrounds	Observed	S/B
4μ	6.3±0.8	2.8±0.1	0.55±0.15	13	~1.9
2μ2e	3.0±0.4	1.4±0.1	1.56±0.33	5	~1.0
2e2μ	4.0±0.5	2.1±0.1	0.55±0.17	7	~1.5
4e	2.6±0.4	1.2±0.1	1.11±0.28	6	~1.1

H→ZZ(*)→4l: π/K→μ

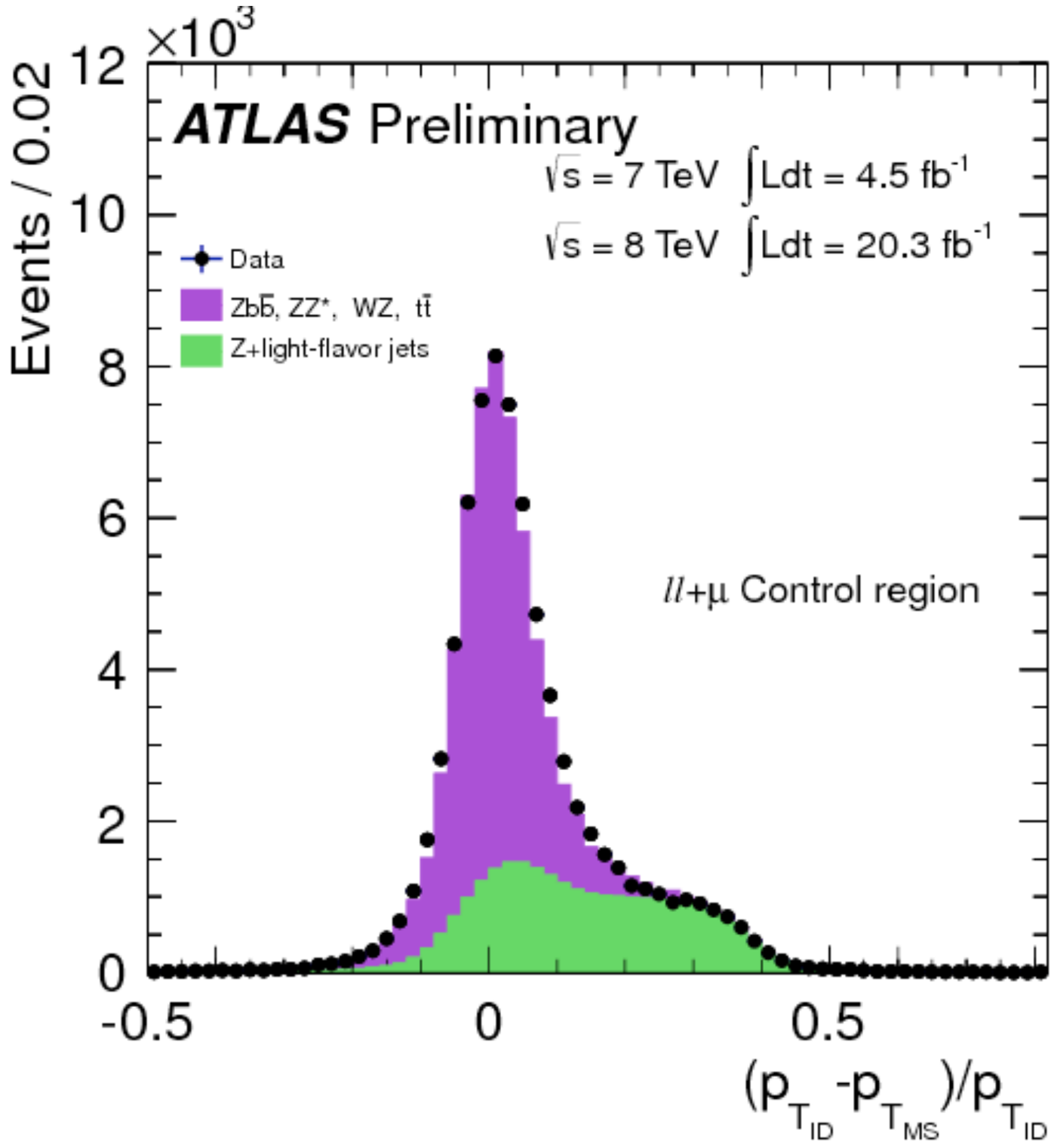
ATLAS Preliminary
√s = 7 TeV ∫Ldt = 4.5 fb-1
√s = 8 TeV ∫Ldt = 20.3 fb-1
Data
Zbb̄, ZZ*, WZ, tt̄
Z+light-flavor jets
ll+μ Control region
Events / 0.02
×10^3
12
10
8
6
4
2
0
-0.5
0
0.5
(p_T_ID - p_T_MS)/p_T_ID

H→ZZ(*)→4l: ll+μμ backgrounds

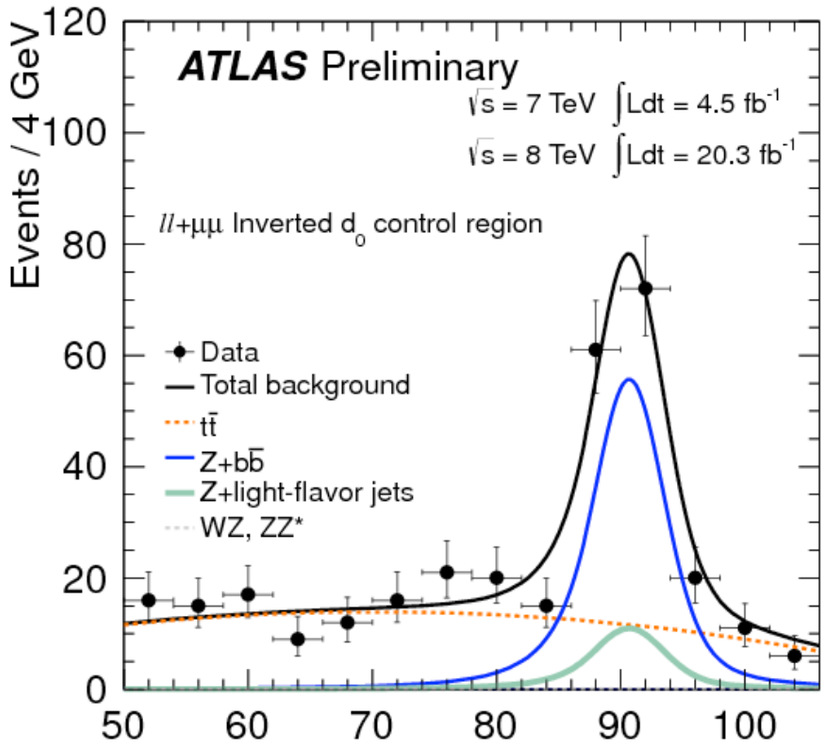

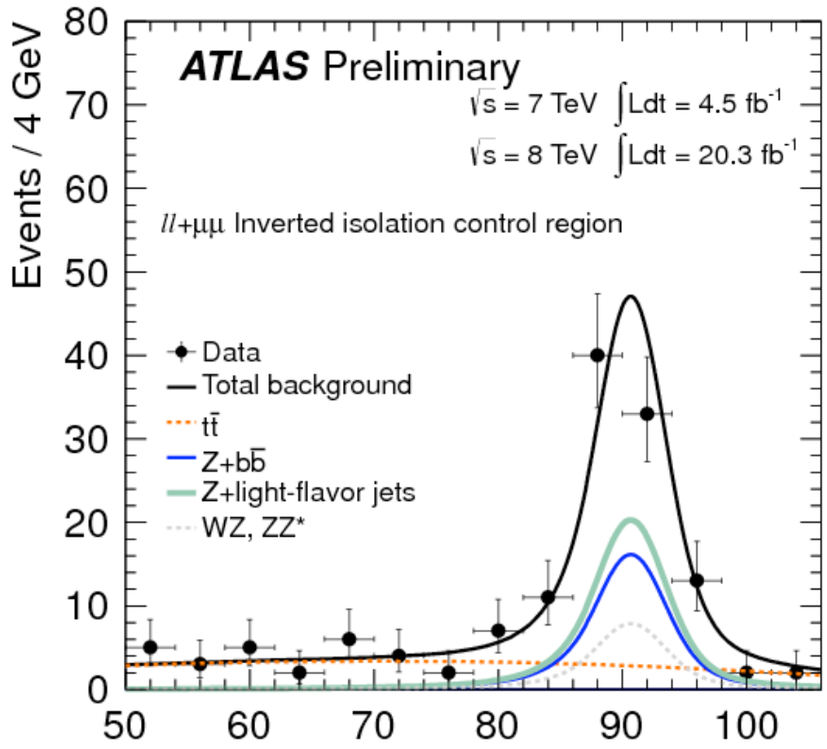

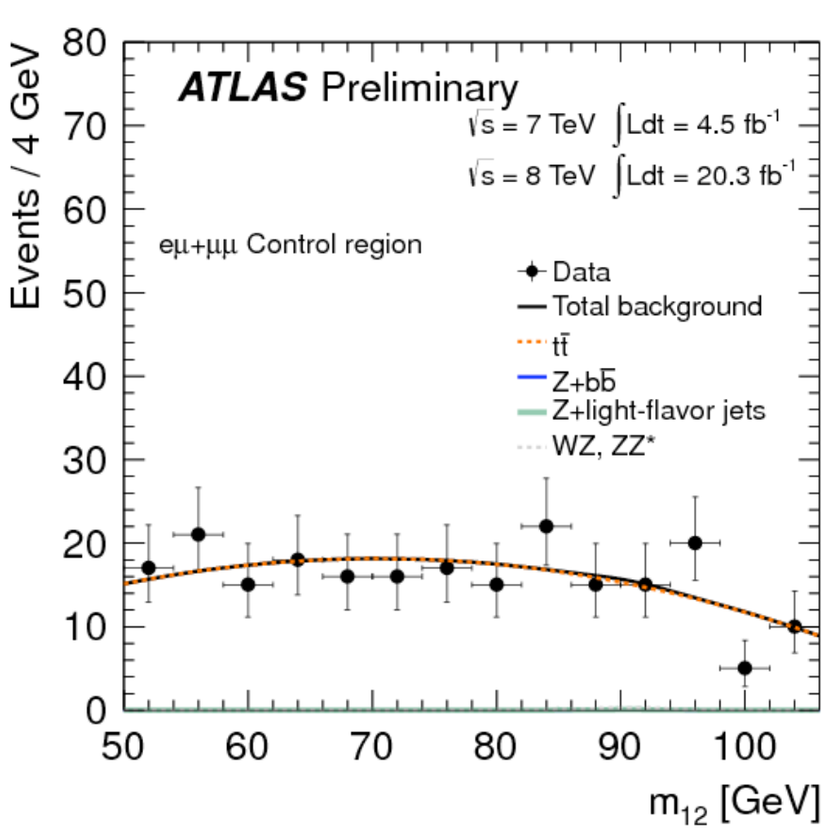

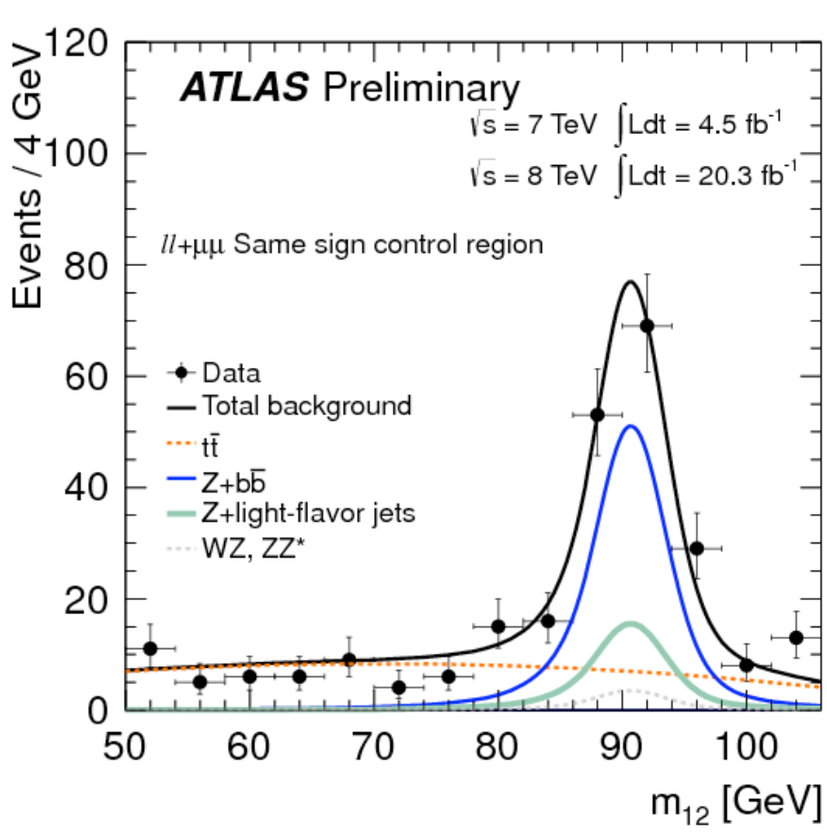

$H \to ZZ^{(*)} \to 4l$: ll+ee backgrounds

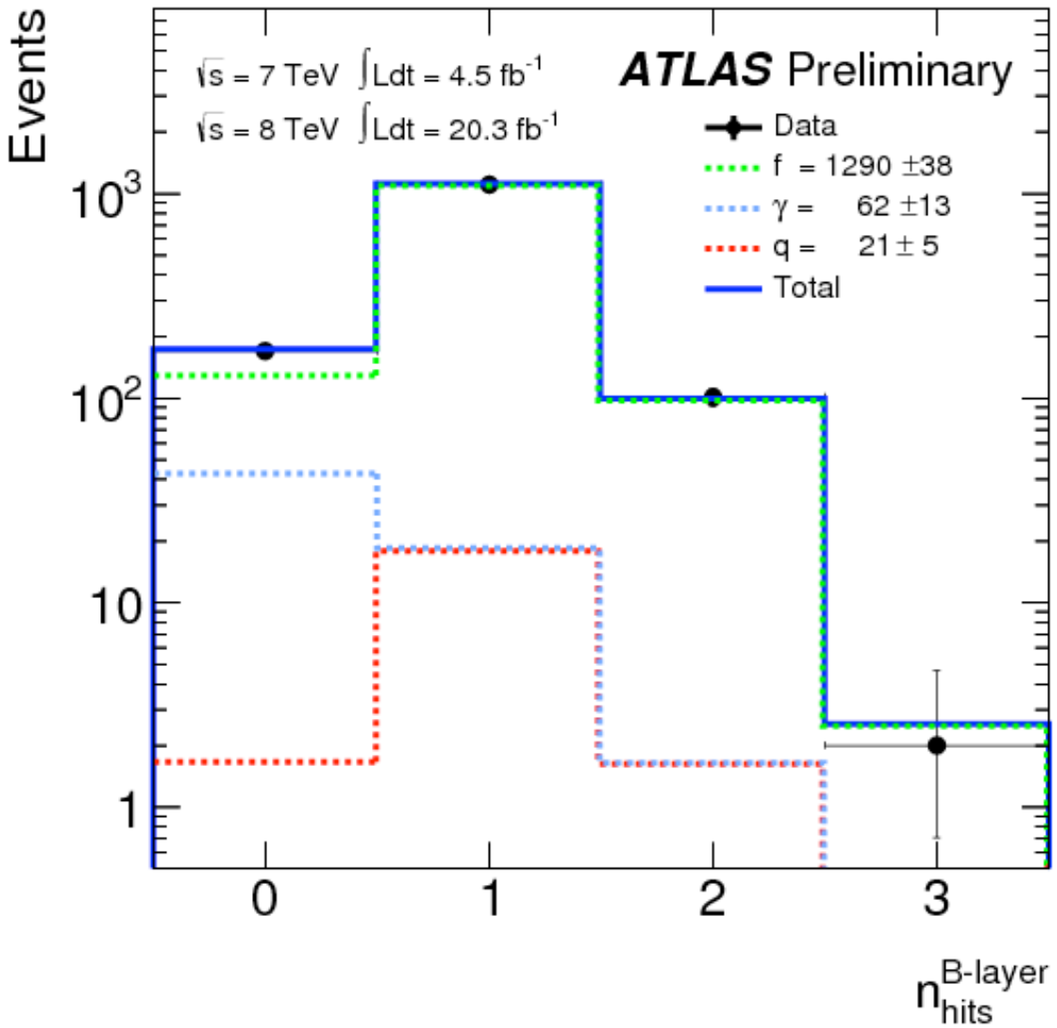

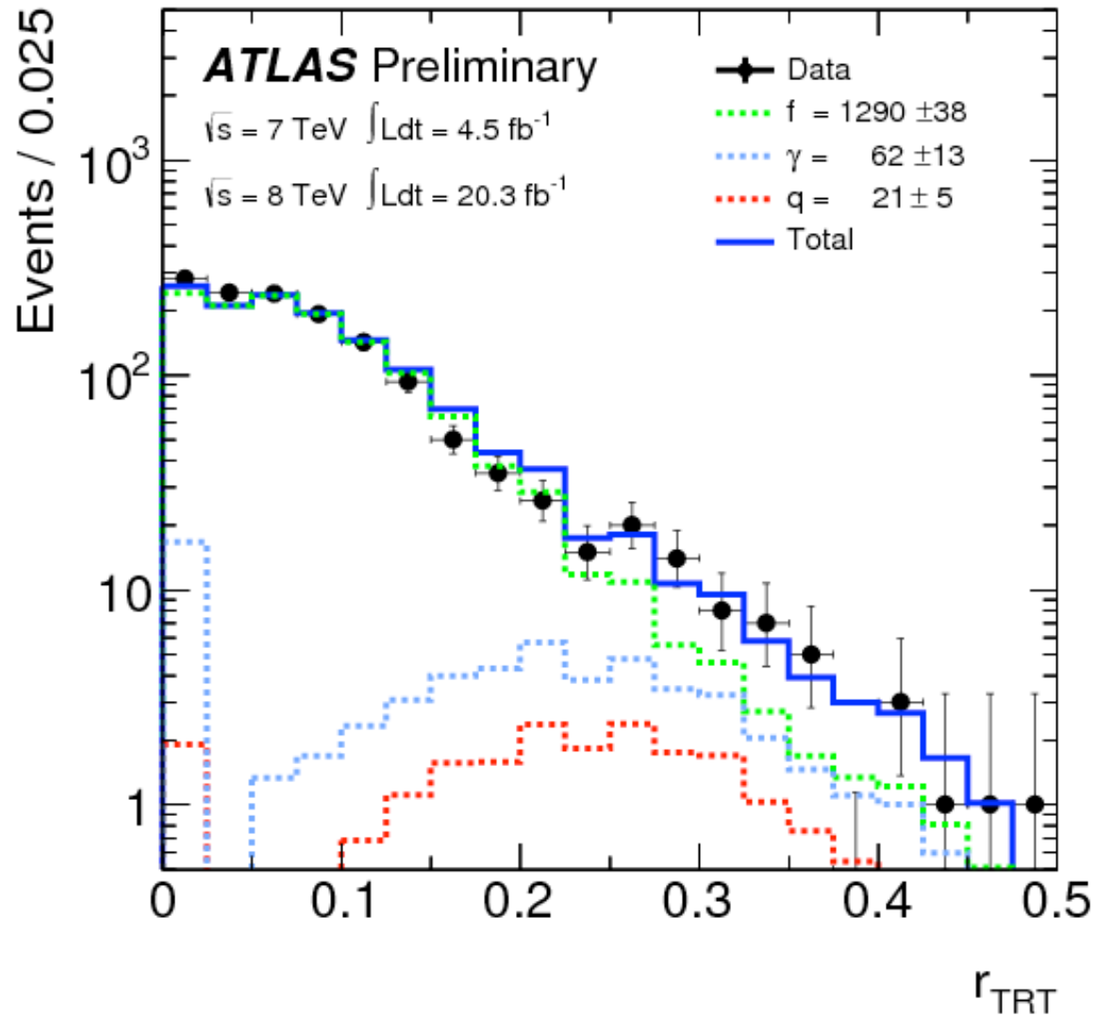

H→ZZ(*)→4l: Inclusive signal strength

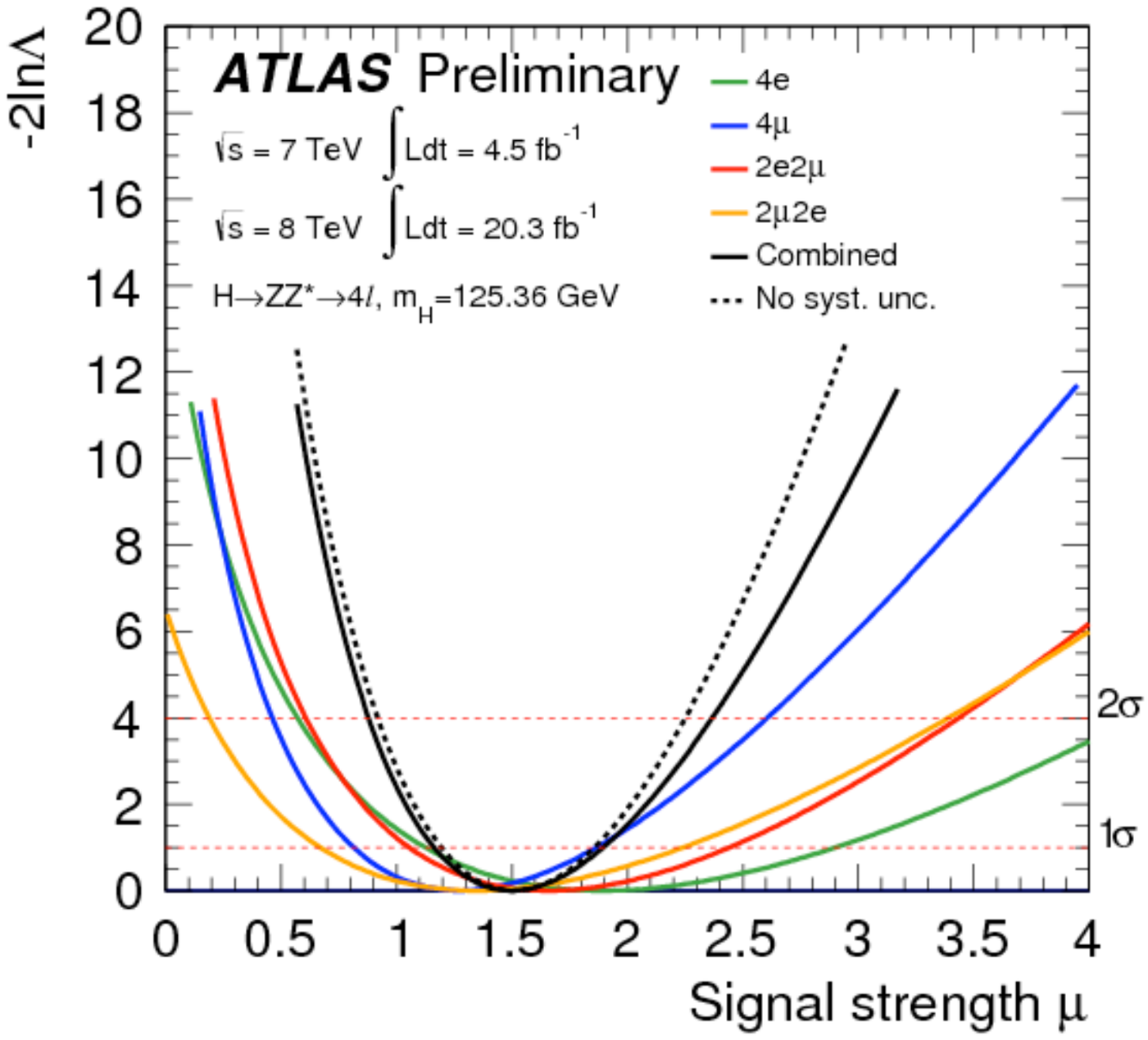

$H \rightarrow ZZ^{(*)} \rightarrow 4l$: BDT Discriminants

NEW!

BDT discriminant introduced to suppress ZZ* contribution
- Inputs: Matrix Element-based Kinematic Discriminant, p_{T4l}, η_{4l}

BDT discriminant introduced to discriminate between VBF signal and other (mainly ggF) contributions
- Inputs: m_{jj}, $\Delta\eta_{jj}$, Leading and Sub-leading jet pT, leading jet η

BDT discriminant introduced to discriminate between VH hadronic signal and other (mainly ggF) signals
- Inputs: m_{jj}, $\Delta\eta_{jj}$, Leading and Sub-leading jet pT, leading jet η

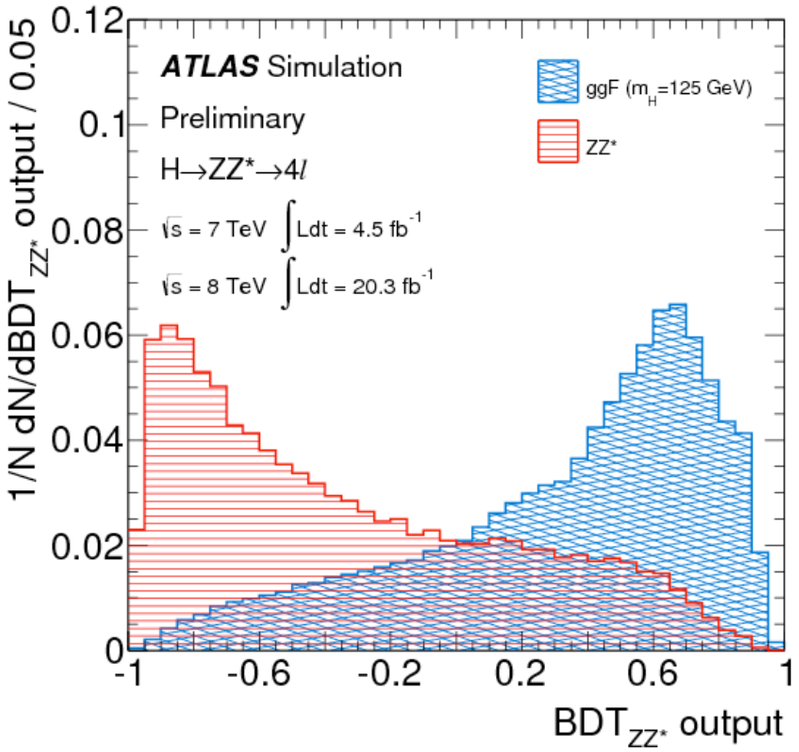

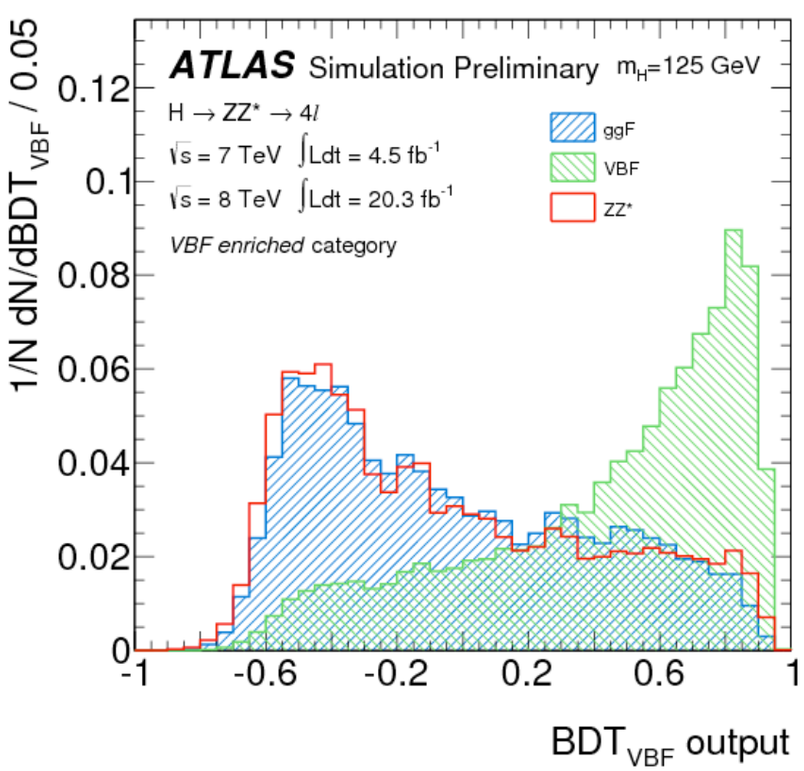

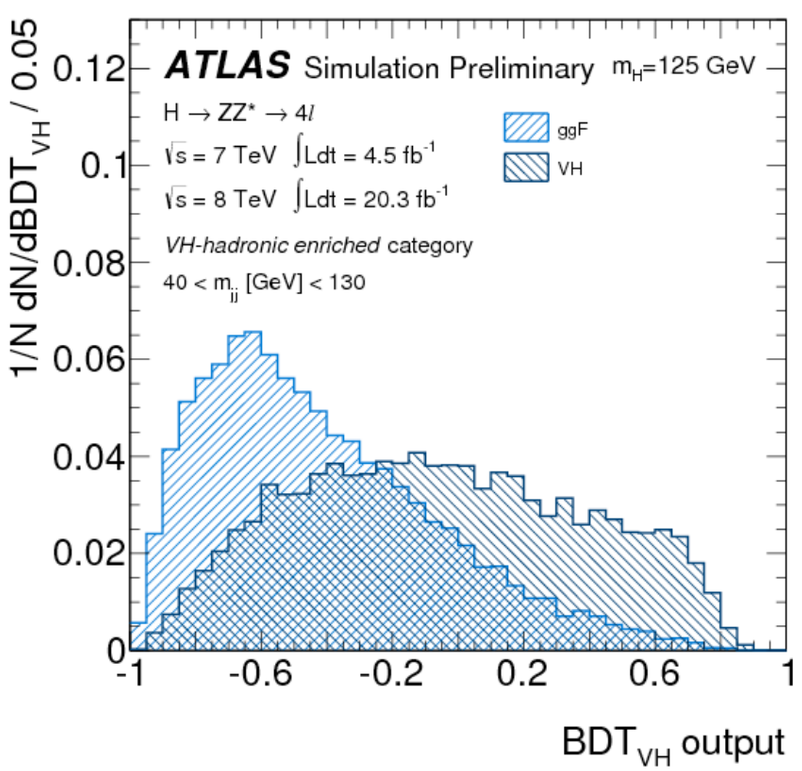

H→ZZ(*)→4l: Event Categorization

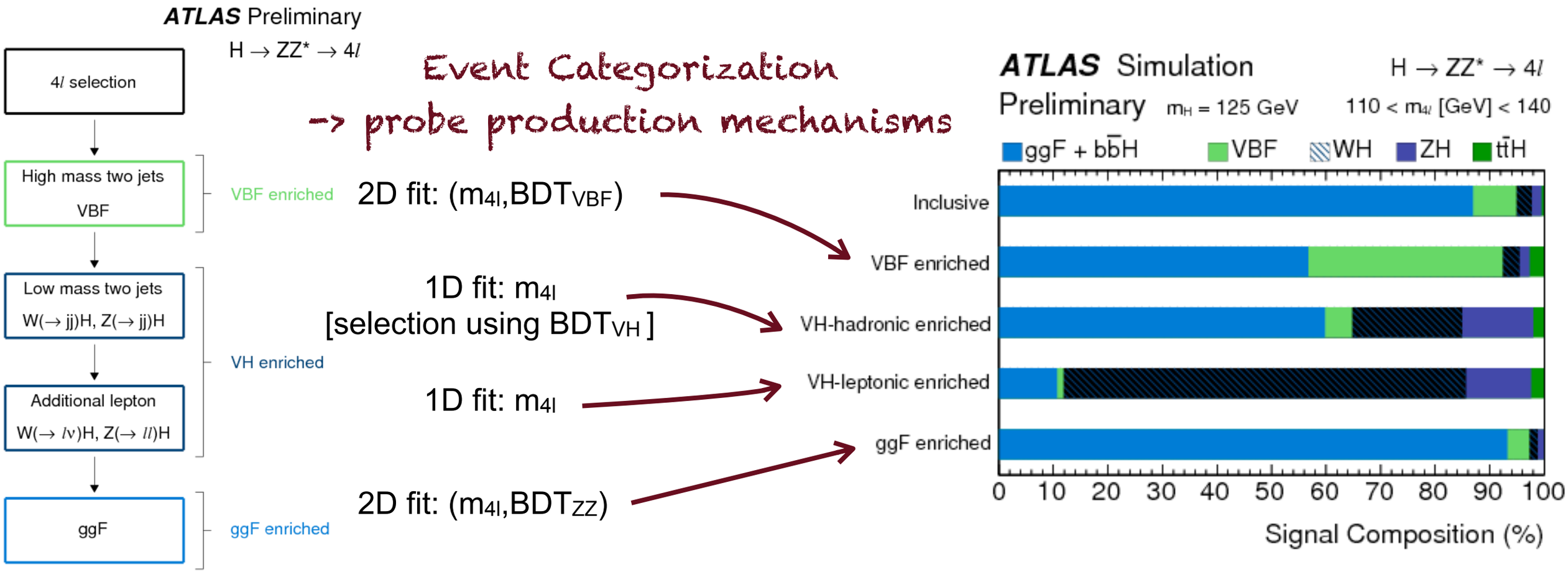

$H \to ZZ^{(*)} \to 4l$: Coupling Results (II)

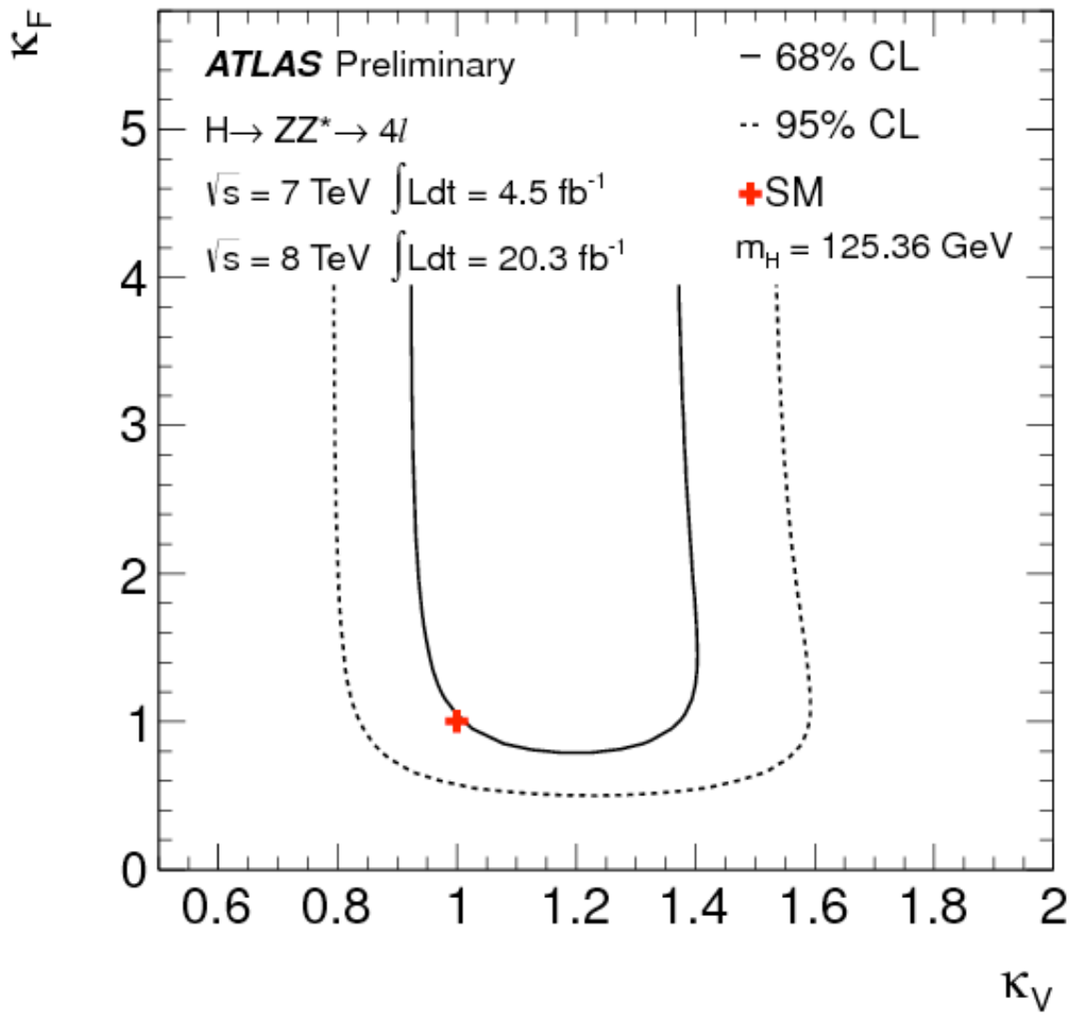

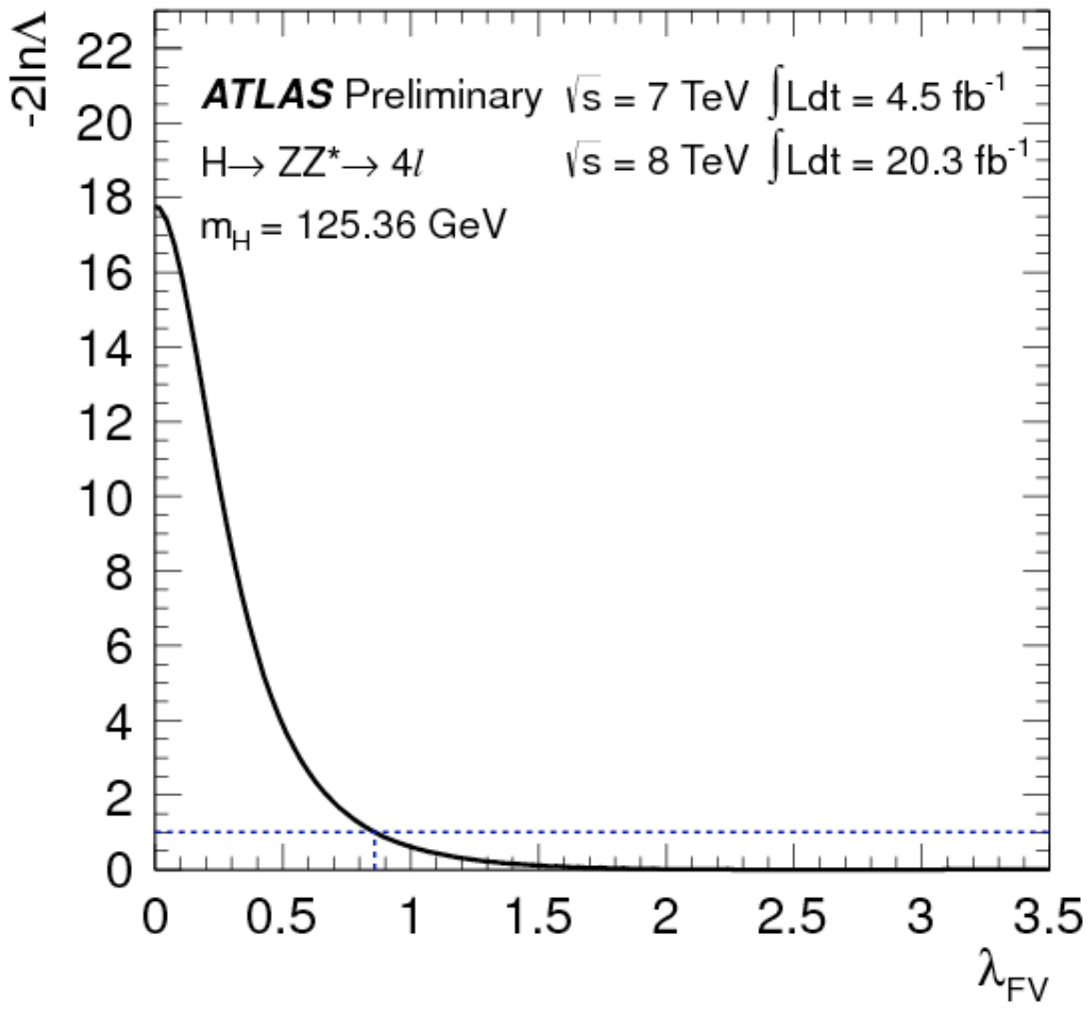

$H\rightarrow\gamma\gamma$: m_H

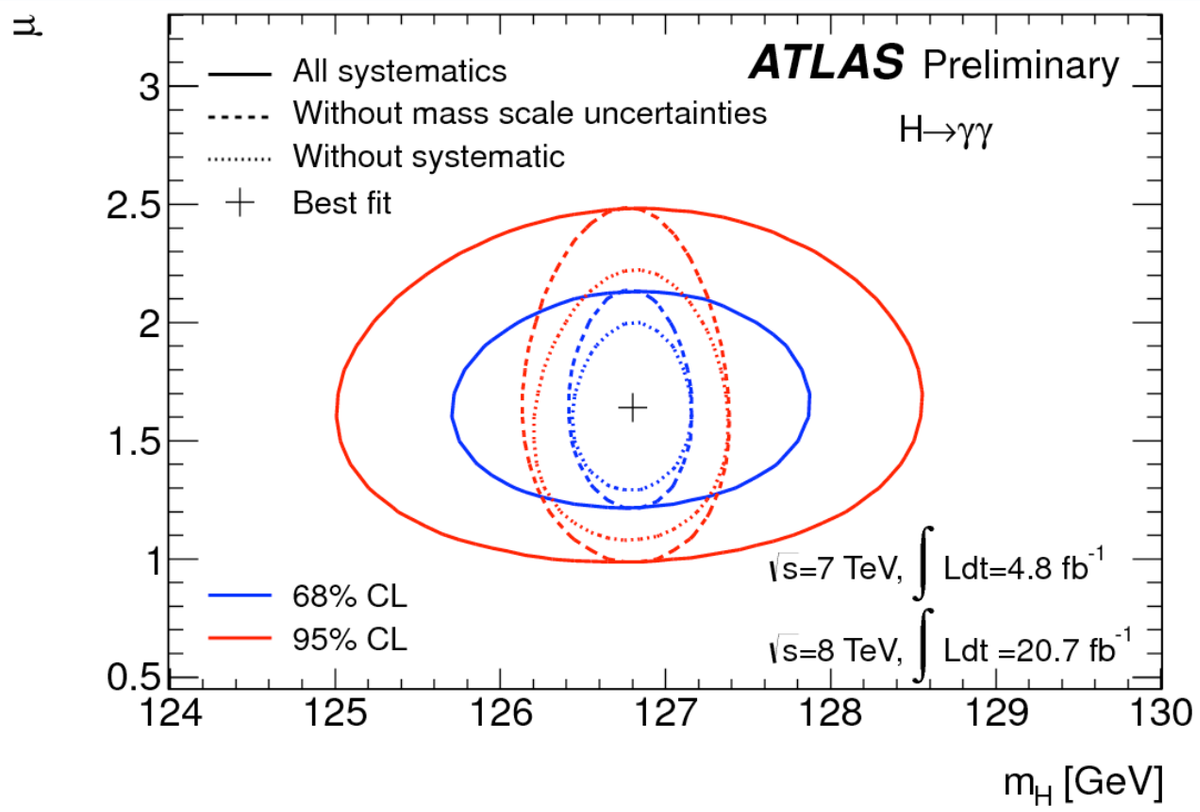

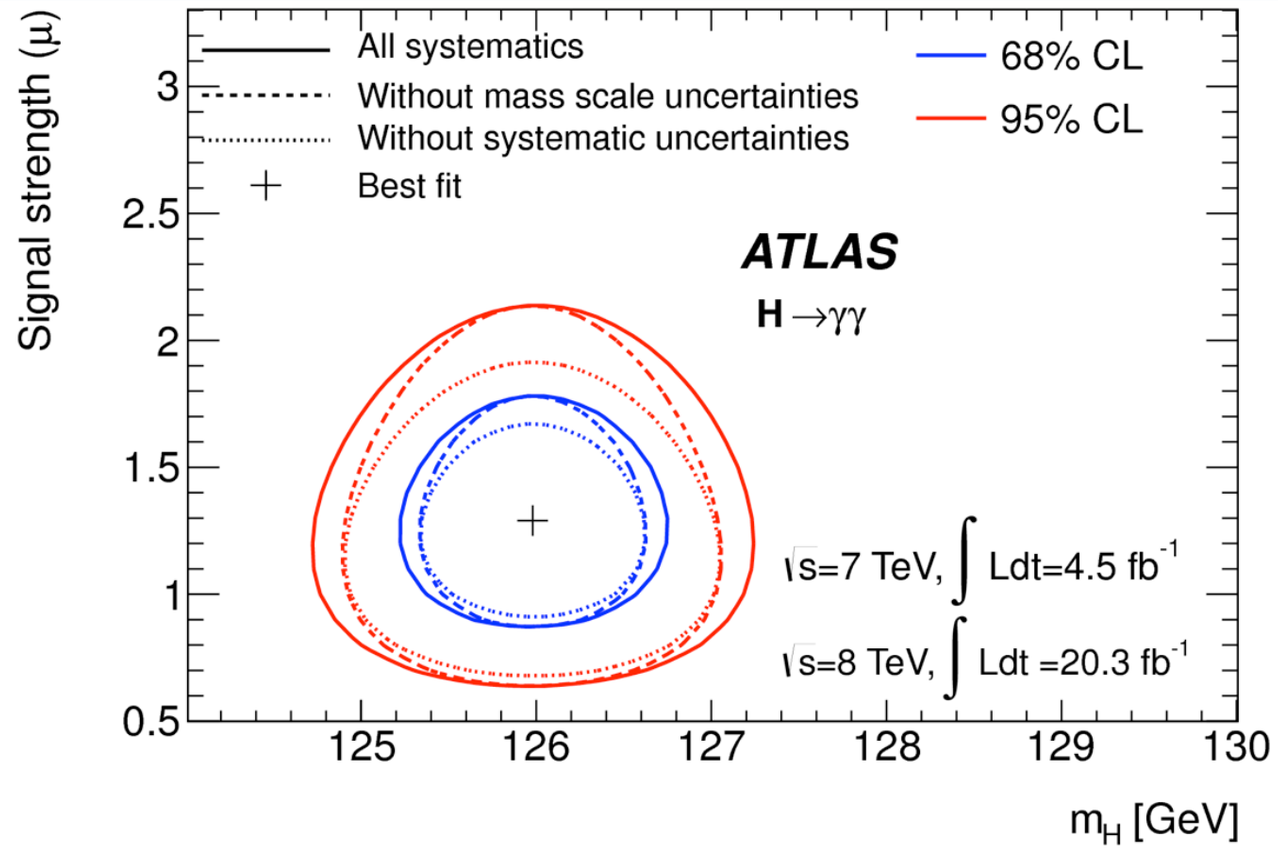

Higgs boson mass measurement using $H\rightarrow\gamma\gamma$:

- OLD : **126.8 ± 0.2 (stat) ± 0.7 (syst) GeV**
- NEW: **125.98 ± 0.42(stat) ± 0.28(syst) GeV**
- consistent with expected change from updated photon energy scale calibration
  - average shift of -0.45 GeV with stat spread ~0.35 GeV expected
  - estimated from the distribution of the mass difference of the common events in the mass sidebands
- statistical uncertainty compatible with expected for given signal level (p-value 16%)
  - larger than in the past: a) lower signal, and b) larger resolution (in the past the observed resolution was better than expected for ideal detector)

$H \to ZZ^{(*)} \to 4l$: m_H

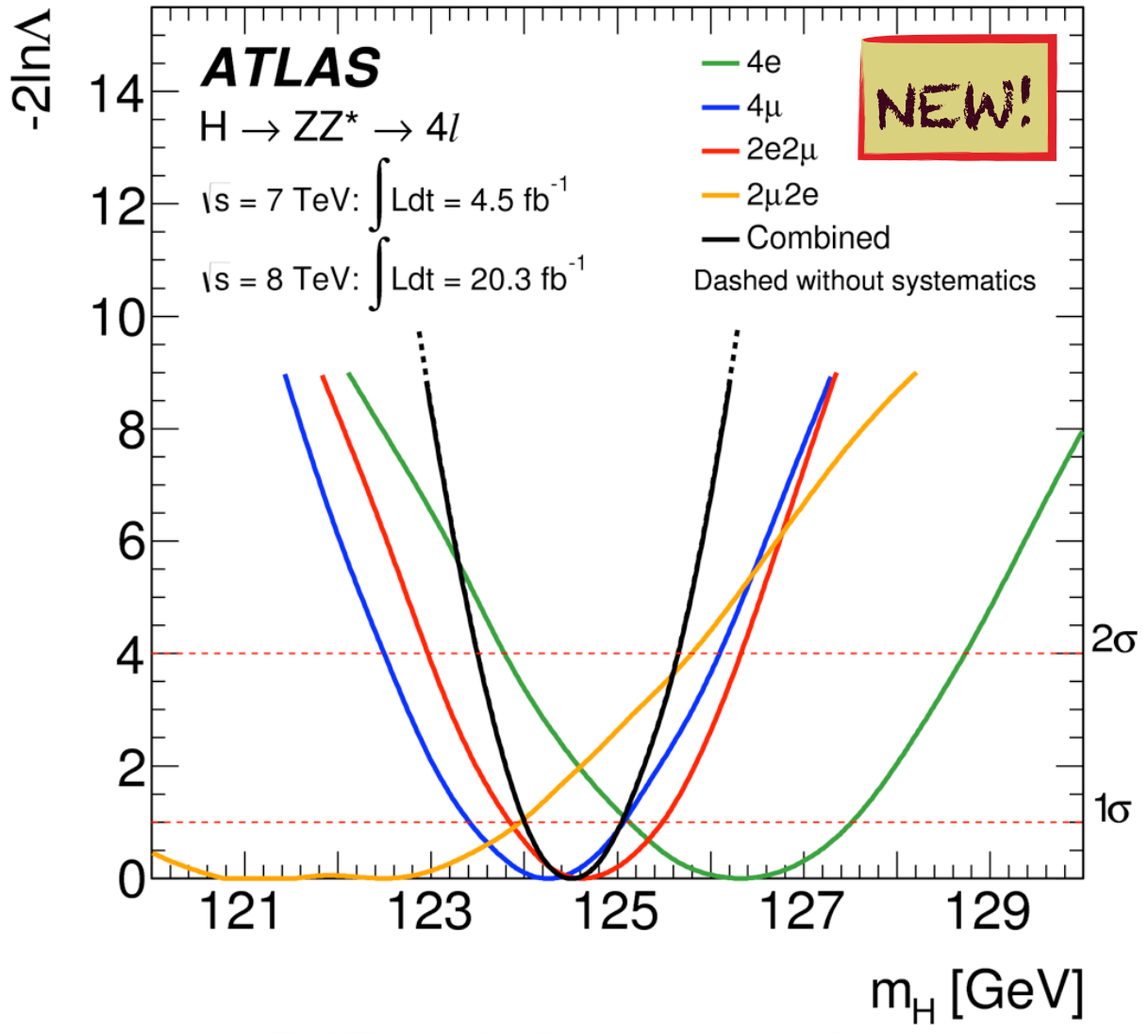

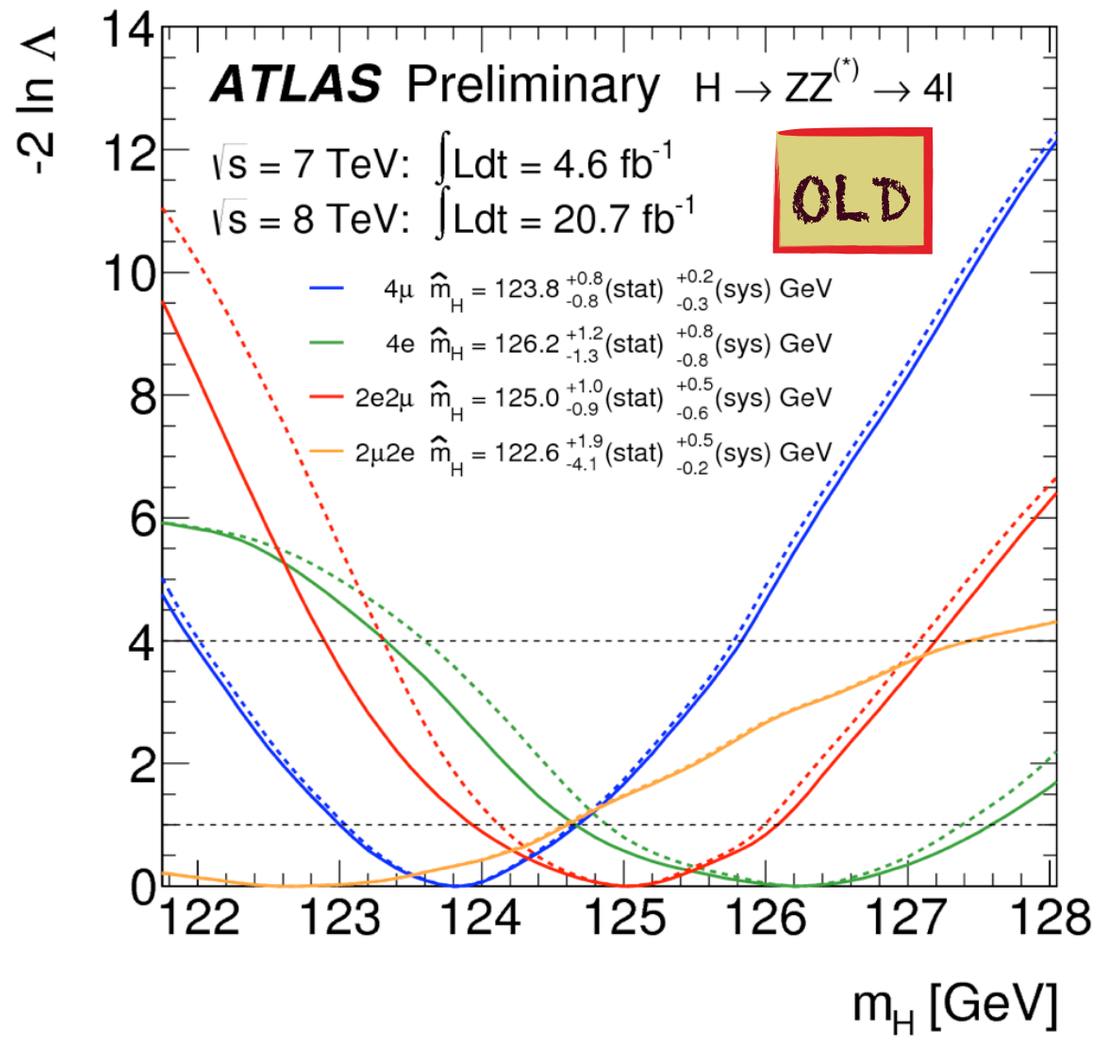

Higgs boson mass measurement using H→ZZ→4l:

- OLD : **$124.3^{+0.6}_{-0.5}(\text{stat})^{+0.5}_{-0.3}(\text{syst})$ GeV**
- NEW : **124.51 ± 0.52(stat) ± 0.06(syst) GeV**
- increases up to 8%
- H→4l consistency leads to -0.8σ adjustment of e/γ energy scale
  - shift -350 MeV for H→γγ mass
- CMS : m_H = **125.7 ± 0.3 (stat) ± 0.3 (syst) GeV**

$H \to ZZ^{(*)} \to 4l$/$H \to \gamma\gamma$: m_H and Γ_H measurement

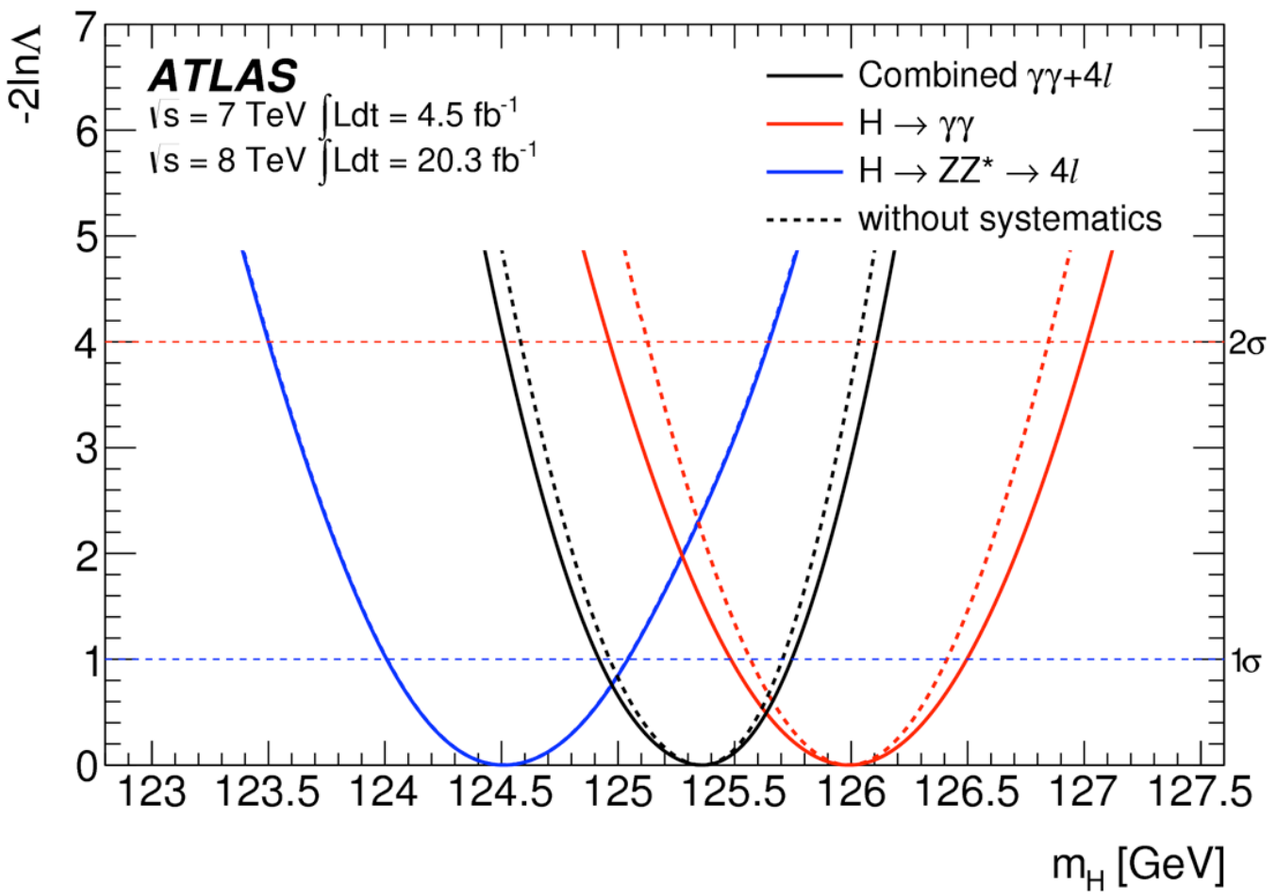

Channel	Mass measurement [GeV]
$H \to \gamma\gamma$	$125.98 \pm 0.42\,(\text{stat}) \pm 0.28\,(\text{syst}) = 125.98 \pm 0.50$
$H \to ZZ^* \to 4\ell$	$124.51 \pm 0.52\,(\text{stat}) \pm 0.06\,(\text{syst}) = 124.51 \pm 0.52$
Combined	$125.36 \pm 0.37\,(\text{stat}) \pm 0.18\,(\text{syst}) = 125.36 \pm 0.41$

individual measurement compatibility: **1.97σ**
- fixing rates to SM expectation →1.6σ
- γ systematics as box →1.8σ

New e/γ calibration, improved analyses and reduce systematics
[previous result: 125.5 ± 0.2 (stat)$^{+0.5}_{-0.6}$ (syst) GeV]

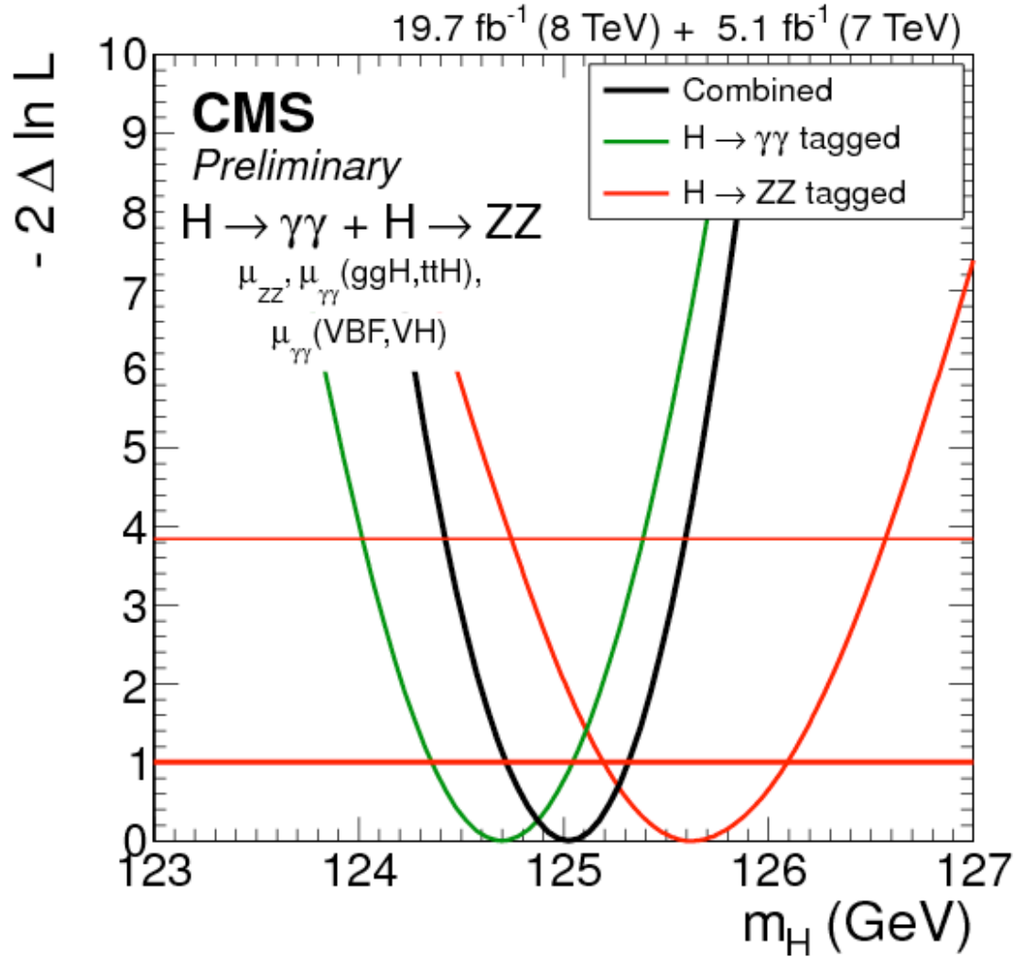

H→γγ: **124.70 ± 0.31(stat) ± 0.15(syst) GeV**

H→ZZ→4l: **125.6 ± 0.4(stat) ± 0.2(syst) GeV**

Combined: **$125.03^{+0.26}_{-0.27}(\text{stat})^{+0.13}_{-0.15}(\text{syst})$ GeV**
individual measurement compatibility: **1.6σ**

Indirect Γ_H measurement: Systematics

	Observed			Median expected		
$R^B_{H^*}$	0.5	**1.0**	2.0	0.5	**1.0**	2.0
cut-based	10.8	**12.2**	14.9	13.6	**15.6**	19.9
ME-based discriminant analysis	6.1	**7.2**	9.9	8.7	**10.2**	14.0

Table 3: The observed and expected 95% CL upper limits on $\mu_{\text{off-shell}}$ in the cut-based and the ME-based discriminant analyses in the 4ℓ channel, within the range of $0.5 < R^B_{H^*} < 2$. The bold numbers correspond to the limit assuming $R^B_{H^*} = 1$. The upper limits are evaluated using the CL_s method, with the alternative hypothesis $R^B_{H^*} = 1$ and $\mu_{\text{off-shell}} = 1$.

Source of systematic uncertainties	95% CL on $\mu_{\text{off-shell}}$
QCD scale for $gg \to ZZ$	9.5
QCD scale for the $gg \to (H^* \to)ZZ$ interference	9.2
QCD scale for $q\bar{q} \to ZZ$	8.8
PDF for $pp \to ZZ$	8.7
EW for $q\bar{q} \to ZZ$	8.7
Luminosity	8.8
electron efficiency	8.7
μ efficiency	8.7
All systematic	10.2
No systematic	8.7

Table 4: The expected 95% CL upper limit on $\mu_{\text{off-shell}}$ in the ME-based discriminant analysis in the 4ℓ channel, with a ranked listing of each systematic uncertainty individually, comparing with no systematic uncertainty or all systematic uncertainties. The upper limits are evaluated using the CL_s method, assuming $R^B_{H^*}$=1.

Indirect Γ_H measurement: Systematics

	Observed			Median expected		
$R^B_{H^*}$	0.5	**1.0**	2.0	0.5	**1.0**	2.0
$2\ell 2\nu$ cut-based	10.4	**11.3**	12.8	8.6	**9.9**	12.9

Table 5: The observed and expected 95% CL upper limit on $\mu_{\text{off-shell}}$ in the $2\ell 2\nu$ channel, within the range of $0.5 < R^B_{H^*} < 2$. The bold numbers correspond to the limit assuming $R^B_{H^*} = 1$. The upper limits are evaluated using the CL_s method, with the alternative hypothesis $R^B_{H^*} = 1$ and $\mu_{\text{off-shell}} = 1$.

Source of systematic uncertainties	95% CL on $\mu_{\text{off-shell}}$
QCD scale for $gg \to ZZ$	7.9
QCD scale for the $gg \to (H^* \to)ZZ$ interference	7.7
QCD scale for $q\bar{q} \to ZZ$	7.6
PDF for $pp \to ZZ$	7.2
EW for $q\bar{q} \to ZZ$	7.1
Parton showering	7.1
Z BG systematic	7.4
Luminosity	7.3
Electron energy scale	7.1
Electron ID efficiency	7.1
Muon reconstruction efficiency	7.1
Jet energy scale	7.1
Sum of remaining systematic uncertainties	7.1
All systematic	9.9
No systematic	7.1

Table 6: The expected 95% CL upper limit on $\mu_{\text{off-shell}}$ in the $2\ell 2\nu$ channel, with a ranked listing of each systematic uncertainty individually, and comparing to including no systematic uncertainty or all systematic uncertainties. The upper limits are evaluated using the CL_s method, assuming $R^B_{H^*}$=1.

Indirect Γ_H measurement: Systematics

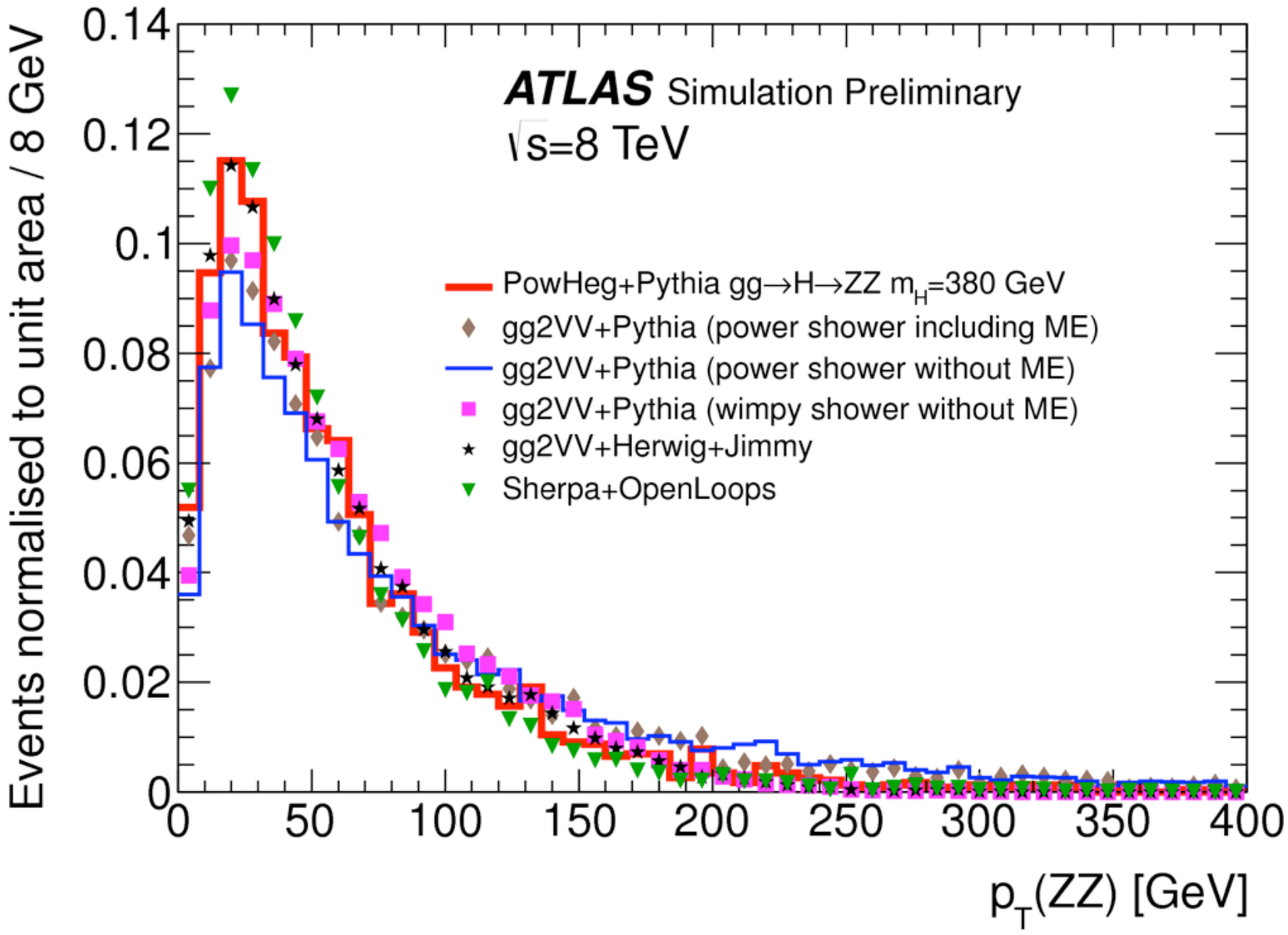

345 GeV< m_{4l} < 415GeV

Indirect Γ_H measurement: Results

Source of systematic uncertainties	95% CL on $\mu_{\text{off-shell}}$
QCD scale for $gg \to ZZ$	6.7
QCD scale for the $gg \to (H^* \to)ZZ$ interference	6.7
QCD scale for $q\bar{q} \to ZZ$	6.4
Z BG systematic	6.2
Luminosity	6.2
PDF for $pp \to ZZ$	6.1
Sum of remaining systematic uncertainties	6.2
No systematic	6.0
All systematic	7.9

Table 8: The expected 95% CL upper limit on $\mu_{\text{off-shell}}$ in the combination of the 4ℓ and $2\ell 2\nu$ channels, with a ranked listing of each systematic uncertainty individually, compared with no systematic uncertainty or all systematic uncertainties. The upper limits are evaluated using the CL_s method assuming $R^B_{H^*}$=1. Only the sources of systematic uncertainty that increase the limit by one significant digit are shown.

$R^B_{H^*}$	Observed 0.5	**1.0**	2.0	Median expected 0.5	**1.0**	2.0	Alternative hypothesis
$\mu_{\text{off-shell}}$	5.6	**6.7**	9.0	6.6	**7.9**	10.7	$R^B_{H^*} = 1, \mu_{\text{off-shell}} = 1$
$\Gamma_H/\Gamma_H^{\text{SM}}$	4.1	**4.8**	6.0	5.0	**5.8**	7.2	$R^B_{H^*} = 1, \Gamma_H/\Gamma_H^{\text{SM}} = 1, \mu_{\text{on-shell}} = 1.51$
$\Gamma_H/\Gamma_H^{\text{SM}}$	4.8	**5.7**	7.7	7.0	**8.5**	12.0	$R^B_{H^*} = 1, \Gamma_H/\Gamma_H^{\text{SM}} = 1, \mu_{\text{on-shell}} = 1$

Table 7: The observed and expected 95% CL upper limit on $\mu_{\text{off-shell}}$ and $\Gamma_H/\Gamma_H^{\text{SM}}$ within the range of $0.5 < R^B_{H^*} < 2$, combining the $ZZ \to 4\ell$ and $ZZ \to 2\ell 2\nu$ channels. The bold numbers correspond to the limit assuming $R^B_{H^*} = 1$. The upper limits are evaluated using the CL_s method, including all systematic uncertainties, with the alternative hypothesis as indicated in the last column. The two measurements of $\Gamma_H/\Gamma_H^{\text{SM}}$ differ only in the choice of the alternative hypothesis. In particular, $\mu_{\text{on-shell}}$ is treated as an auxiliary measurement in both cases in the fit and hence takes a value close to the observed value of $\mu_{\text{on-shell}} \sim 1.5$.

H→γγ: Spin/CP

- Discriminating variable:
polar angle of γ wrt z-axis of the Collins-Soper frame (minimize effect of ISR)
- Analysis similar to “rate/mass” analysis
  - $p_{T\gamma 1}$>0.35 $m_{\gamma\gamma}$ and $p_{T\gamma 2}$>0.25 $m_{\gamma\gamma}$
  [Minimize $m_{\gamma\gamma}$ and cosθ* correlations for background]
- H→γγ is a low S/B final state (inclusive ~3%)
  - Simultaneous fit
    $m_{\gamma\gamma}$ and |cosθ*| in signal region
    $m_{\gamma\gamma}$ in side-bands

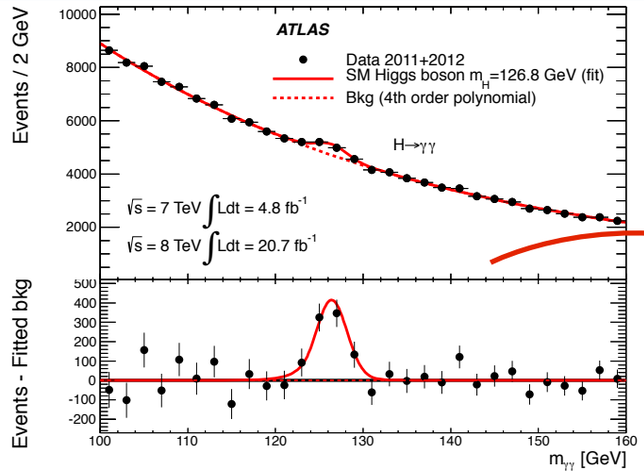

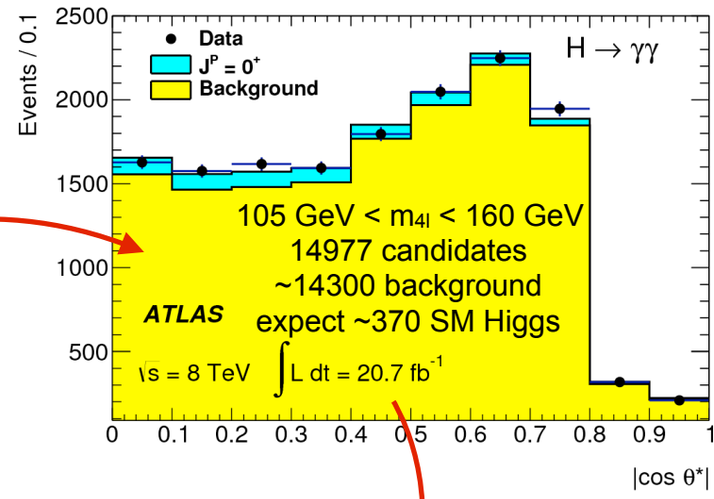

$$|\cos\theta^*| = \frac{|\sinh(\Delta\eta^{\gamma\gamma})|}{\sqrt{1+(p_T^{\gamma\gamma}/m_{\gamma\gamma})^2}} \frac{2p_T^{\gamma 1}p_T^{\gamma 2}}{m_{\gamma\gamma}^2}$$

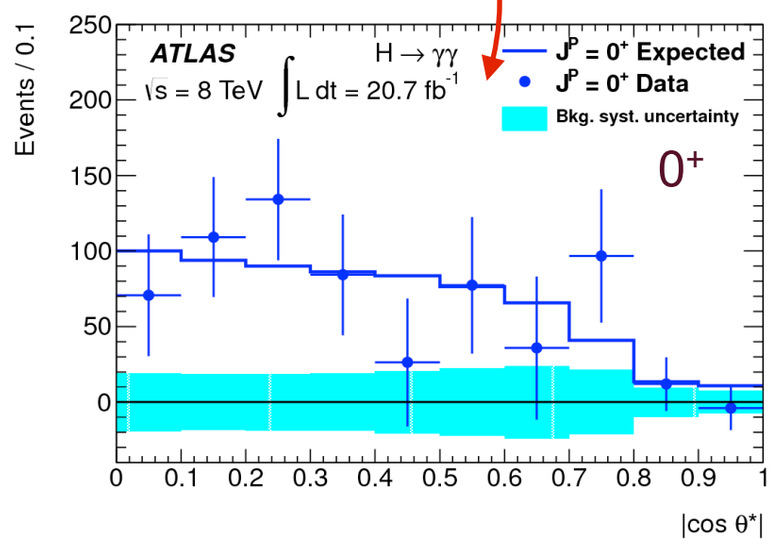

The 2^+ hypothesis is disfavored with respect to the 0^+ hypothesis.

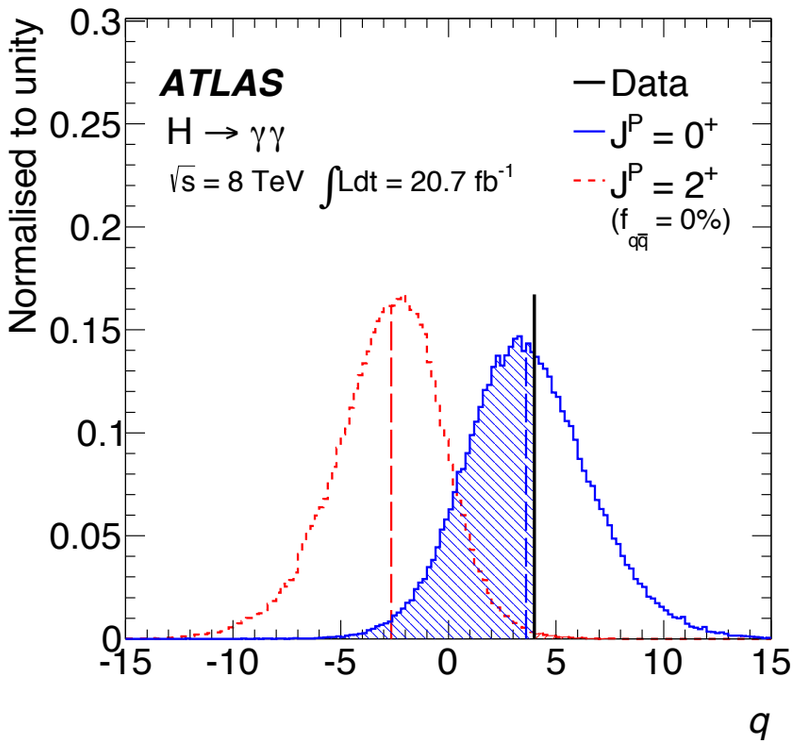

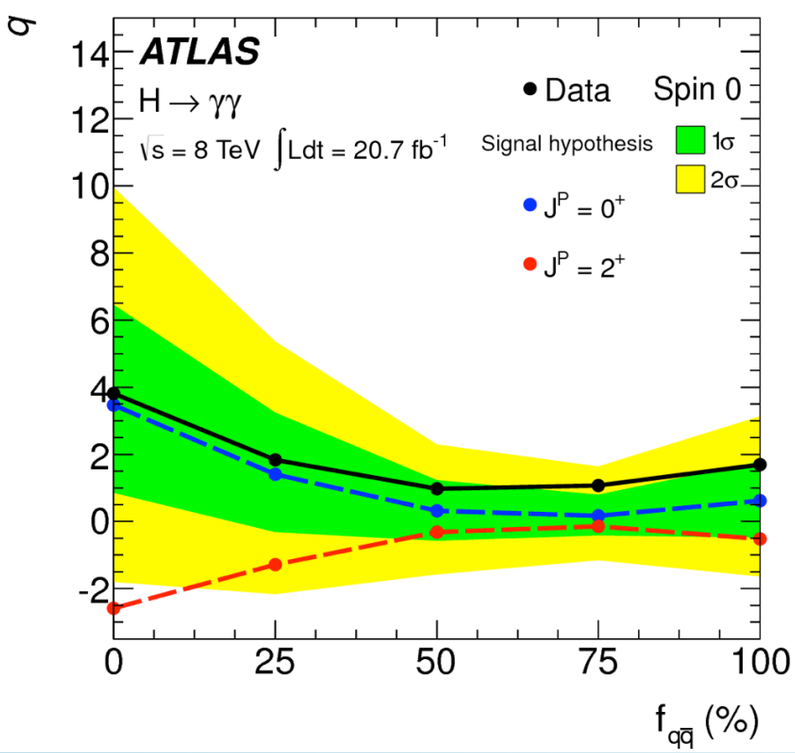

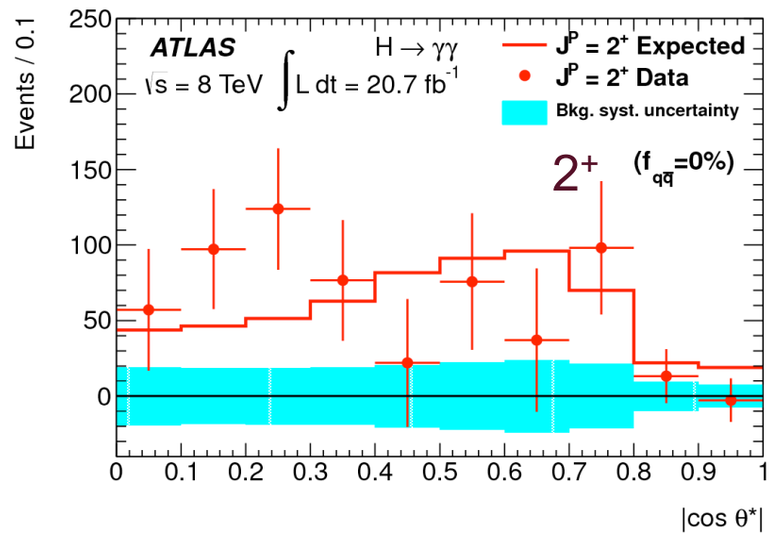

H→ZZ→4l Spin/CP

Ideal channel for spin/CP studies
- High S/B and full event reconstruction
- Spin/CP-sensitive observables:
  5 production angles and
  2 di-lepton invariant masses

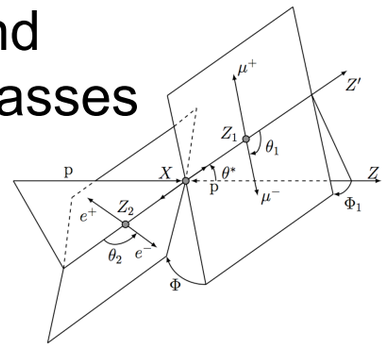

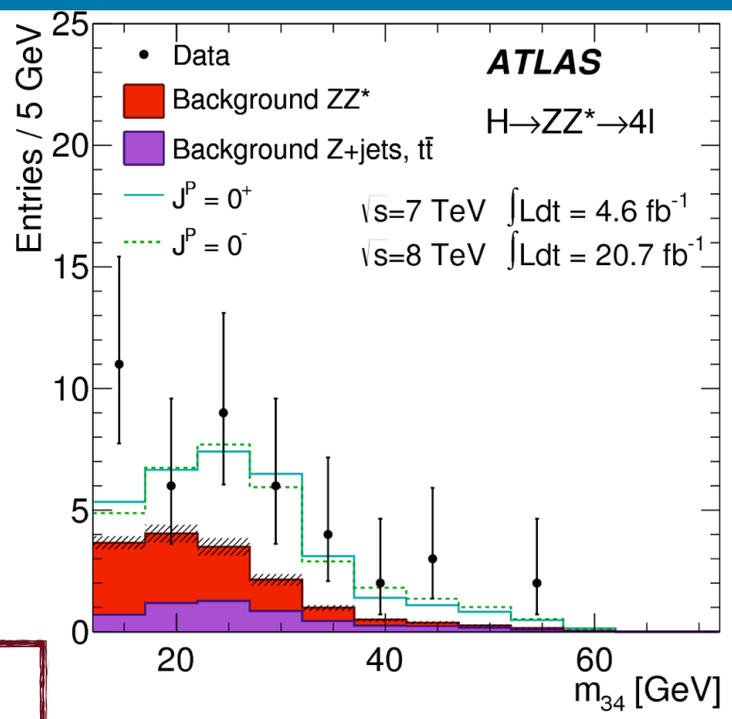

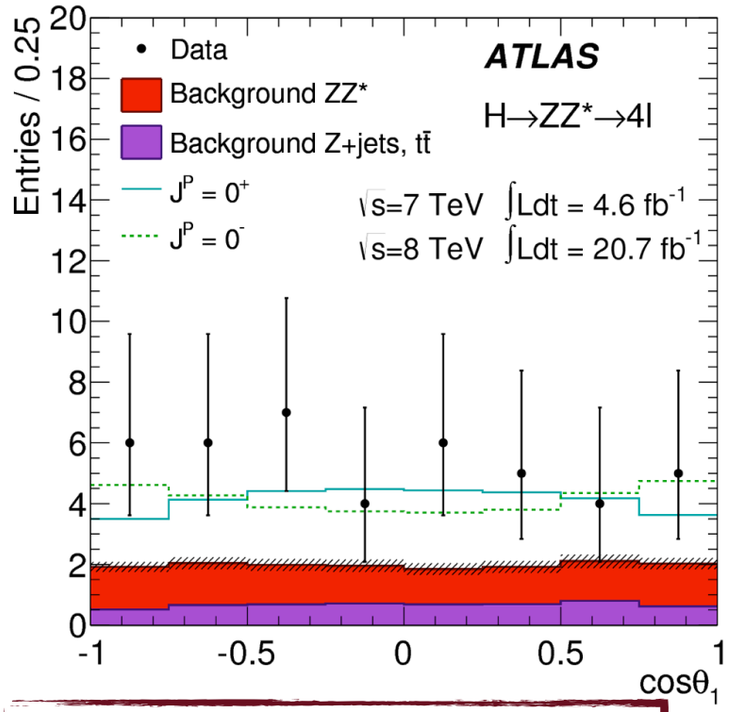

Two approaches:
- Separate BDT for each hypothesis
- ME corrected for acceptance/pairing effects

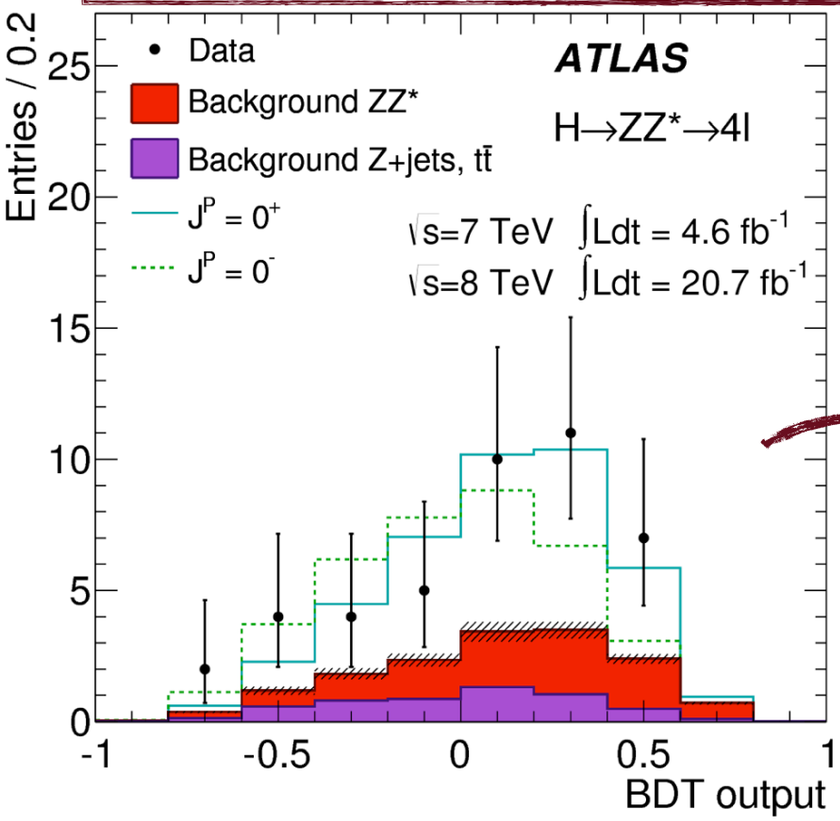

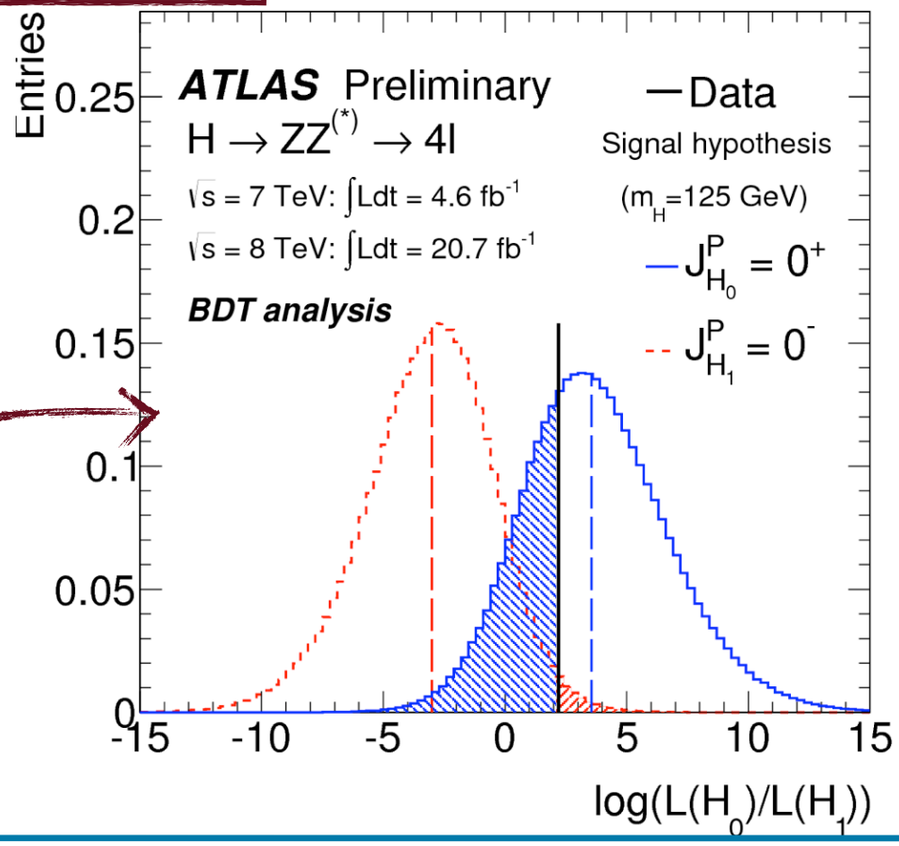

All studied alternative hypotheses disfavored wrt the 0^+ hypothesis.

	CL	J^{CP}
Spin-0	97.8%	0^-
Spin-1	94.0%	1^-
	99.8%	1^+
Spin-2	97.4%	2^+ 100% qq
	96.1%	2^+ 75% qq
	96.5%	2^+ 50% qq
	96.4%	2^+ 25% qq
	83.1%	2^+ 0% qq

H→WW→lνlν: Spin

- Restricted to “different flavour” (eμ) events and no jets
- Rate analysis already exploits spin-0 nature of SM Higgs boson
  - Relax spin-sensitive requirements, while keeping background under control
- m_{ll}, $\Delta\varphi_{ll}$, p_{Tll}, m_T sensitive to spin

Two BDT classifiers are used:
- BDT_{0+}: SM Higgs signal against the sum of all backgrounds
- BDT_{JP}: J^P signal against the sum of all backgrounds
- Perform 2D-fit in (BDT_{0+},BDT_{JP})

pT spectrum uncertainties found to have small effect

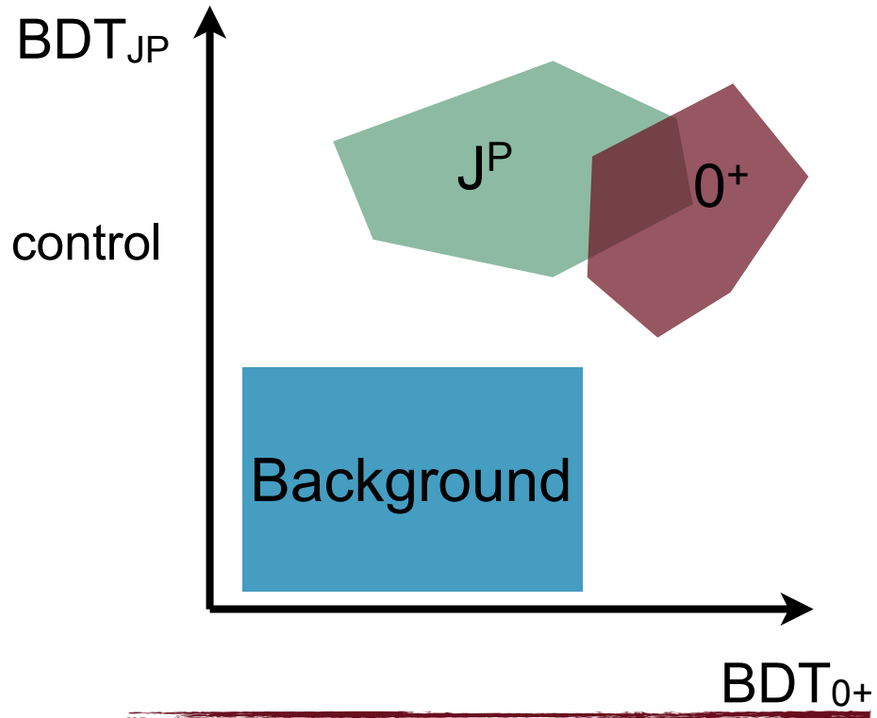

All studied alternative hypotheses are disfavored with respect to the 0^+ hypothesis.

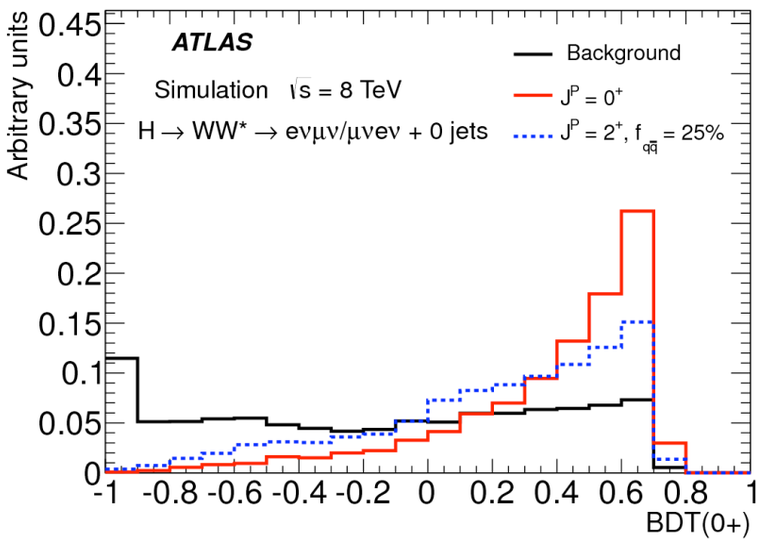

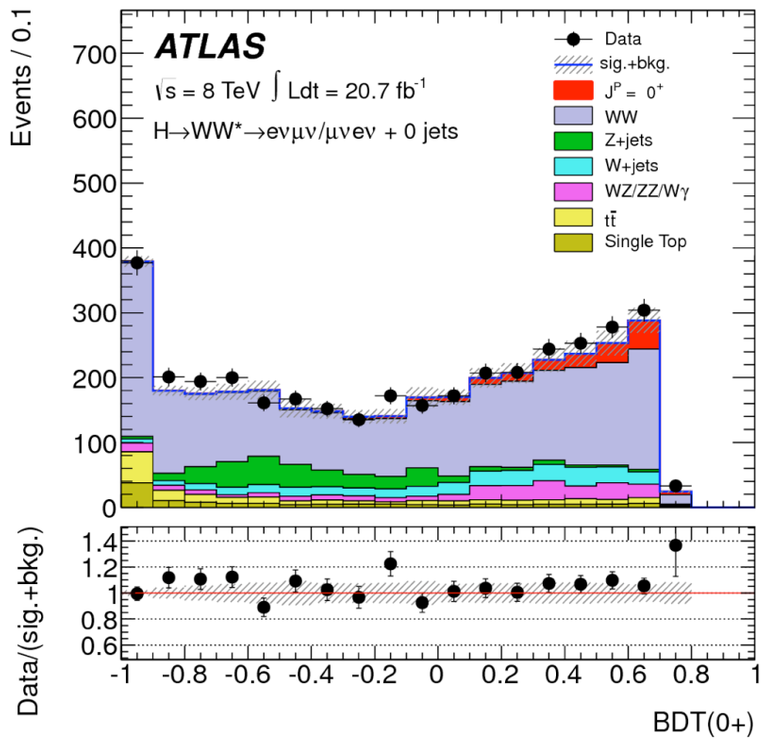

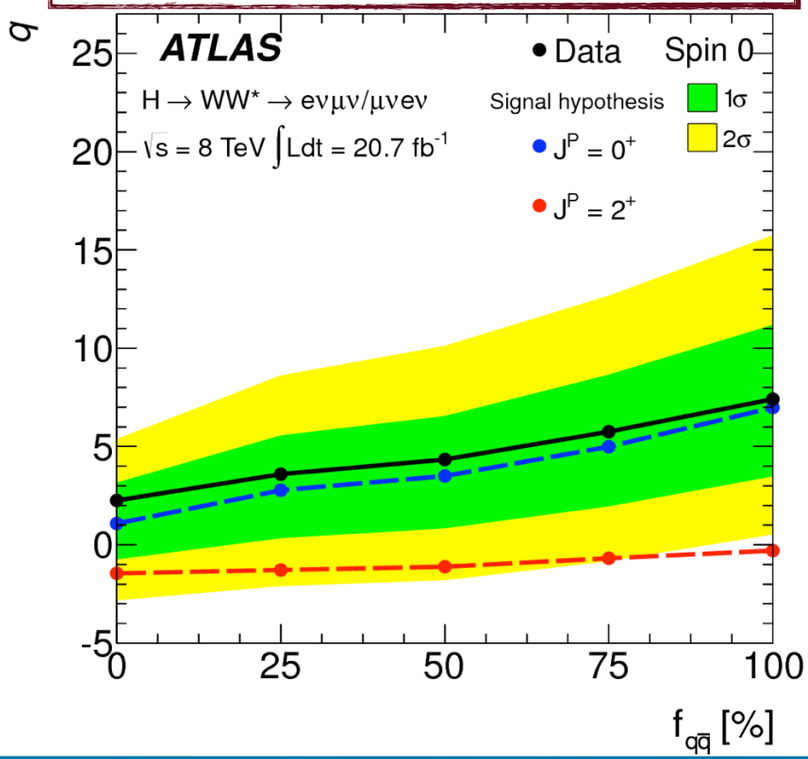

Indirect Γ_H measurement: Results

NEW!

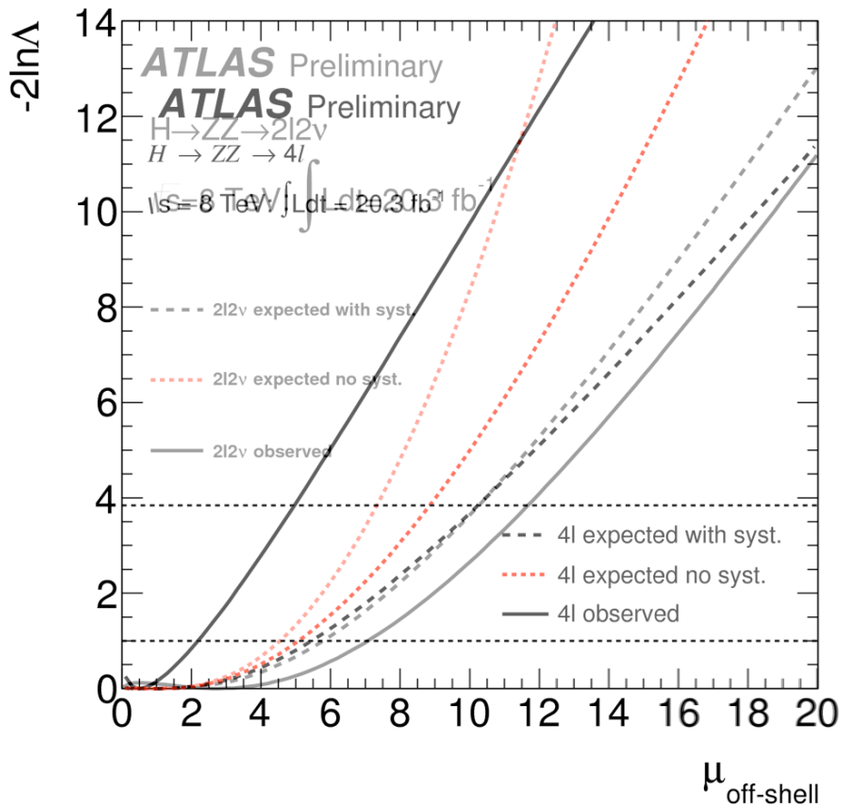

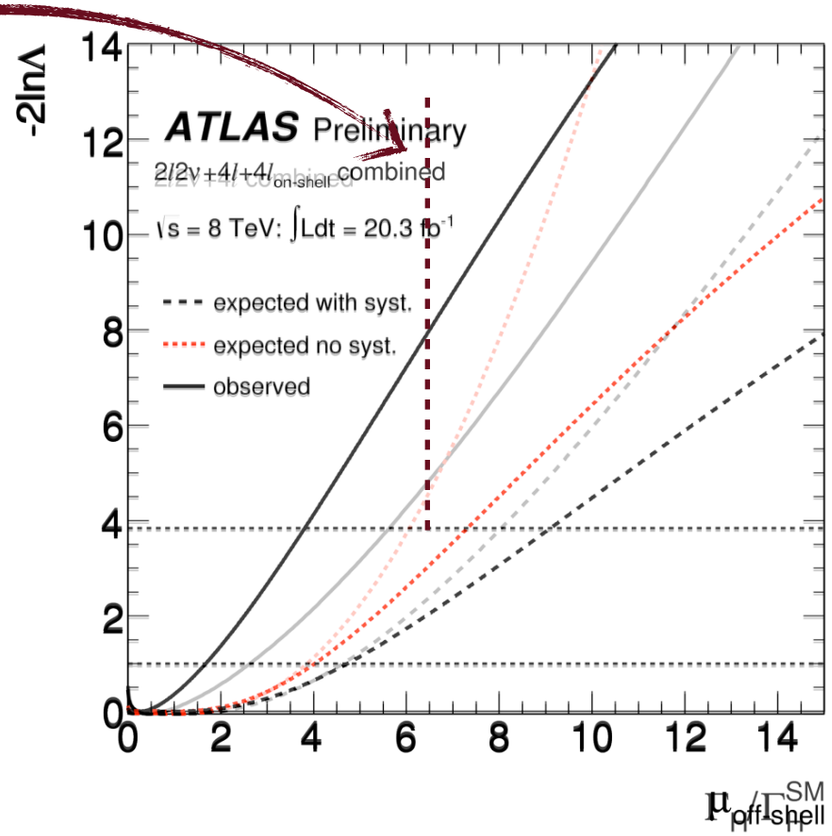

Results are expressed as a function of the unknown K-factor for the gg→ZZ background.

Assuming background K-factors same as for signal:

- $\Gamma_H/\Gamma_{SM} < 4.8$ (5.8) at 95% CLs with alternative hypothesis $R^B_{H^*}=1$, $\Gamma_H/\Gamma_{SM}=1$ and $\mu_{on\text{-}shell}=1.51$
- $\Gamma_H/\Gamma_{SM} < 5.7$ (8.5) at 95% CLs with alternative hypothesis $R^B_{H^*}=1$, $\Gamma_H/\Gamma_{SM}=1$ and $\mu_{on\text{-}shell}=1.00$